I

Pergamon

www.elsevier.com/locate/neuroscience

PII: S0306-4522(00)00335-3

Neuroscience Vol. 101, No. 1, pp. 89–100, 2000

0306-4522/00 $20.00+0.00

DONEPEZIL DOSE-DEPENDENTLY INHIBITS ACETYLCHOLINESTERASE ACTIVITY IN VARIOUS AREAS AND IN THE PRESYNAPTIC CHOLINERGIC AND THE POSTSYNAPTIC CHOLINOCEPTIVE ENZYME-POSITIVE STRUCTURES IN THE HUMAN AND RAT BRAIN

P. KASA,*† H. PAPP,* P. KASA JR‡ and I. TOROK§

*Alzheimer's Disease Research Centre and ‡Department of Pharmaceutical Technology, University of Szeged, H-6720 Szeged, Hungary

§Erzsébet Hospital, H-6800 Hódmezovásárhely, Hungary

Abstract—In the symptomatic treatment of mild to moderately severe dementia associated with Alzheimer's disease, donepezil (E2020) has been introduced for the inhibition of acetylcholinesterase activity in the human brain. However, there is no morphological evidence as to how this chemical agent affects the acetylcholinesterase-positive structures in the various areas of the human and the rat CNS. This study demonstrates by histochemical means that donepezil exerts a dose-dependent inhibitory effect *in vitro* on acetylcholinesterase activity. The most sensitive areas were the cortex and the hippocampal formation. Within the different layers of the cortex, the cholinoceptive acetylcholinesterase-positive postsynaptic pyramidal cell bodies were more sensitive than the presynaptic cholinergic axonal processes. In the cortex, the cell body staining was already abolished by even 2×10^{-8} M donepezil, whereas the axonal staining could be eliminated only by at least 5×10^{-8} M donepezil. In the hippocampus, the axonal acetylcholinesterase reaction end-product was eliminated by 5×10^{-7} M donepezil. The most resistant region was the putamen, where the staining intensity was moderately reduced by 1×10^{-6} M donepezil. In the rat brain, the postsynaptic cholinoceptive and presynaptic cholinergic structures were inhibited by nearly the same dose of donepezil as in the human brain. These histochemical results provide the first morphological evidence that, under *in vitro* circumstances, donepezil is not a general acetylcholinesterase inhibitor in the CNS, but rather selectively affects the different brain areas and, within these, the cholinoceptive and cholinergic structures. The acetylcholinesterase staining in the nerve fibers (innervating the intracerebral blood vessels of the human brain and the extracerebral blood vessels of the rat brain) and at the neuromuscular junction in the diaphragm and gastrocnemius muscle of rat, was also inhibited dose dependently by donepezil.

It is concluded that donepezil may be a valuable tool with which to influence both the pre- and the postsynaptic acetylcholinesterase-positive structures in the human and rat central and peripheral nervous systems. © 2000 IBRO. Published by Elsevier Science Ltd. All rights reserved.

Key words: acetylcholinesterase, Alzheimer's disease, CNS, donepezil, histochemistry, peripheral nervous system.

Donepezil (*R,S*-1-benzyl-4-[(5,6-dimethoxy-1-indanon)-2-yl]methylpiperidine hydrochloride) (E2020) is a central-acting second-generation cholinesterase inhibitor that is used in the treatment of Alzheimer's disease (AD).[12,45,57,65,73] Neuropathologically, the affected brain is characterized by the presence of senile plaques and neurofibrillary tangles,[46,47] and the loss of different transmitter-containing axons. Brain regions that are associated with cognitive, learning and memory functions, and particularly the neocortex and hippocampus, are most affected by the characteristic neuropathology of AD. It has been proposed that the degeneration of cholinergic neurons that is associated with the loss of cholinergic neurotransmission in the neocortex and other brain areas may contribute significantly to the cognitive function deterioration observed in subjects with AD. It has therefore been suggested that pharmacological enhancement of cholinergic neurotransmission may alleviate the symptoms in AD. According to the cholinergic hypothesis of the disease,[38,72] the inhibition of acetylcholinesterase (AChE) activity may be one of the most realistic approaches to the symptomatic treatment of AD.

Many neuropharmacological,[2] pharmacokinetic[2,49] and clinical[3,20,55] studies have been performed on the effects of donepezil on the cognitive functions.[10,56] Its mechanism of action is to increase the central cholinergic activity by inhibiting AChE activity in the brain,[62] thereby increasing the level of acetylcholine (ACh) at the synaptic sites. Donepezil has been shown to be clinically effective and well tolerated in the treatment of the symptoms of mild to moderately severe AD.[7,22] Although the use of AChE inhibitors is the most highly developed approach for the treatment of AD,[39] there has as yet been no demonstration of the precise morphological site(s) of its action. Nor is it known how AChE inhibitors with known central effects influence the enzyme activities in the peripheral nervous system (PNS). Biochemically, donepezil has been demonstrated to inhibit AChE activity in the cortex,[4,5,31] the hippocampus, the striatum and the hypothalamus of the rat brain.[5] Histochemical procedures, however, display advantages over biochemical methods because they allow detection of the effects of donepezil at a single cell level and at the single synaptic site, such as the peripherally located neuromuscular junction. In the present histochemical study, therefore, our aims were: (i) to investigate the regional selectivity of donepezil on AChE activity in the non-demented human brain; (ii) to compare the AChE inhibitory effects of donepezil in the non-demented human brain with those observed in the rat brain; and (iii) to investigate the AChE inhibitory effect of donepezil at the myoneuronal

†To whom correspondence should be addressed. Tel./Fax: +36-62-544569.
E-mail address: kp@comser.szote.u-szeged.hu (P. Kasa).

Abbreviations: ACh, acetylcholine; AChE, acetylcholinesterase; AD, Alzheimer's disease; NBM, nucleus basalis of Meynert; OD, optical density; PNS, peripheral nervous system; SO, supraoptic nucleus.

junction. It was also necessary to establish the effects of this agent on the intensity of AChE staining, in the cholinergic axons innervating the extra- and intracerebral blood vessels.

EXPERIMENTAL PROCEDURES

Materials

Donepezil (*R,S*-1-benzyl-4-[(5,6-dimethoxy-1-indanon)-2-yl]methyl-piperidine hydrochloride) was generously donated by Y. Kay (Eisai Co., Tsukuba Research Laboratory, Ibarakai, Japan). Acetylthiocholine iodide, copper sulfate, potassium ferricyanide, sodium maleate, 3,3′-diaminobenzidine.4HCl, nickel chloride, hydrogen peroxide (H_2O_2), sodium citrate and Tris–HCl buffers were from Sigma Chemical Co. (St Louis, MO, USA). Paraformaldehyde was purchased from Merck KGaA (Darmstadt, Germany). The DPX histological mountant was from Fluka Chemie Ag (Buchs, Germany).

Tissue preparation from human brains

Five brains with no history of previous mental disturbance were obtained at autopsy (mean age 64.8 ± 3.6 years). The interval between death and autopsy was less than 4 h. The left half of the human brain was sliced coronally into approximately 1 cm slabs, which were fixed by immersion for 24–36 h in an ice-cold 0.1 M phosphate-buffered (pH 7.4) 4% paraformaldehyde solution. After fixation, the samples were cryoprotected in 30% sucrose solution until they sank to the bottom of the container. The samples contained cortical areas, the hippocampal complex and the basal part of the brain. Forty-micrometer-thick sections were cut on a freezing microtome and incubated for AChE activity.[29,67]

Tissue preparation from rat brains

These investigations were performed in accordance with the ethical guidelines for animal investigations of the Hungarian Ministry of Welfare. Experiments were carried out in accordance with the European Communities Council Directive (24 November 1986; 86/609/EEC) and the Albert Szent-Györgyi Medical University Guidelines for Ethics in Animal Experiments. All efforts were made to minimize to reduce the number of animals used (a total of 30 animals was used). After ether anesthesia, adult Sprague–Dawley rats (weighing 200–250 g) were perfused transcardially for 30 min with cold (4°C) 4% paraformaldehyde solution (200 ml, freshly prepared from paraformaldehyde), buffered with 0.1 M Na phosphate (pH 7.4). The brains were immediately removed and immersed overnight in a similar fixative at 4°C. After cryoprotection for 24 h in 30% sucrose solution, coronal sections were cut at 30 μm on a freezing microtome. The samples were collected in ice-cold 0.1 M phosphate buffer (pH 7.4) and processed as free-floating sections for the histochemical staining of AChE.[29,67]

Tissue preparation from muscles

After perfusion fixation the left gastrocnemius muscle and the left part of the diaphragm of rats were dissected and immersed in a 4% paraformaldehyde solution containing 0.1 M Na phosphate buffer (pH 7.4). The samples were cryoprotected for 24 h in 30% sucrose solution. Thereafter under a dissecting microscope with the use of transparent light, the central area of the diaphragm containing the phrenic nerve arborization was cut out. Twenty-micrometer-thick sections were cut with a freezing microtome and incubated for AChE histochemical staining.[29,67]

Acetylcholinesterase histochemistry

To determine the possible inhibitory effects of donepezil on AChE histochemical staining, sections from human brain, rat cerebra and different muscles (diaphragm and gastrocnemius muscle) were preincubated for 20 min in a 0.1 M phosphate buffer solution (pH 7.4) which contained different doses of donepezil (5×10^{-9}, 2×10^{-8}, 5×10^{-8}, 5×10^{-7} and 1×10^{-6} M). Thereafter, without washing, the control and treated brain and muscle samples were placed in an incubation medium that contained the same dose of donepezil as was present in the preincubation solution. Control samples were incubated in the absence of donepezil, since it has been demonstrated that donepezil interacts with Trp279 and Phe330, which are present in AChE but not in the butyrylcholinesterase.[34] The muscles were incubated for 7 min, the rat brain tissues for 60 min and the human brain samples for 2 h at 25°C with constant agitation in a dark box. The incubation solution was prepared as described previously.[29,67] The medium consisted of acetylthiocholine iodide (1.8 mM), sodium citrate (0.1 M), copper sulfate (0.03 M), potassium ferricyanide (5.0 μM) and sodium maleate (0.1 M; pH 6.0). After incubation the sections were placed for 30 s at room temperature in a solution containing 0.05% 3,3′-diaminobenzidine.4HCl, 0.3% nickel chloride and 0.03% hydrogen peroxide in Tris–HCl buffer. All mounted sections were dehydrated in graded alcohols, cleared in xylene and mounted in DPX.

Image analysis

The intensity of AChE histochemical staining was evaluated by measuring the optical density (OD). The OD in an area comprising the stained neuronal perikarya, dendrites and axons was determined with a Quantimet 500MC Image Analysis System (Leica Cambridge) linked to a JVC-Color camera mounted on a Leica Laborlux "S" Leitz microscope.

The histochemical reactions were visualized and the digitized image (256 gray levels) was displayed on a color monitor with 1024×768 pixel resolution. The inhibitory effect of donepezil on AChE staining was evaluated. Each site was sampled within a rectangular box created on the computer monitor. In the case of the cortical area, the long axis of the box extended from the cortical surface to the white matter. Five fields of each site were chosen at random. The fields of interest were measured and the OD measurements were averaged. The OD of the white matter in the same section served as the background value. The absolute OD of the area of interest was obtained by subtracting the OD of the background from the OD of the area of interest. All measurements were made under the same optical and light conditions. The OD values obtained are expressed as percentages of the AChE-stained untreated control section (taken as 100%).

RESULTS

Inhibition of acetylcholinesterase activity in the human brain

The histochemical localization of AChE activity in the different areas of the human CNS has been well described in several reports.[15,17,30,35,40–43,50,54,59] We confirmed the findings of these previous studies, demonstrating that regional and laminar variations of the AChE-positive structures can be observed in non-demented control brain samples. The areas studied contained different amounts of AChE-positive fibers and various numbers of stained neuronal perikarya in different cortical layers (Fig. 1A). In the hippocampal complex very dense AChE staining was present in sectors CA3 and CA2. Moderate AChE activity was observed in areas CA4 and CA1 (Fig. 2A). Intensive axonal and perikaryonal staining was exhibited in the putamen (Fig. 2E) and in the nucleus basalis of Meynert (NBM) (Fig. 3A). There was strong cell body AChE positivity in the globus pallidus externus, the diagonal band of Broca (vertical and horizontal parts) and the supraoptic nucleus (SO) (Fig. 3B).

The AChE-positive structures in the different areas of the human brain were sensitive to donepezil in a dose-dependent manner. Donepezil (2×10^{-8} M) inhibited most of the AChE-positive neurons and reduced the axonal staining in the temporal cortex (Fig. 1B) and slightly decreased the staining intensity in hippocampal areas CA1 and CA4 (Fig. 2B). The application of 2×10^{-8} M donepezil, however, did not affect the AChE activity in the basal part of the forebrain. At 5×10^{-8} M, donepezil severely reduced the axonal staining in sector CA1 and inhibited the enzyme activity in the area CA4 (Fig. 2C). At 5×10^{-7} M, donepezil abolished the perikaryonal and axonal staining in the hippocampal formation (Fig. 2D). The AChE activity in the cholinergic neuronal

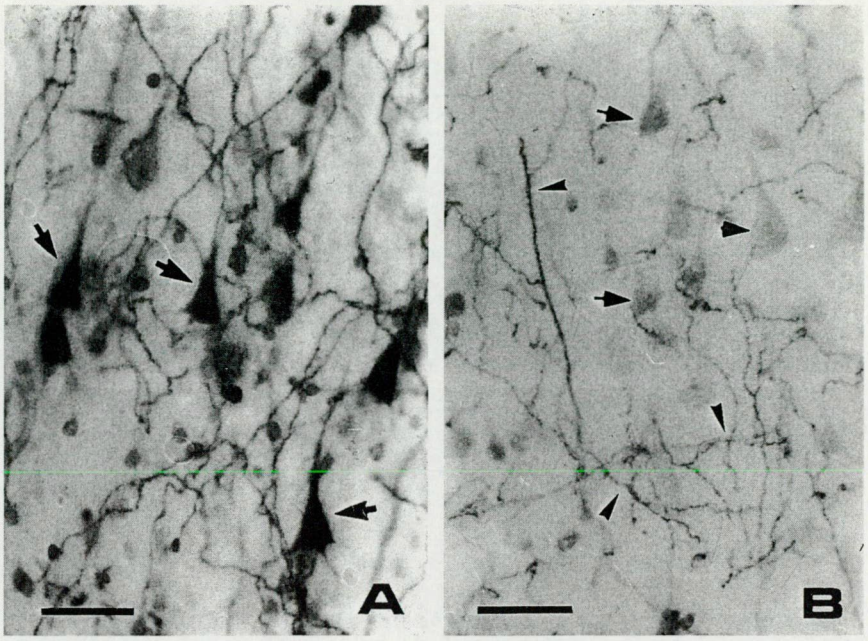

Fig. 1. Photographs showing the differences in AChE activity between the control (A) and the donepezil-treated (B) human temporal cortex. Note the presence of intensely stained pyramidal cells (arrows) and the AChE-positive nerve fibers in the control sample (A), and the disappearance of AChE activity from most of the neuronal perikarya (arrows) in the 2×10^{-8} M donepezil-treated sample (B). A stained neuron can rarely be observed in the donepezil-treated sample, although some AChE positivity is still present in many cholinergic nerve fibers (arrowheads) (B). Scale bar = 50 μm.

perikarya and axons in the putamen was resistant to 5×10^{-8} M donepezil (Fig. 2F) and slightly decreased by 5×10^{-7} M donepezil (Fig. 2G). At 1×10^{-6} M, however, the inhibitor moderately reduced the AChE positivity in the axons in the putamen, but intense staining persisted in the cholinergic cell body (Fig. 2H).

The AChE-positive neuronal perikarya present in the diagonal band of Broca (vertical and horizontal parts), the NBM, the globus pallidus (external and internal parts) and the SO nucleus were more resistant than the cholinergic axons in the same area to different concentrations of donepezil. At 5×10^{-9} M, donepezil had no effect, 5×10^{-8} M slightly inhibited the AChE staining, while 5×10^{-7} M donepezil had a very pronounced reducing effect on the axonal AChE staining. Despite the reduction in the staining intensity in the cell processes, the reaction end-product in a large number of the neuronal perikarya in the NBM was only moderately reduced by 1×10^{-6} M donepezil (Fig. 3C). In the SO nucleus, an inhibition similar to that in the NBM was observed, except that the dendritic processes were eliminated and the perikaryonal staining was reduced (Fig. 3D) by 5×10^{-7} M donepezil.

A more detailed microscopic evaluation of the inhibitory effects of different doses of donepezil on AChE-positive cell bodies and axons in the entorhinal cortex, temporal cortex, insular cortex and hippocampus is presented in Table 1. The effects of donepezil on axonal and cell body staining in the SO nucleus, the globus pallidus (external and internal parts), the diagonal band (vertical and horizontal areas), the NBM and the putamen are demonstrated (Table 2).

Inhibition of acetylcholinesterase activity in the rat brain

In general, our study accords well with the earlier histochemical results in revealing the AChE-positive structures in the different areas of the control rat brain.[28] In the coronal section of the control, untreated brain at the interaural 6.2 mm level,[50] AChE staining is present (among others) in the frontoparietal cortex (Fig. 4A), the hippocampus (Fig. 4C) and the caudate–putamen (Fig. 4F).

The various concentrations of donepezil (5×10^{-9}, 2×10^{-8}, 5×10^{-8}, 5×10^{-7} and 1×10^{-6} M) dose-dependently inhibited the AChE staining in the various areas of the treated brain. In detail, the histochemical staining revealed that 5×10^{-9} M donepezil reduced the reaction end-product in the cell bodies more effectively than that in the axons in the frontoparietal cortex. The AChE reaction end-product was significantly reduced in the cortical cholinergic axons and abolished from the neuronal perikarya with 2×10^{-8} M donepezil (Fig. 4B). All the axonal AChE staining disappeared from the cortex and the cell bodies in hippocampal areas CA1 and CA4 on inhibition with 5×10^{-8} M donepezil. However, in other areas of the hippocampus, and especially in CA3, CA2 and the supragranular zone of the dentate gyrus, many AChE-positive axons remained (Fig. 4D). On application of 5×10^{-7} M donepezil, all of the AChE positivity disappeared from the axons in the hippocampus (Fig. 4E), but AChE staining surprisingly still remained in some cell bodies of the medial septum, the diagonal band nucleus, the NBM and the axons and cholinergic neurons in the caudate–putamen (Fig. 4G). AChE-positive structures could be detected in the caudate–putamen and in the basolateral nucleus of amygdala even after 1×10^{-6} M donepezil treatment (Fig. 4H).

Details of the inhibitory effects of various doses of donepezil on the AChE-positive cell bodies and axons in the different areas of the rat brain are provided in Table 3.

Inhibition of acetylcholinesterase activity in nerve fibers innervating the cerebral blood vessels

The histochemical demonstration of cholinergic innervation

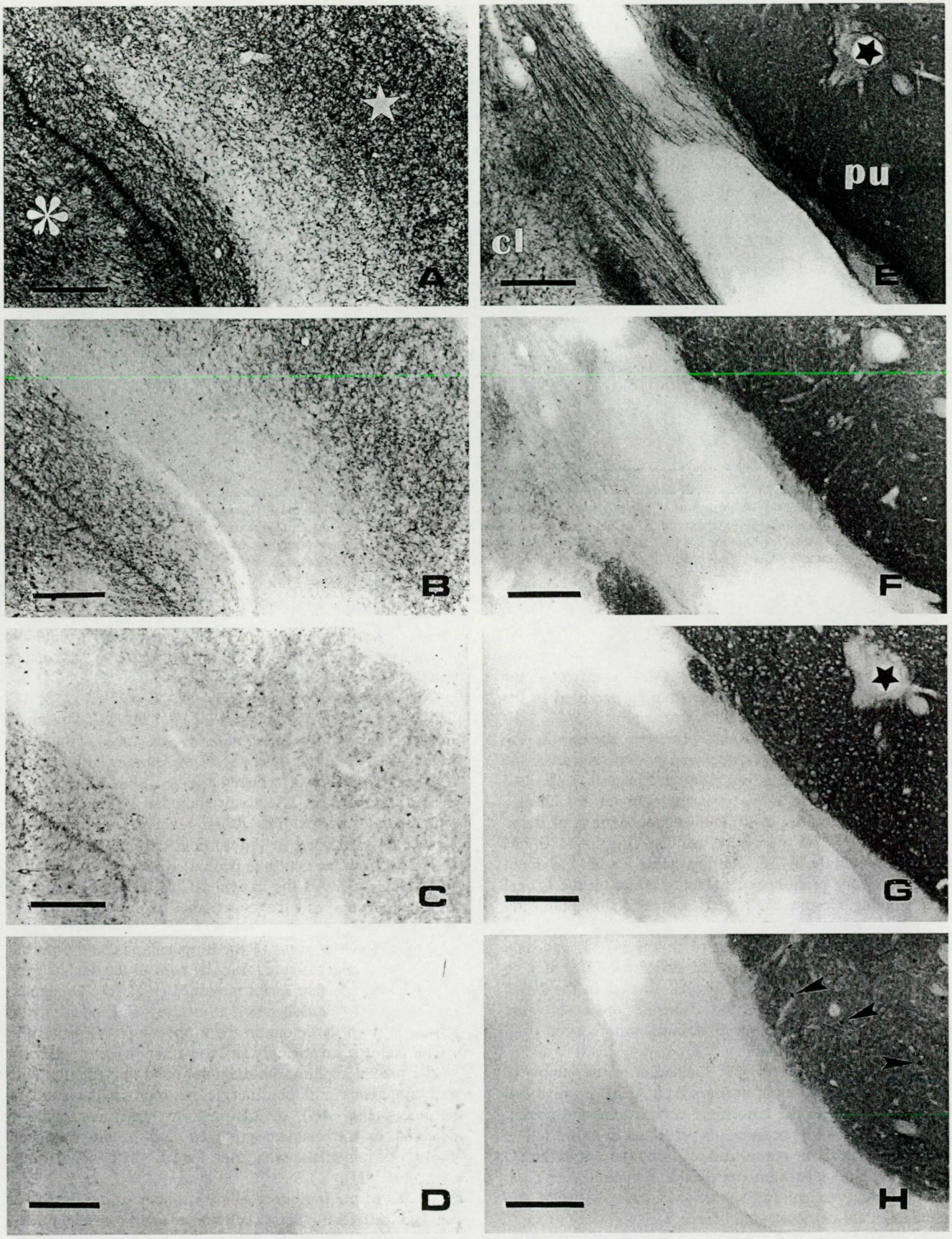

Fig. 2. Photographs showing the effects of different doses of donepezil on AChE staining in the hippocampus (A–D) and putamen (E–H) of the human brain. In the control hippocampus intense perikaryonal staining is present in area CA4 (asterisk). Moderate AChE positivity may be seen in sector CA1 (star) (A). The application of 2×10^{-8} M donepezil slightly reduced the axonal staining in the sectors CA1 and CA4 (B), while 5×10^{-8} M donepezil eliminated most of the axonal AChE reaction in sector CA1 and severely reduced it in area CA4 (C). No AChE positivity could be discerned in any part of the hippocampus after the application of 5×10^{-7} M donepezil (D). In the control putamen (pu), intense enzyme staining is present in the cholinergic fibers and cell bodies (E). No or a slight reduction in AChE activity could be detected after the application of 5×10^{-8} M (F) or 5×10^{-7} M donepezil (G). At 1×10^{-6} M, donepezil slightly inhibited the AChE staining in the cholinergic axons, whereas intense AChE positivity remained in the neuronal perikarya (arrowheads) (H). Note the intense AChE staining in claustrum (cl) (E) and the dose-dependent reduction of the AChE reaction end-product (F–H). The identical areas in the different sections are labeled (stars). Scale bar = 500 μm.

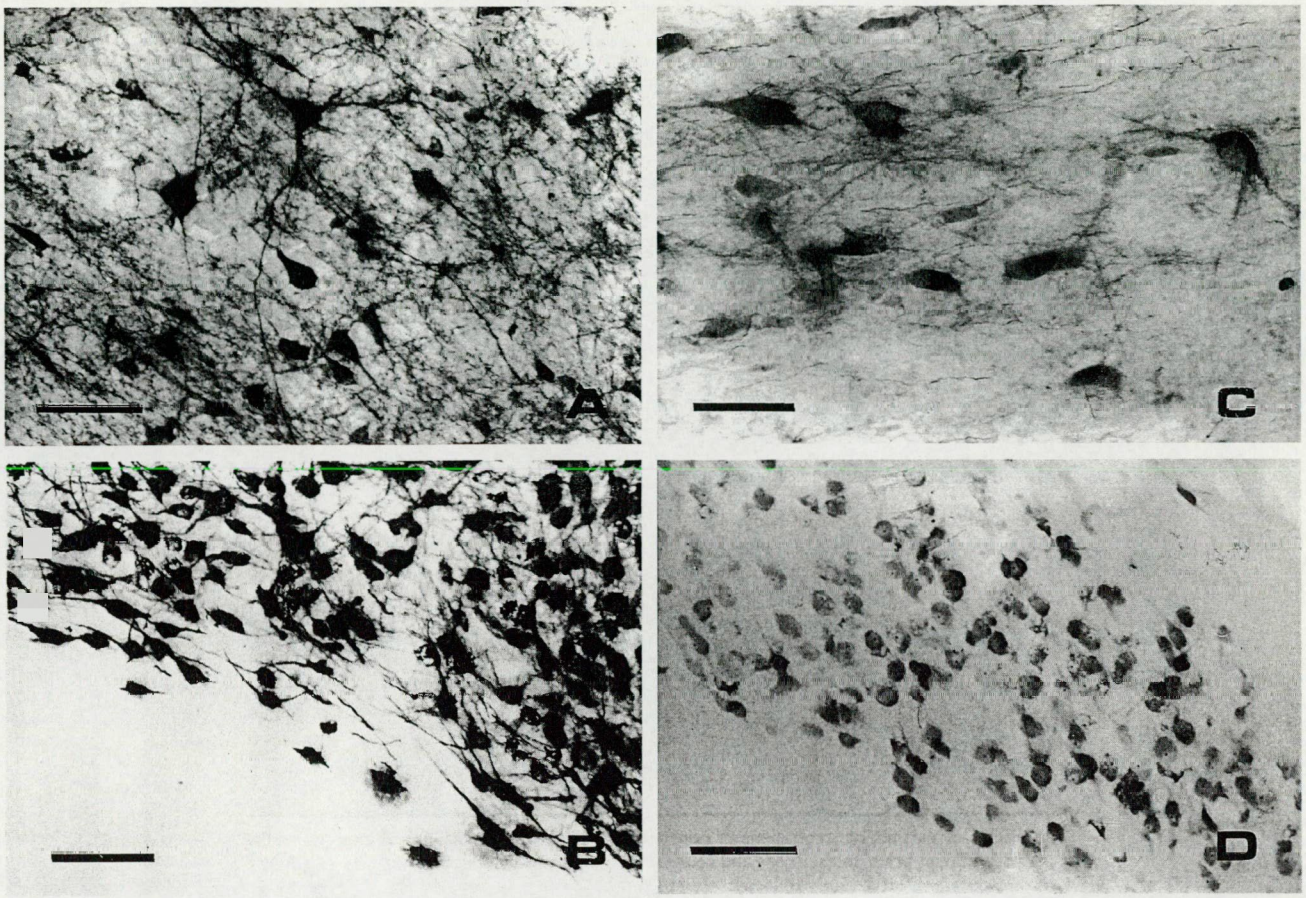

Fig. 3. Photographs showing the AChE-positive structures in the control (A, B) and the donepezil-treated (C, D) NBM and SO of the human brain. In the control NBM, the AChE positivity is present in the cholinergic cell bodies and the neuropil (A). At 1×10^{-6} M, the drug reduced the neuropil staining, but it is still present in the neuronal perikarya (C). In the control SO nucleus, the large multipolar neurons display AChE positivity in the neuronal perikarya and its dendrites (B). On application of 5×10^{-7} M donepezil abolished the AChE reaction end-product from the dendrites and reduced the staining in the cell bodies (D). Scale bar = 100 μm.

of the cerebral blood vessels is an important issue in the normal human brain, in individuals with AD and in animal models. This study has demonstrated the cholinergic innervation of the different extracerebral (Fig. 5A) and intracerebral (Fig. 5B, D) blood vessels in the rat and human. AChE histochemical staining revealed that donepezil dose-dependently inhibited the AChE staining reaction in the nerve fibers innervating the blood vessels. In rat brain samples treated *in vitro* with 2×10^{-8} M donepezil, the number and intensity of AChE-positive nerve fibers were reduced in the extracerebral blood vessels (Fig. 5C), while on treatment with 5×10^{-8} M donepezil they were abolished from the nerve fibers in the extracerebral blood vessels in the rat (Fig. 5E) and in the intracerebral vessels in humans (Fig. 5F).

Inhibition of acetylcholinesterase activity at the neuromuscular junction

In accord with the earlier findings,[26] AChE histochemical staining is present at the control neuromuscular junction of the rat (Fig. 5G). With the same doses as in the brain, it was demonstrated that 2×10^{-8} M donepezil only slightly (Fig. 5H), while 5×10^{-7} M donepezil effectively (Fig. 5I) reduced the AChE-positive staining at the neuromuscular junction in the diaphragm and gastrocnemius muscle of the rat.

Densitometric demonstration of the inhibitory effect of donepezil on acetylcholinesterase staining in different areas of the human and the rat brain

For a quantitative analysis of the inhibitory effect of donepezil we measured the changes in the OD of the AChE histochemical staining. The results revealed a dose-dependent inhibitory effect of donepezil in the various areas of the cortex, the hippocampus, the caudate–putamen and the NBM. The quantitative OD results, relating to the inhibitory effects of donepezil, on the AChE histochemical staining in the human and the rat brain are summarized in Fig. 6A and 6B, respectively.

DISCUSSION

We confirmed the results of previous biochemical and neuropharmacological studies that donepezil inhibits AChE activity in the rat brain. In addition, the present histochemical study reveals for the first time the AChE-inhibitory effect of donepezil in various human brain areas and its effects on different cholinergic and cholinoceptive neuronal structures in the human and rat CNS.

Our AChE histochemical study resulted in four principal findings. First, an important feature of this study is that AChE-positive postsynaptic neuronal perikarya in the cortex and the hippocampus are structures that are more sensitive to

Table 1. Microscopic evaluation of the inhibitory effects of different doses of donepezil on the histochemical staining in acetylcholinesterase-positive axons and cell bodies in different cortical and hippocampal areas of the human brain

Brain area	Inhibitory effect on	Dose of donepezil Control	$5x10^{-9}$	$2x10^{-8}$	$5x10^{-8}$	$5x10^{-7}$ M
Entorhinal cortex	Cell body	+	-/+	-	-	-
	Axon	+	+/-	+/-	-	-
Temporal cortex	Cell body	+	-/+	-	-	-
	Axon	+	+/-	-/+	-	-
Insular cortex	Cell body	+	-/+	-	-	-
	Axon	+	+/-	-/+	-	-
Hippocampus CA1	Cell body	+	+	+/-	-/+	-
	Axon	+	+	+/-	+/-	-
Hippocampus CA3-2	Cell body	+	+	+/-	+/-	-
	Axon	+	+	+	+/-	-
Hippocampus CA4	Cell body	+	+	+/-	+/-	-
	Axon	+	+	+	+/-	-

The effects of various concentrations of donepezil on the AChE histochemical staining in the various human brain areas, axons and neuronal perikarya are indicated: no effect: +; slightly reduced: +/−; moderately reduced: −/+; severely reduced or abolished: −.
The shaded area emphasizes the inhibitory effects of the different doses of donepezil.

donepezil than the presynaptic cholinergic fibers in the cortex and in the hippocampus. Second, the most resistant cholinergic fibers are present in the putamen, the basolateral nucleus of the amygdala, the olfactory tubercle and the lateral habenular nucleus. Third, the most resistant cholinergic neuronal perikarya are present in the NBM, the medial septum, the diagonal band (vertical and horizontal parts) and the globus pallidus. Fourth, the staining intensity in the cholinergic cell bodies of the putamen, which are marginally involved in AD, was only slightly inhibited with donepezil.

Effects of donepezil on the human CNS

In biochemical experiments, donepezil has been shown to inhibit AChE activity in the human brain[44] and in human erythrocytes.[44] Neurochemical studies have demonstrated that presynaptic cholinergic markers, such as choline acetyltransferase activity, the ACh level and the high-affinity choline uptake are significantly reduced in the cortex, the hippocampus and the NBM in AD. Since the neocortex and the hippocampal formation are known to be major sites of the neuropathological changes in AD, inhibition of the residual AChE activity in these areas might well be beneficial in alleviating the cholinergic hypofunction in AD.[18,52] Indeed, in clinical applications, donepezil is used for the treatment of memory loss and the behavioral deterioration associated with the ACh deficit in AD.

Biochemical experiments have demonstrated that AChE and its different molecular forms (soluble and membrane-bound) are reduced in the brain in AD[1,11] and anomalous AChE activity appears in the senile plaques[16,61] and cerebrospinal fluid.[64] This histochemical study revealed the noteworthy finding that the AChE activity present in the postsynaptic cholinoceptive cortical pyramidal cell body is more sensitive than the presynaptic cholinergic axons to donepezil. (It is interesting to note that the cholinergic neurons present in the NBM, which receives cholinergic innervations and may therefore be regarded as cholinoceptive, are not as sensitive to donepezil as the purely cholinoceptive pyramidal cells within the cortical layers.) In other brain areas, such as the putamen, which is not involved in the AD neuropathology, the cholinergic axons and the cell bodies are very resistant to donepezil treatment. Our results therefore provide the first morphological evidence of a difference in the effects of donepezil on the presynaptic cholinergic and postsynaptic cholinoceptive sites in the human brain. This study has demonstrated that the selectivity of donepezil is more pronounced towards the soluble form of AChE (G1 form), which is known to be located mainly in the cell body, than towards the membrane-bound AChE (G4 form), which is to be found predominately on the outer surface of axonal membranes of the cholinergic cells.[27] Similarly to our results, in biochemical experiments where donepezil was added to soluble and crude mitochondrial fractions obtained from non-demented or AD brain, the AChE activity was inhibited in the soluble and the particulate fractions at a low concentration of the inhibitor.[44] Donepezil inhibits the

Table 2. Microscopic evaluation of the inhibitory effects of different doses of donepezil on the histochemical staining in acetylcholinesterase-positive axons and cell bodies in the various areas of the human brain

Brain area	Inhibitory effect on	Dose of donepezil Control	$5x10^{-9}$	$2x10^{-8}$	$5x10^{-8}$	$5x10^{-7}$	$1x10^{-6}$ M
Supraoptic	Axon	+	+	+	-/+	-	-
nucleus	Cell body	+	+	+	+/-	-/+	-
Globus pallidus	Axon	+	+	+	-/+	-/+	-
(external part)	Cell body	+	+	+	+/-	-/+	-
Globus pallidus	Axon	+	+	+	-/+	-/+	-
(internal part)	Cell body	+	+	+	+/-	-/+	-
Diagonal band	Axon	+	+	+	+/-	-/+	-
(vertical part)	Cell body	+	+	+	+	+/-	-/+
Diagonal band	Axon	+	+	+	+/-	-/+	-
(horizontal part)	Cell body	+	+	+	+	+/-	-/+
Nucl. basalis	Axon	+	+	+	+/-	-/+	-
(Meynert)	Cell body	+	+	+	+	+/-	-/+
Putamen	Axon	+	+	+	+	+/-	-/+
	Cell body	+	+	+	+	+	+/-

The effects of various concentrations of donepezil on the AChE histochemical staining in the various human brain areas, axons and neuronal perikarya are indicated: no effect: +; slightly reduced: +/−; moderately reduced: −/+; severely reduced or abolished: −.
The shaded area emphasizes the inhibitory effects of the different doses of donepezil.

Table 3. Microscopic evaluation of the inhibitory effects of different doses of donepezil on the histochemical staining in acetylcholinesterase-positive cell bodies and axons in various areas of the rat brain

Brain area	Inhibitory effect on	Control	Dose of donepezil $5x10^{-9}$	$2x10^{-8}$	$5x10^{-8}$	$5x10^{-7}$	$1x10^{-6}$ M
Frontoparietal	Cell body	+	+/-	-	-	-	-
cortex	Axon	+	+	+/-	-	-	-
Hippocampus	Cell body	+	+/-	-/+	-	-	-
CA1	Axon	+	+	-/+	-/+	-	-
Hippocampus	Cell body	+	+	-/+	-	-	-
CA4	Axon	+	+	+/-	+/-	-	-
Septum	Axon	+	+	+/-	-/+	-	-
	Cell body	+	+	+	+/-	-/+	-
Nucl. basalis	Axon	+	+	+/-	-/+	-	-
(Meynert)	Cell body	+	+	+	+	+/-	-
Putamen	Axon	+	+	+	+	+/-	-/+
	Cell body	+	+	+	+	+	+/-

The effects of various concentrations of donepezil on the AChE histochemical staining in the various rat brain areas, axons and neuronal perikarya are indicated: no effect: +; slightly reduced: +/−; moderately reduced: −/+; severely reduced or abolished: −.
The shaded area emphasizes the inhibitory effects of the different doses of donepezil.

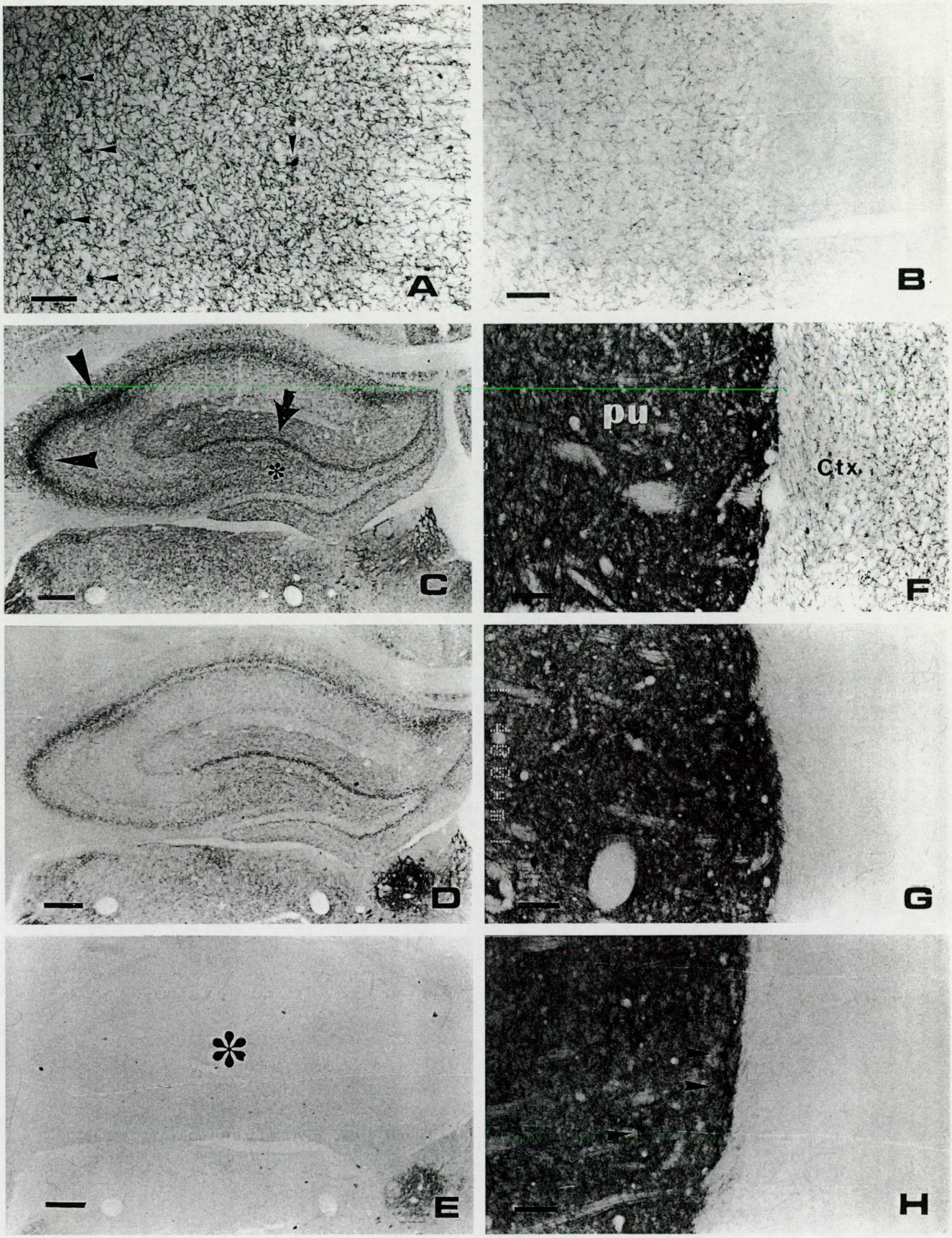

Fig. 4. Photographs showing the AChE positivity in the frontoparietal cortex (A), hippocampus (C) and putamen (pu) (F) of control rat brain. Note the presence of intensely stained pyramidal cells (arrowheads) and the moderately enzyme-positive nerve fibers (A). At 2×10^{-8} M, donepezil abolished the AChE positivity in the cortical pyramidal cells (B). In the control hippocampus intense axonal staining is present in area CA2 and CA3 (arrowheads) and in some neuronal perikarya in sector CA4 (asterisk) (C). On application of 5×10^{-8} M donepezil all of the AChE positivity disappeared from the cells in area CA1 and CA4, but many enzyme stained axons remained in sector CA2, CA3 and the supragranular zone of the dentate gyrus (D). At 5×10^{-7} M, donepezil abolished the AChE staining from the hippocampus (asterisk) (E) and slightly reduced it in the putamen (G). Enzyme-positive axons and neuronal cell bodies could be detected in the caudate–putamen even after 1×10^{-6} M donepezil treatment (H). Scale bar = 100 μm.

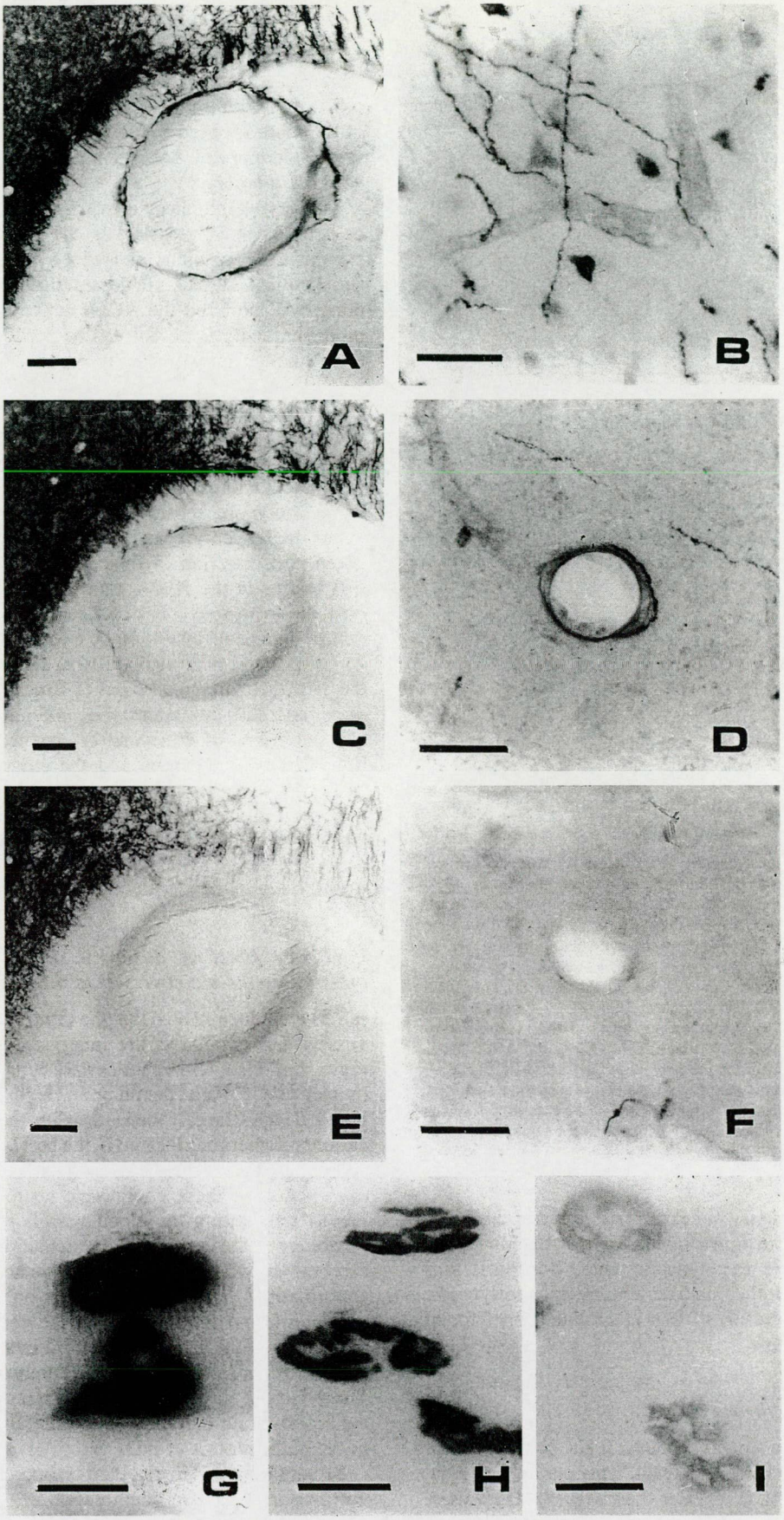

Fig. 5. Photographs showing the cholinergic innervations of the extracerebral innervation of blood vessels in a control rat (A), an intracerebral blood vessel in the control human brain (B, D), the neuromuscular junction in the diaphragm of a control rat (G) and the same structures after treatment with different doses of donepezil (C, E, F, H, I). In the control sample of the rat brain, an extracerebral blood vessel is surrounded by a number of AChE-positive nerve fibers (A). At 2×10^{-8} M, donepezil reduced (C), while 5×10^{-8} M abolished the nerve fiber staining surrounding the blood vessels in the rat (E) and in the human brain (F). In the neuromuscular junction, heavy AChE reaction end-product is present in the diaphragm of the control sample (G). On application of 2×10^{-8} M donepezil slightly (H), but 5×10^{-7} M donepezil strongly reduced the enzyme staining in the motor end-plate in the diaphragm of the rat. Scale bar = 50 μm.

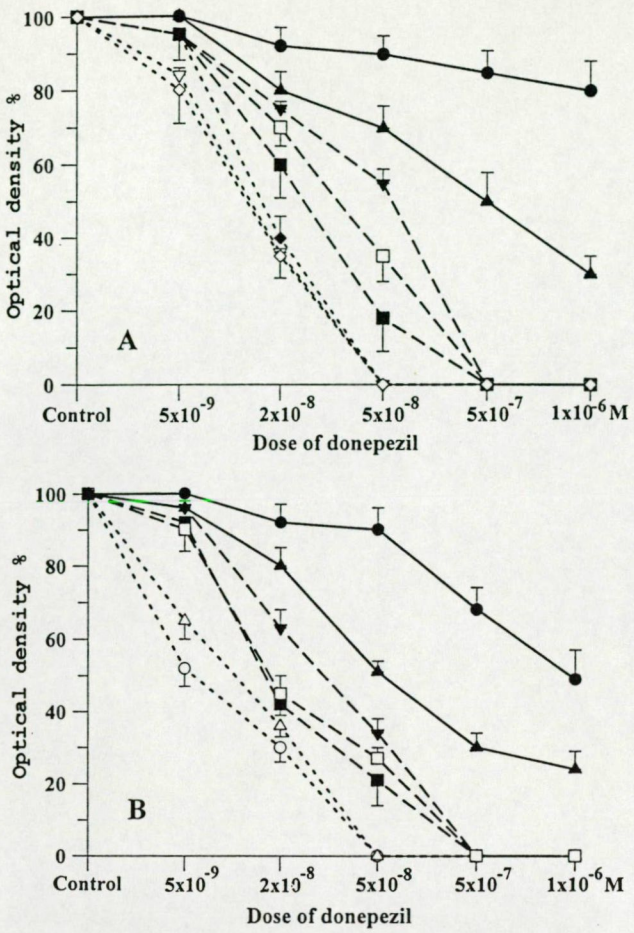

Fig. 6. (A) Changes in optical density (OD) in the AChE histochemical staining in the various areas of the human brain after treatment with different doses of donepezil. The OD of the AChE histochemical reaction in the control sample is taken as 100%. Five fields of each area of interest were measured ($n = 5$) and the OD results were averaged. Symbols are as follows: putamen (●), NBM (▲), hippocampus CA1 (■), hippocampus CA3 and CA2 (▼), hippocampus CA4 (□), temporal cortex (◆), entorhinal cortex (▽), insular cortex (◇). (B) Changes in optical density (OD) in the AChE histochemical staining in the various areas of the rat brain after treatment with different doses of donepezil. The OD of the AChE histochemical reaction in the control sample is taken as 100%. Five fields of each area of interest were measured (n = 5) and the OD results were averaged. Symbols are as follows: caudate–putamen (●), NBM (▲), hippocampus CA1 (■), hippocampus CA3 and CA2 (▼), hippocampus CA4 (□), fronto-parietal cortex (○), primary olfactory cortex (△).

postsynaptic AChE activity better than the presynaptic AChE activity, which is quite remarkable. By slowing down the hydrolysis of ACh at the synaptic sites, donepezil will enhance the effect of the residual cholinergic presynaptic elements in AD. The result of this is similar to that found for heptyl-physostigmine.[53]

Effect of donepezil on the rat CNS

In biochemical experiments, donepezil has been shown to inhibit the AChE activity in the brain,[48] the cortex[4,5] and the hippocampus[5] of the rat. It elevates the extracellular levels of catecholamines[19] and ACh in the cerebral cortex[19] and the hippocampus.[2] It will affect the *N*-methly-D-aspartate receptors[71] in the rat brain and interact with nicotinic receptors expressed in fibroblast cells.[66] *In vitro* experiments revealed that the IC_{50} of donepezil on AChE activity present in the homogenate of the rat brain cortex is around 10^{-8} M,[4,71] which is somewhat less than suggested by our OD experiments. The differences can be explained, however, in terms of the methods used in the various studies. In *in vivo* animal studies, donepezil has been demonstrated to improve the working memory.[4,5]

The *in vivo* inhibitory effect of donepezil on AChE activity has also been investigated in the frontal cortex, the hippocampus, the striatum and the hypothalamus of the rat.[5] Biochemical studies suggested that the different doses of donepezil inhibited the AChE activity in the frontal cortex more markedly than that can be found in the striatum. Our histochemical results clearly demonstrate that the different neuronal elements (cell bodies and axonal processes) in the various brain regions are differently affected, even within the same region, such as the cortex, the hippocampus, the NBM and the striatum. This therefore provides firm morphological evidence that the cholinoceptive pyramidal neuronal perikarya are more sensitive than the cholinergic presynaptic axons in the cortex and the hippocampus of the rat to a given concentration of donepezil. In contrast, the neuronal cell bodies in the NBM, from where the cholinergic axons emanate to various areas of the cortex, are moderately resistant to donepezil inhibition. We found that the most resistant AChE-positive neuronal perikarya are located in the putamen, the NBM, the diagonal band of Broca and some cells in the hypothalamus. An alternative interpretation is that higher concentrations of donepezil are needed to inhibit AChE in basal forebrain neurons and the striatum because of their higher AChE activity. Via the AChE-inhibitory effect of donepezil in neuropharmacological experiments, a microdialysis technique has shown that oral administration of donepezil leads to an increase in the level of ACh in the cerebral cortex of rats.[33]

Inhibitory effect of donepezil on the cholinergic nerves innervating the blood vessels to the brain

It is well documented that the intra- and extracerebral blood vessels and capillaries are innervated not only with aminergic, but also with cholinergic nerve fibers, in both the human[13,14,24,68,74] and the rat brain.[21,36,58,60,70] The brain cortical blood flow is largely dependent on the normal function of cholinergic neurons located in the basal forebrain and projecting their axons to the cortex[36] (see also Refs 60 and 70). A dysfunction of these cholinergic neurons or their axon terminals innervating the blood vessels may therefore lead to pathology of the cortical microcirculation. Indeed, a disturbed cerebral blood flow has been demonstrated.[8,14,51,74] The abnormalities may be dependent on cerebral endothelial cells, profound irregularities in the course of the vessels,[69] thickening of the vascular basement membrane[23] and a reduction or loss of innervation in the cerebral microvasculature.[25] These factors may play significant roles in the dysfunction of the blood–brain barrier, in the cerebral microcirculation and in the pathogenesis of AD.[6,9,63]

Factors believed to stabilize or improve the blood circulation may result in an amelioration of the symptoms in AD. Alternatively, the modulation of the cholinergic neurotransmission may result in changes in memory performance in AD[13] patients. Indeed, if AChE inhibitors (e.g., donepezil) are used to reduce the AChE activity in the cholinergic nerves, it might be suspected that the ACh remaining in the

cholinergic nerves innervating the intra- and extracerebral blood vessels may regulate the blood circulation in AD more effectively than without treatment. In our histochemical experiments, the AChE activity was inhibited by 2×10^{-8} M donepezil, and totally abolished by 5×10^{-8} M donepezil. Application of this drug and/or other AChE inhibitors to ameliorate the blood circulation in the treatment of AD is therefore an important possibility.

Effect of donepezil on the rat neuromuscular junction

Both human and animal *in vivo* studies have demonstrated a peripheral effect of donepezil. The oral administration of donepezil inhibited the pectoral muscle cholinesterase activity in young rats in a dose-dependent manner.[32] Donepezil at or above 2.5 mg/kg caused fasciculation, a peripheral cholinergic sign of the activation of neuromuscular transmission.[33] In nerve–hemidiaphragm preparations, an intracellular recording technique revealed that the application of 1×10^{-9} M donepezil increased the amplitude, the time-to-peak and the half-decay time of miniature end-plate potentials.[37] In our *in vitro* experiments, the AChE activity in the neuromuscular junction was reduced by 2×10^{-8} M donepezil, suggesting a local effect of donepezil on the postsynaptic membrane of the neuromuscular junction. In human studies, muscle cramps were registered as a side-effect in patients receiving a high dose of donepezil (10 mg daily during a 24 week trial);[57] this could be attributed to the inhibition of AChE activity in the postsynaptic membrane folding at the neuromuscular junction. When the effects of donepezil on the cholinergic structures in the CNS and PNS are compared, however, the drug is observed histochemically to be more selective for the brain cholinoceptive neuronal perikarya than for the neuromuscular junction. In the cortex, the AChE positivity in the pyramidal cells can be abolished by 2×10^{-8} M donepezil, while at the neuromuscular junction a similar level of inhibition can be achieved only with 5×10^{-7} M. The results of this study reveal the importance of the regional, cellular and tissue specificity of the effects of donepezil on AChE activity.

Acknowledgements—We are grateful to Dr Z. Rakonczay for his generous help relating to the experiments. This work was supported by OTKA (T022683 and T032458), ETT (584/1996) and a Széchenyi Professorship to P.K.

REFERENCES

1. Atack J. R., Perry E. K., Bonham J. R., Perry R. H., Tomlinson B. E., Blessed G. and Fairbairn A. (1983) Molecular forms of acetylcholinesterase in senile dementia of Alzheimer type: selective loss of the intermediate (10S) form. *Neurosci. Lett.* **40**, 199–204.
2. Barner E. L. and Gray S. L. (1998) Donepezil use in Alzheimer disease. *Ann. Pharmacother.* **32**, 70–77.
3. Burns A., Rossor M., Hecker J., Gauthier S., Petit H., Moller H. J., Rogers S. L. and Friedhoff L. T. (1999) The effects of donepezil in Alzheimer's disease—results from a multinational trial. *Dement. Geriatr. Cogn. Disord.* **10**, 237–244.
4. Cheng D. H., Ren H. and Tang X. C. (1996) Huperzine A, a novel promising acetylcholinesterase inhibitor. *NeuroReport* **8**, 97–101.
5. Cheng D. H. and Tang X. C. (1998) Comparative studies of huperzine A, E2020, and tacrine on behaviour and cholinesterase activities. *Pharmac. Biochem. Behav.* **60**, 377–386.
6. Crawford J. G. (1998) Alzheimer's disease risk factors as related to cerebral blood flow: additional evidence. *Med. Hypotheses* **50**, 25–36.
7. Doody R. S. (1999) Clinical profile of donepezil in the treatment of Alzheimer's disease. *Gerontology* **45**, 23–32.
8. Eberling J. L., Jagust W. J., Reed B. R. and Baker M. G. (1992) Reduced temporal lobe blood flow in Alzheimer's disease. *Neurobiol. Aging* **13**, 483–491.
9. Esiri M. M., Nagy Z., Smith M. Z., Barnetson L. and Smith A. D. (1999) Cerebrovascular disease and threshold for dementia in the early stages of Alzheimer's disease. *Lancet* **354**, 919–920.
10. Evans M., Ellis A., Watson D. and Chowdhury T. (2000) Sustained cognitive improvement following treatment of Alzheimer's disease with donepezil. *Int. J. Geriatr. Psychiatry* **15**, 50–53.
11. Fishman E. B., Siek G. C., MacCallum R. D., Bird E. D., Volicer L. and Marquis J. K. (1986) Distribution of the molecular forms of acetylcholinesterase in human brain: alterations in dementia of the Alzheimer type. *Ann. Neurol.* **19**, 246–252.
12. Forette F. and Boller F. (1997) Trends in Alzheimer's disease treatment and prevention. In *Alzheimers Disease and Related Disorders* (eds Iqbal K., Swaab D. F., Winblad B. and Wisniewski H. M.). John Wiley and Sons, Chichester.
13. Furey M. L., Pietrini P., Haxby J. V., Alexander G. E., Lee H. C., VanMeter J., Grady C. L., Shetty U., Rapoport S. I., Schapiro M. B. and Freo U. (1997) Cholinergic stimulation alters performance and task-specific regional cerebral blood flow during working memory. *Proc. natn. Acad. Sci. USA* **94**, 6512–6516.
14. Geaney D. P., Soper N., Shepstone B. J. and Cowen P. J. (1990) Effect of central cholinergic stimulation on regional cerebral blood flow in Alzheimer disease. *Lancet* **335**, 1484–1487.
15. Geula C. and Mesulam M. M. (1989) Cortical cholinergic fibers in aging and Alzheimer's disease: a morphometric study. *Neuroscience* **33**, 469–481.
16. Geula C. and Mesulam M. M. (1989) Special properties of cholinesterases in the cerebral cortex of Alzheimer's disease. *Brain Res.* **498**, 185–189.
17. Geula C. and Mesulam M. M. (1996) Systematic regional variations in the loss of cortical cholinergic fibers in Alzheimer's disease. *Cereb. Cortex* **6**, 165–177.
18. Giacobini E. and Becker R. (1991) New cholinesterase inhibitors for treatment Alzheimer's disease. In *Alzheimer's Disease: Basic Mechanisms, Diagnosis and Therapeutic Strategies* (eds Iqbal K., McLachlan D. R. C., Winblad B. and Wisniewski H. M.). John Wiley and Sons, Chichester.
19. Giacobini E., Zhu X. D., Williams E. and Sherman K. A. (1996) The effect of the selective reversible acetylcholinesterase inhibitor E2020 on extracellular acetylcholine and biogenic amine levels in rat cortex. *Neuropharmacology* **35**, 205–211.
20. Greenberg S. M., Tennis M. K., Brown L. B., Gomez-Isla T., Hayden D. L., Schoenfeld D. A., Walsh K. L., Corwin C., Daffner K. R., Friedman P., Meadows M. E., Sperling R. A. and Growdon J. H. (2000) Donepezil therapy in clinical practice: a randomized crossover study. *Arch. Neurol.* **57**, 94–99.
21. Itakura T., Yamamoto K., Tohyama M. and Shimizu N. (1977) Central dual innervation of arterioles and capillaries in the brain. *Stroke* **8**, 360–365.
22. Jacobsen F. M. and Comas D. L. (1999) Donepezil for psychotropic-induced memory loss. *J. clin. Psychiatry* **60**, 698–704.
23. Kalaria R. N. (1992) The blood–brain barrier and cerebral microcirculation in Alzheimer disease. *Cerebrovasc. Brain Metab. Rev.* **4**, 226–260.
24. Kalaria R. N. (1996) Cerebral vessels in ageing and Alzheimer's disease. *Pharmac. Ther.* **72**, 193–214.
25. Kalaria R. N. and Ballard C. (1999) Overlap between pathology of Alzheimer disease and vascular dementia. *Alzheimer Dis. Assoc. Disord.* **13**, 115–123.
26. Kasa P. and Csillik B. (1966) Electron microscopic localization of cholinesterase by a copper-lead-thiocholine technique. *J. Neurochem.* **13**, 1345–1349.
27. Kasa P. and Rakonczay Z. (1982) Histochemical and biochemical demonstration of the molecular forms of acetylcholinesterase in peripheral nerve of rat. *Acta histochem.* **70**, 244–257.
28. Kasa P. (1986) The cholinergic systems in brain and spinal cord. *Prog. Neurobiol.* **26**, 211–272.
29. Kasa P., Karcsu S., Kovacs I. and Wolff J. R. (1996) Cholinoceptive neurons without acetylcholinesterase activity and enzyme-positive neurons without cholinergic synaptic innervation are present in the main olfactory bulb of adult rat. *Neuroscience* **73**, 831–844.
30. Kasa P., Rakonczay Z. and Gulya K. (1997) The cholinergic system in Alzheimer's disease. *Prog. Neurobiol.* **52**, 511–535.

31. Kosasa T., Kuriya Y., Matsui K. and Yamanishi Y. (1999) Effect of donepezil hydrochloride (E2020) on basal concentration of extracellular acetylcholine in the hippocampus of rats. *Eur. J. Pharmac.* **380**, 101–107.
32. Kosasa T., Kuriya Y., Matsui K. and Yamanishi Y. (1999) Inhibitory effects of donepezil hydrochloride (E2020) on cholinesterase activity in brain and peripheral tissues of young and aged rats. *Eur. J. Pharmac.* **386**, 7–13.
33. Kosasa T., Kuriya Y. and Yamanishi Y. (1999) Effect of donepezil hydrochloride (E2020) on extracellular acetylcholine concentration in the cerebral cortex of rats. *Jpn. J. Pharmac.* **81**, 216–222.
34. Kryger G., Silman I. and Sussman J. L. (1998) Three-dimensional structure of a complex of E2020 with acetylcholinesterase from *Torpedo californica*. *J. Physiol., Paris* **92**, 191–194.
35. de Lacalle S., Lim C., Sobreviela T., Mufson E. J., Hersh L. B. and Saper C. B. (1994) Cholinergic innervation in the human hippocampal formation including the entorhinal cortex. *J. comp. Neurol.* **345**, 321–344.
36. Lacombe P., Sercombe R., Vaucher E. and Seylaz J. (1997) Reduced cortical vasodilatory response to stimulation of the nucleus basalis of Meynert in the aged rat and evidence for a control of the cerebral circulation. *Ann. N.Y. Acad. Sci.* **826**, 410–415.
37. Lin J. H., Hu G. Y. and Tang X. C. (1997) Comparison between huperzine A, tacrine, and E2020 on cholinergic transmission at mouse neuromuscular junction in vitro. *Acta pharmac. sin.* **18**, 6–10.
38. Mayeux R. (1990) Therapeutic strategies in Alzheimer's disease. *Neurology* **40**, 175–180.
39. McGleenon B. M., Dynan K. B. and Passmore A. P. (1999) Acetylcholinesterase inhibitors in Alzheimer's disease. *Br. J. clin. Pharmac.* **48**, 471–480.
40. Mesulam M. M. and Geula C. (1988) Nucleus basalis (Ch4) and cortical cholinergic innervation in the human brain: observations based on the distribution of acetylcholinesterase and choline acetyltransferase. *J. comp. Neurol.* **275**, 216–240.
41. Mesulam M. M. and Geula C. (1992) Overlap between acetylcholinesterase-rich and choline acetyltransferase-positive (cholinergic) axons in human cerebral cortex. *Brain Res.* **577**, 112–120.
42. Mesulam M. M., Geula C. and Morán A. (1987) Anatomy of cholinesterase inhibition in Alzheimer's disease: effect of physostigmine and tetrahydroaminoacridine on plaques and tangles. *Ann. Neurol.* **22**, 683–691.
43. Mesulam M. M., Hersh L. B., Mash D. C. and Geula C. (1992) Differential cholinergic innervation within functional subdivisions of the human cerebral cortex: a choline acetyltransferase study. *J. comp. Neurol.* **318**, 316–328.
44. Mimori Y., Nakamura S. and Yukawa M. (1997) Abnormalities of acetylcholinesterase in Alzheimer's disease with special reference to effect of acetylcholinesterase inhibitor. *Behav. Brain Res.* **83**, 25–30.
45. Misson J. and Kendall M. J. (1997) Therapeutic advances: donepezil for the treatment of Alzheimer's disease. *J. clin. Pharmac. Ther.* **22**, 251–255.
46. Nagy Z., Esiri M. M., Joachim C., Jobst K. A., Morris J. H., King E. M., Hindley N. J., McDonald B., Litchfield S., Barnetson L. and Smith A. D. (1998) Comparison of pathological diagnostic criteria for Alzheimer's disease. *Alzheimer Dis. Assoc. Disord.* **12**, 182–189.
47. Nagy Z., Hindley N. J., Braak H., Braak E., Yilmazer-Hanke D. M., Schultz C., Barnetson L., King E. M., Jobst K. A. and Smith A. D. (1999) The progression of Alzheimer's disease from limbic regions to the neocortex: clinical, radiological and pathological relationships. *Dement. geriatr. cogn. Disord.* **10**, 115–120.
48. Nochi S., Asakawa N. and Sato T. (1995) Kinetic study on the inhibition of acetylcholinesterase by 1-benzyl-4-[5,6-dimethoxy-1-indanon)-2-yl]methylpiperidine hydrochloride (E2020). *Biol. Pharmac. Bull.* **18**, 1145–1147.
49. Ohnishi A., Mihara M., Kamakura H., Tomono Y., Hasegawa J., Yamazaki K., Morishita N. and Tanaka T. (1993) Comparison of the pharmacokinetics of E2020, a new compound for Alzheimer's disease, in healthy young and elderly subjects. *J. clin. Pharmac.* **33**, 1086–1091.
50. Paxinos G. and Watson C. (1982) *The Rat Brain in Stereotaxic Coordinates*. Academic Press, New York.
51. Postiglione A., Lassen N. A. and Holman B. L. (1993) Cerebral blood flow in patients with dementia of Alzheimer's type. *Aging* **5**, 19–26.
52. Rakonczay Z. and Kovacs I. (1998) Cholinesterases in Alzheimer's disease and cholinesterase inhibitors in Alzheimer's therapy. *Acta biol. hung.* **49**, 55–70.
53. Rakonczay Z., Torok I. and Kasa P. (1999) Preferential inhibition of acetylcholinesterase molecular forms in normal human brain. *Neurobiology* **7**, 75–77.
54. Ransmayr G., Cervera P., Hirsch E., Ruberg M., Hersh L. B., Duyckaerts C., Hauw J. J., Delumeau C. and Agid Y. (1989) Choline acetyltransferase-like immunoreactivity in the hippocampal formation of control subjects and patients with Alzheimer's disease. *Neuroscience* **32**, 701–714.
55. Rogers S. L. (1998) Perspectives in the management of Alzheimer's disease: clinical profile of donepezil. *Dement. geriatr. cogn. Disord.* **9**, 29–42.
56. Rogers S. L., Doody R. S., Mohs R. C. and Friedhoff L. T. (1998) Donepezil improves cognition and global function in Alzheimer disease: a 15-week, double-blind, placebo-controlled study. Donepezil Study Group. *Arch. intern. Med.* **158**, 1021–1031.
57. Rogers S. L., Farlow M. R., Doody R. S., Mohs R. and Friedhoff L. T. (1998) A 24-week, double-blind, placebo-controlled trial of donepezil in patients with Alzheimer's disease. Donepezil Study Group. *Neurology* **50**, 136–145.
58. Saito A., Wu J. Y. and Lee T. J. (1985) Evidence for the presence of cholinergic nerves in cerebral arteries: an immunohistochemical demonstration of choline acetyltransferase. *J. cerebr. Blood Flow Metab.* **5**, 327–334.
59. Saper C. B. (1990) Cholinergic system. In *The Human Nervous System* (ed. Paxinos G.). Academic Press, New York.
60. Sato A. and Sato Y. (1992) Regulation of regional cerebral blood flow by cholinergic fibers originating in the basal forebrain. *Neurosci. Res.* **14**, 242–274.
61. Schätz C. R., Geula C. and Mesulam M. (1990) Competitive substrate inhibition in the histochemistry of cholinesterase activity in Alzheimer's disease. *Neurosci. Lett.* **117**, 56–61.
62. Shunting E. Y. and Uchida K. M. (1997) Donepezil: an anticholinesterase inhibitor for Alzheimer's disease. *Am. J. Health-System Pharmacy* **54**, 2805–2810.
63. Skoog I., Kalaria R. N. and Breteler M. M. (1999) Vascular factors and Alzheimer disease. *Alzheimer Dis. Assoc. Disord.* **13**, 106–114.
64. Smith A. D., Jobst K. A., Navaratnam D. S., Shen Z. X., Priddle J. D., McDonald B., King E. and Esiri M. M. (1991) Anomalous acetylcholinesterase in lumbar CSF in Alzheimer's disease. *Lancet* **338**, 1538.
65. Sramek J. J. and Cutler N. R. (1999) Recent developments in the drug treatment of Alzheimer's disease. *Drugs Aging* **14**, 359–373.
66. Svensson A-L. and Nordberg A. (1997) Interaction of tacrine, galanthamine, NXX-066 and E2020 with neuronal α4β2 nicotinic receptors expressed in fibroblast cells. In *Alzheimer's Disease: Biology, Diagnosis and Therapeutics* (eds Iqbal K., Winblad B., Nishimura T., Takeda M. and Wisniewski H. M.). John Wiley and Sons, Chichester.
67. Tago H., Kimura H. and Maeda T. (1986) Visualization of detailed acetylcholinesterase fiber and neuron staining in rat brain by a sensitive histochemical procedure. *J. Histochem. Cytochem.* **34**, 1431–1438.
68. Tong X. K. and Hamel E. (1999) Regional cholinergic denervation of cortical microvessels and nitric oxide synthase-containing neuron in Alzheimer's disease. *Neuroscience* **92**, 163–175.
69. de la Torre J. C. (1997) Hemodynamic consequences of deformed microvessels in the brain in Alzheimer's disease. *Ann. N.Y. Acad. Sci.* **826**, 75–91.
70. Vaucher E. and Hamel E. (1995) Cholinergic basal forebrain neurons project to cortical microvessels in the rat: electron microscopic study with anterogradely transported *Phaseolus vulgaris* leucoagglutinin and choline acetyltransferase immunocytochemistry. *J. Neurosci.* **15**, 7427–7441.
71. Wang X. D., Chen X. Q., Yang H. H. and Hu G. Y. (1999) Comparison of the effects of cholinesterase inhibitors on [3H]MK-801 binding in rat cerebral cortex. *Neurosci. Lett.* **272**, 21–24.
72. Weinstock M. (1995) The pharmacotherapy of Alzheimer's disease based on the cholinergic hypothesis: an update. *Neurodegeneration* **4**, 349–356.
73. Wilkinson D. (1998) Clinical experience with donepezil (Aricept) in the UK. *J. neural. Transm.* **54**, Suppl., 311–315.
74. Wilson K., Bowen D., Francis P. and Tyrrell P. (1991) Effect of central cholinergic stimulation on regional cerebral blood flow in Alzheimer's disease. *Br. J. Psychiatry* **158**, 558–562.

(*Accepted* 2 *July* 2000)

II

ELSEVIER

Neuroscience Letters 278 (2000) 117–119

Neuroscience Letters

www.elsevier.com/locate/neulet

Human amyloid-β1–42 applied in vivo inhibits the fast axonal transport of proteins in the sciatic nerve of rat

Peter Kasa[a,*], Henrietta Papp[a], Imre Kovacs[a], Monika Forgon[a], Botond Penke[b], Haruyasu Yamaguchi[c]

[a]Alzheimer's Disease Research Centre, Albert Szent-Györgyi Medical University, Somogyi B. ut 4, H-6720 Szeged, Hungary
[b]Department of Medical Chemistry, Albert Szent-Györgyi Medical University, H-6720 Szeged, Hungary
[c]College of Medical Care and Technology, Gunma University, Gunma 371, Japan

Received 23 June 1999; accepted 18 October 1999

Abstract

Human amyloid-β1–42 has been suggested to be a pathogenetic factor in Alzheimer's disease. The precise mechanism by which this peptide causes the degeneration of neurons in the affected brain is not yet fully understood. By using immunohistochemistry we explored the inhibitory effects of human amyloid-β1–42 applied in vivo on the fast axonal transport of acetylcholinesterase, the amyloid precursor protein, the vesicular acetylcholine transporter and synaptophysin in the sciatic nerve of rat. Our findings provide evidence for the in vivo neurotoxic effect of human amyloid-β peptide.

Keywords: Alzheimer's disease; Amyloid; Axonal transport; Immunohistochemistry; Neurotoxicity; Sciatic nerve

Characteristic neuropathological features of Alzheimer's disease (AD) include the cerebral deposition of human amyloid-β1–42 (Aβ1–42) in the senile plaques and the degeneration of cholinergic nerve cells (see Ref. [9] for a review). The disease is characterized by a neuronal dysfunction in which the microtubule-associated tau-protein is abnormally hyperphosphorylated, which in turn may cause a disruption of the microtubule network and affect the axonal transport. If this suggestion is correct, it may be assumed that substances that are rapidly transported axonally should accumulate in the axon after Aβ treatment. It was earlier demonstrated that proteins, including acetylcholinesterase (AChE) [6], amyloid precursor protein (APP) [10], synaptophysin (SYN) [3] and vesicular acetylcholine transporter (VAChT) [11], accumulate in damaged nerves and are good markers of axonal lesions. There has been no previous report of the in vivo effects of human Aβ1–42 on the axonal transport of these proteins. We therefore used membrane-bound proteins to demonstrate the neurotoxic effects of Aβ1–42 on axonal transport.

Adult male Sprague–Dawley rats (250–300 g) were anaesthetized and 1.0 μl human Aβ1–42 (20 μM) freshly solubilized solution [12] was injected under the epineurium of the left sciatic nerve. The right sciatic nerve served as control and was injected with the Aβ solution vehicle. Experiments were carried out under a protocol approved by the Animal Research Committee of the Albert Szent-Györgyi Medical University (No. 2/19/2).

One day postinjection, control and Aβ1–42-injected nerves were dissected out and fixed by immersion for 12 h in 4% paraformaldehyde solution. Twenty micrometers thick longitudinal sections were cut on a freezing microtome. AChE histochemistry was performed as described earlier [7]. For immunohistochemistry, the free-floating sections were incubated either in 1:2000 diluted anti-APP A4 serum (Mab 22C11, Boehringer) or in 1:64 000 diluted polyclonal goat anti-VAChT serum (Ab1578, Chemicon) or in 1:1000 diluted monoclonal anti-synaptophysin antibody (clone SY 38, Boehringer). For the detection of Aβ positivity, the sections were incubated in 1:16 000 diluted polyclonal rabbit anti-Aβ serum raised against a synthetic peptide consisting of residues 1–28 of Aβ (G42CL). The reaction end-products of histochemistry and of immunohistochemistry were visualized with a solution of 0.05% 3,3′-diaminobenzidine tetrahydrochloride (Sigma) as chromogen and intensified by nickel chloride. To exclude the mechanical damaging effect of oedema that may occur in

* Corresponding author. Tel.: +36-62-454-569; fax: +36-62-454-569.
E-mail address: kp@comser.szote.u-szeged.hu (P. Kasa)

0304-3940/00/$ - see front matter
PII: S0304-3940(99)00863-0

the injected area, the weights of the excised samples were measured.

In general, the results demonstrated that exogenously applied human Aβ1–42 can disturb the axonal transport of AChE, APP, VAChT and SYN in the sciatic nerve of rat. The accumulation of immunoreactivities was restricted to the area where Aβ1–42 was present.

In detail, Aβ staining could not be detected in the control nerve trunk of rat (Fig. 1A). After application of the human Aβ1–42, however, a dark staining could be observed at the injection site among the myelinated axons (Fig. 1B) and at the node of Ranvier (Fig. 1C,D). In control sciatic nerve, AChE staining was demonstrated in the cholinergic axons as described earlier [6] (Fig. 1E). In the nerve trunk treated with Aβ1–42 for 24 h, a considerable accumulation of AChE occurred at the injected site (Fig. 1F,G).

In the control sciatic nerve, no immunohistochemical staining of APP, VAChT and SYN could be observed. 24 h after the injection of Aβ1–42, the APP (Fig. 1H), the VAChT (Fig. 1I) and the SYN (Fig. 1J) reaction was present

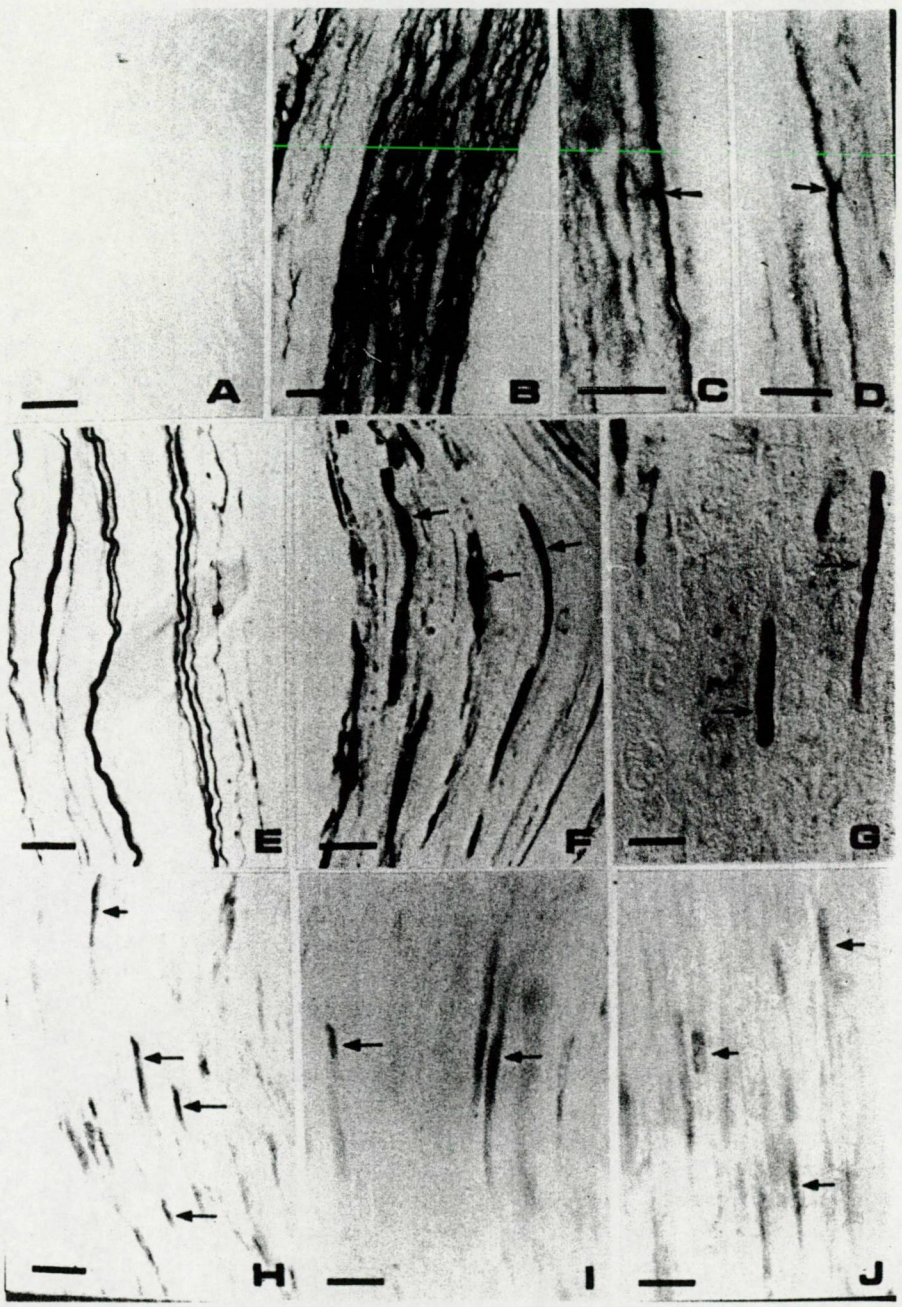

Fig. 1. Effects of Aβ1–42 on the transport of AChE, APP, VAChT and SYN in the sciatic nerve of rat. Aβ staining can not be observed in the control samples (A). After in vivo application Aβ1–42 is present among the myelinated axons (B) and at the node of Ranvier (arrow, C,D). The reaction end-product of AChE is revealed in the control samples (E). 24 h after Aβ1–42 treatment, high accumulations of AChE (arrows, F,G), APP (arrows, H), VAChT (arrows, I) and SYN (arrows, J) are visible in the axons. Scale bars, 30 μm.

in the axonal swellings, indicating local axonal injuries. No oedema developed in the vehicle-injected and Aβ1–42-treated samples. The weights of the excised samples did not vary significantly (vehicle-injected: 5.692 (0.641, SD ($n = 3$) mg; Aβ1–42-injected: 5.809 (0.708, SD ($n = 3$) mg, $P > 0.5$).

The mechanism whereby Aβ can block the fast axonal transport of AChE, APP, VAChT and SYN is not clear at present. Several hypotheses have been put forward to explain the neurotoxic effect of Aβ. It has been amply demonstrated that the aggregated and soluble forms of the peptide are very harmful to neurons and endothelial cells both in vitro and in vivo [2,4,5,8,13,14]. Extracellularly applied Aβ was internalized selectively by hippocampal CA1 neurons [1] and caused the accumulation of amyloidogenic carboxy terminal fragments of APP. In our experiments, the immunohistochemical localization of the injected peptide suggests that it could be internalized into the axoplasm at the nodes of Ranvier. If this is the case, Aβ may inhibit the transport inside the axon by affecting dynein, the dynactin complex [17] and the kinesin system [15], which is known to be responsible for the fast axonal transport. When Aβ is applied exogenously, the accumulation of APP is regulated by tau-protein kinase I/glycogen synthase kinase-3β, resulting in an impairment of axonal transport and in the cytoplasmic accumulation of APP [16].

The results of this study support the suggestion that AD may be initiated by a failure in axonal transport, which is followed by neuronal degeneration.

This work was supported by OTKA (T022683), ETT (584/1996) and a Széchenyi Professorship to P.K.

[1] Bahr, A., Hoffman, K.B., Yang, A.J., Hess, U.S., Glabe, C.G. and Lynch, G., Amyloid β protein is internalized selectively by hippocampal field CA1 and causes neurons to accumulate amyloidogenic carboxyterminal fragments of the amyloid precursor protein. J. Comp. Neurol., 397 (1998) 139–147.

[2] Crawford, F., Suo, Z., Fang, C., Sawar, A., Su, G., Arendash, G. and Mullan, M., The vasoactivity of A beta peptides. Ann. Acad. Sci. N.Y., 826 (1997) 35–46.

[3] Dahlström, A.B., Czernik, A.J. and Li, J.-Y., Organelles in fast axonal transport. What molecules do they carry in anterograde versus retrograde directions, as observed in mammalian systems? Mol. Neurobiol., 6 (1992) 157–177.

[4] Forloni, G., Lucca, E., Angeretti, N., Della Torre, P. and Salmona, M., Amidation of beta-amyloid peptide strongly reduced the amyloidogenic activity without alteration of the neurotoxicity. J. Neurochem., 69 (1997) 2048–2054.

[5] Giovanelli, L., Scali, C., Faussone-Pellegrini, M.S., Pepeu, G. and Casamenti, F., Long-term changes in the aggregation state and toxic effects of beta-amyloid injected into the rat brain. Neuroscience, 87 (1998) 349–357.

[6] Kasa, P., Acetylcholinesterase transport in the central and peripheral nervous tissue: the role of tubules in the enzyme transport. Nature, 218 (1968) 1265–1267.

[7] Kasa, P., Karcsu, S., Kovacs, I. and Wolff, J.R., Cholinoceptive neurons without acetylcholinesterase activity and enzyme-positive neurons without cholinergic synaptic innervation are present in the main olfactory bulb of adult rat. Neuroscience, 73 (1996) 831–844.

[8] Kasa, P., Pákáski, M. and Penke, B., Synthetic human beta-amyloid has selective vulnerable effects on different types of neurons. In M. Nicolini, P.F. Zatta and B. Corani (Eds.), Alzheimer's Disease and Related Disorders, Pergamon, Oxford, 1993, pp. 311–312.

[9] Kasa, P., Rakonczay, Z. and Gulya, K., The cholinergic system in Alzheimer's disease. Prog. Neurobiol., 52 (1997) 511–535.

[10] Koo, E.H., Sisodia, S.S., Archer, D.R., Martin, J.L., Weidemann, A., Beyreuther, K., Fischer, P., Masters, C.L. and Price, D.L., Precursor of amyloid protein in Alzheimer disease undergoes fast anterograde axonal transport. Proc. Natl. Acad. Sci. USA, 87 (1990) 1561–1565.

[11] Li, J.-Y., Dahlström, A.-M., Hersh, L.B. and Dahlström, A., Fast axonal transport of the vesicular acetylcholine transporter (VAChT) in cholinergic neurons in the rat sciatic nerve. Neurochem. Int., 32 (1998) 457–467.

[12] Pákáski, M., Farkas, Z., Kasa Jr., P., Forgon, M., Papp, H., Zarandi, M., Penke, B. and Kasa Sr, P., Vulnerability of small GABAergic neurons to human β-amyloid pentapeptide. Brain Res., 796 (1998) 239–246.

[13] Pákáski, M., Papp, H., Forgon, M., Kasa Jr., P. and Penke, B., Effects of beta-amyloid on cholinergic, cholinoceptive and GABAergic neurons. Acta Biol. Hung., 49 (1998) 43–54.

[14] Seilheimer, B., Bohrmann, B., Bondolfi, L., Müller, F., Stüber, D. and Döbeli, H., The toxicity of the Alzheimer's peptide correlates with a distinct fiber morphology. J. Struct. Biol., 119 (1997) 59–71.

[15] Stenoien, D.L. and Brady, S.T., Immunochemical analysis of kinesin light chain function. Mol. Biol. Cell., 8 (1997) 675–689.

[16] Takashima, A., Yamaguchi, H., Noguchi, K., Michel, G., Ishiguro, K., Sato, K., Hoshino, T., Hoshi, M. and Imahori, K., Amyloid β peptide induces cytoplasmic accumulation of amyloid protein precursor via tau protein kinase I/glycogen synthase kinase-3β in rat hippocampal neurons. Neurosci. Lett., 198 (1995) 83–86.

[17] Waterman-Storer, C.M., Karki, S.B., Kuznetsov, S.A., Tabb, J.S., Weiss, D.G., Langford, G.M. and Holzbaur, E.L., The interaction between cytoplasmic dynein and dynactin is required for fast axonal transport. Proc. Natl. Acad. Sci. USA, 94 (1997) 12180–12185.

III

ELSEVIER

Brain Research 909 (2001) 159–169

BRAIN RESEARCH

www.elsevier.com/locate/bres

Research report

Presenilin-1 and its N-terminal and C-terminal fragments are transported in the sciatic nerve of rat

Peter Kasa*, Henrietta Papp, Magdolna Pakaski

Alzheimer's Disease Research Centre, Department of Psychiatry, University of Szeged, Somogyi B. ut 4, H-6720 Szeged, Hungary

Accepted 22 May 2001

Abstract

The axonal transport of presenilin-1 was investigated in a spinal cord–sciatic nerve–neuromuscular junction model system in the rat. The technique of unilateral sciatic nerve ligation, using double ligatures, was combined with immunohistochemical staining and Western blotting to examine the axonal transport of the protein. Immunohistochemical studies involving the use of polyclonal antibodies for either the N-terminal or the C-terminal domain of presenilin-1 furnished evidence that both fragments may be present not only in the neuronal cell bodies, but also in the motoric and sensory axons and the motoric axon terminals at the neuromuscular junctions. After double ligation of the sciatic nerve for 6, 12 or 24 h, progressive immunostaining of presenilin-1 occurred above the upper ligature and to a lesser extent below the lower ligature. Double staining of the sciatic nerve for presenilin-1 and for amyloid precursor protein revealed overlapping immunoreactivity. Western blotting confirmed the accumulation of the ~20-kDa C-terminal and ~25-kDa N-terminal fragments and the full-length 45-kDa holoprotein of presenilin-1 both above and below the ligature. It is concluded that besides the larger amounts of C-terminal and N-terminal fragments, a smaller quantity of intact presenilin-1 may be present and conveyed bidirectionally in the sciatic nerve of the rat. These results lend further support to the suggestion that presenilin-1 may leave the *trans*-Golgi network and be found in the axons and axon terminals of the various neurons.

Theme: Disorders of the nervous system

Topic: Degenerative disease: Alzheimer's — beta-amyloid

Keywords: Alzheimer's disease; Axonal transport; Immunohistochemistry; Presenilin-1; Sciatic nerve; Western blot

1. Introduction

Molecular genetic studies [41] have demonstrated that mutations of presenilin genes (PS-1 and PS-2), and in particular PS-1, are associated with a majority of the early-onset cases of familial Alzheimer's disease (AD). PS-1 has been localized in senile plaques [4,9,16,47], but see Ref. [46], and neurofibrillary tangles [4,16] in the brain of AD individuals. In the brain and in vitro tissue cultures, PS-1 has been found in the cell bodies, where it is associated with the perinuclear envelope, the endoplasmic reticulum and the *trans*-Golgi network [2,7,9,26,29]. In some studies, it has been concluded that PS-1 can not be found beyond the Golgi network (e.g. in the axons) [2,6]. In contrast, other authors have demonstrated PS-1 in the axons [10,12,27,29,34,40] and the axon terminals [4]. Ray et al. [36] found that PS-1 may reach the plasma membrane, while Beher et al. [3] provided evidence that fragments of PS-1 are present in synaptic plasma membranes. They suggested that PS-1 may exit from the cell body and reach the synaptic organelles. The transport of PS-1 fragments in neuritic processes has also been postulated [4], but there is no direct morphological evidence for the axonal transport of PS-1. The existence of PSs in the axons is therefore debated and further evidence is needed to clarify this question. Our aim in the present work was to study the axonal localization and axonal transport of PS-1 by immunohistochemical means. Western blot analysis was applied for a semiquantitative demonstration of translocated PS-1 in the double-ligated sciatic nerve of the rat. The axonal presence and transport of PS-1 were

*Corresponding author. Tel./fax: +36-62-544-569.
E-mail address: kp@comser.szote.u-szeged.hu (P. Kasa).

0006-8993/01/$ – see front matter
PII: S0006-8993(01)02679-8

compared with those of the amyloid precursor protein (APP) and acetylcholinesterase (AChE), substances which are well documented in the different types of axons.

2. Materials and methods

The University Committee for the Care of Experimental Animals approved all experimental procedures. The experiments were performed in accordance with the ethical guidelines for animal investigations of the Hungarian Ministry of Welfare and in accordance with the European Communities Council Directive (24 November 1986; 86/609/EEC). Efforts were made to minimize animal suffering and the number of animals used. After surgery, the animals were kept in cages separately under a 12-h light/dark cycle, with lights on at 06:00 h; food and water were freely available.

2.1. Materials

The substances used in this study were acetylthiocholine iodide, bioMax light autoradiographic film, ethopropazine.HCl, ethylenediaminetetraacetic acid (EDTA), 3,3'-diaminobenzidine tetrahydrochloride (DAB), horseradish peroxidase (HRP)-conjugated anti-mouse IgG, leupeptin, phenylmethanesulfonyl fluoride (PMSF) and pepstatin A, all from Sigma–Aldrich (St. Louis, MO, USA); anti-Alzheimer precursor protein A4 (Mab 22C11) from Boehringer (Mannheim, Germany); polyclonal (AB1575 and AB5308) anti-PS-1 from Chemicon International Inc. (Temecula, CA, USA); HMW-SDS marker kit, LMW-SDS marker kit and Hybond ECL nitrocellulose membrane from Amersham Pharmacia Biotech (Buckinghamshire, UK); Supersignal Western blot chemiluminescence reagent from Pierce (Rockford, IL, USA); sodium dodecylsulfate (SDS) and paraformaldehyde from Merck KgaA (Darmstadt, Germany); biotin-SP-conjugated sheep anti-mouse IgG, biotin-SP-conjugated goat anti-rabbit IgG, biotin-SP-conjugated rabbit anti-goat IgG, HRP-conjugated anti-rabbit IgG and HRP-conjugated streptavidin from Jackson (West Grove, PA, USA); DPX histological mountant from Fluka Chemie AG, (Buchs, Germany); and Histoclear II and Histomount from National Diagnostics (Atlanta, GA, USA). All other reagents were of either laboratory or analytical grade from various suppliers.

2.2. Animals

Adult male Sprague–Dawley rats (4–5 months old, 400–450 g) were used in this study. The animals were anaesthetized with a cocktail of ketamine (70 mg/kg) and xylazine (10 mg/kg), administered intraperitoneally. The left sciatic nerve of the rat was exposed and ligated distally to the obturator internus muscle, using black silk thread. To visualize and quantify the anterograde and retrograde transport of the C-terminal and N-terminal fragments, full-length PS-1 and the holoprotein of APP, a double-ligation procedure was applied. The right sciatic nerve was also exposed and a silk thread was placed loose around the nerve in the same location in the sham controls. The rats were allowed to recover for 6, 12 or 24 h prior to sacrifice. The ligated left sciatic nerve was removed; this contained a 4-mm segment above the proximal ligature, a 4-mm middle segment, and a 4-mm segment below the distal ligature. Nerve segments that were similar in size were excised from the sham-operated animals.

2.3. Tissue preparation for immunohistochemical and histochemical investigations

After different time intervals, the rats were anaesthetized with diethyl ether and perfused transcardially (200 ml) for 30 min with cold (4°C) 4% paraformaldehyde solution (freshly prepared from paraformaldehyde powder), buffered with 0.1 M Na-phosphate (pH 7.4). A segment of the spinal cord (lumbar intumescentia), the spinal ganglia (L5 and L6), sensory axons distal to the L5–L6 spinal ganglia, the sciatic nerve from control and ligated animals and the abductor digiti quinti of the plantar muscle from the control leg were immediately removed and immersed overnight in a similar fixative at 4°C. After cryoprotection for 24 h in 30% sucrose solution, the spinal cord, the sensory ganglia and the muscle samples were cut at 24 μm on a freezing microtome, while the sciatic and sensory nerves were cut at a thickness of 15 μm on a cryostat. The spinal cord, the spinal ganglia and the muscle samples were collected in ice-cold 0.1 M phosphate-buffered saline (PBS) (pH 7.4) and processed as free-floating sections, while the cryostat sections were mounted on glass slides for immunohistochemical and histochemical staining.

2.4. Immunohistochemistry for single and double-stained samples

The sections of the spinal cord, the L5 and L6 spinal ganglia, the control and the double-ligated sciatic nerves, the connecting sensory nerves and the muscle samples were soaked for 10 min in 3% H_2O_2, washed in PBS and treated with 0.1 M PBS containing 0.3% Triton X-100 for 20 min, and then with 0.1 M PBS containing 5% normal serum for 60 min. Separate sections were incubated with 0.1 M PBS containing one of the primary antibodies for 2 days at room temperature. This was followed by incubation in normal serum for 30 min, in biotin-SP-conjugated secondary antibody (1:500) for 90 min, and then in streptavidin–HRP (1:1000) for 90 min. The sections were washed twice in 0.1 M PBS for 10 min between sera. When single staining was applied, the peroxidase complex was visualized by incubating the sections with 0.05 M Tris–HCl (pH 7.6) containing 0.05% DAB, 0.1% $NiCl_2$ and 0.005% H_2O_2, resulting in a bluish-black colour.

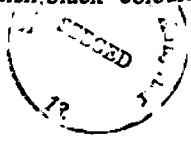

When double-stained sections were prepared (stained either for PS-1 and APP or for AChE and PS-1), the samples were developed first in DAB dissolved in 0.05 M Tris–HCl buffer. The staining resulted in a brownish colour. After this step, the samples were mounted on glass slides in 0.05 M Tris–HCl buffer and photos were taken from the areas where the brownish colour was detected. Thereafter, the sections were treated for 30 min with 0.6% H_2O_2 to eliminate the possibly persistent activity of the marker enzyme. In the case of PS-1, the second staining was for APP, while the histochemical reaction for AChE was followed by either PS-1 or APP immunohistochemistry. After staining for the second antibody, the peroxidase complex was visualized by incubating the sections in a DAB–$NiCl_2$ mixture. In these double-stained sections, a brownish colour could be detected in some axons; in some others, the brownish colour was intermingled with a bluish-black colour; and in yet other axons, the bluish-black staining appeared as a separate entity. In parallel incubations, the primary antibody was omitted, and the specificity of the immunoreactivity was tested. No immunostaining was observed in such samples. The sections were thereafter mounted, air-dried, dehydrated in an ethyl alcohol series, cleared in Histoclear, and finally coverslipped by using Histomount. Photos were taken under normal light field microscopy conditions (Nikon Microphot-FXA microscope).

2.5. Acetylcholinesterase histochemistry

To determine whether PS-1 and/or APP are localized in sensory and/or motoric fibres in the ligated sciatic nerves, AChE histochemical staining was performed. Sections from sensory nerves emanating from the spinal ganglia towards the spinal cord and the sciatic nerves were prepared as previously described [22,43]. Some of the sections which were double-stained for AChE and PS-1, or for AChE and APP, were mounted in 0.05 M Tris–HCl-covered glass slides after AChE staining, and the AChE reaction end-product was photographed for further documentation.

2.6. Preparation of the sciatic nerve for SDS–PAGE

The control and ligated sciatic nerves were removed after ligation for 6, 12 or 24 h. Segments 4 mm in length of the sciatic nerves of the sham-operated control animals, and 4-mm segments from above the proximal ligature, from between the two ligatures, and from below the distal ligature of the sciatic nerve were excised on ice and immediately placed into a buffer solution which contained 50 mM Tris–HCl buffer (pH 7.5), 150 mM NaCl, 2 mM EDTA, 2 mM PMSF, 2 μg/ml leupeptin, 1 μg/ml pepstatin and detergents (1% Nonidet-P-40 and 0.1% sodium deoxycholate). Thereafter, the samples were homogenized. As the amount of PS-1 in the sciatic nerve was expected to be low, samples from two animals were pooled for PS-1 isolation. After centrifugation (10 000×g for 1 h at 4°C), proteins in the supernatant solutions were measured by the method of Hess [14]. For analysis, 40 μg of protein was supplemented with Laemmli sample buffer and, after boiling for 5 min, loaded on 9.0% PAGE for electrophoresis [28].

2.7. Western blot analysis

To ascertain whether only the C-terminal and N-terminal fragments, or the holoprotein of PS-1, or all of these, are transported in the sciatic nerve of rat, we used various polyclonal antibodies: AB5308 for the detection of intact 45-kDa holoprotein and the C-terminal fragment [amino acids 275–367] and AB1575 to recognize the full-length and the N-terminal fragment [amino acids 14–33] of PS-1.

The separated proteins were transferred to nitrocellulose membranes by using the BioRad Mini-Protean II system. Membranes were blocked in 5% non-fat dry milk with 0.2% Tween-20 in 50 mM Tris-buffered saline (TBS) for 1 h at room temperature. For the labelling of the fragments and the holoprotein of PS-1, the antibodies were used in a dilution of 1:1000 in TBS containing 1% non-fat dry milk. The membranes were incubated with the different primary antibodies overnight at room temperature. After the membranes had been washed five times in TBS, the filters were incubated with HRP-conjugated goat anti-rabbit IgG (1:5000) or HRP-conjugated rabbit anti-goat IgG (1:5000) as secondary antibody for 1 h at room temperature, followed by washing as described above. Bound antibodies were detected with the Supersignal Western blot chemiluminescence reagent, and this was followed by exposure to an autoradiography film.

2.8. Quantitation of blots

Optical densities of immunoreactive bands were quantified by means of the NIH-Image program (NIH, USA). The intensity of the control band was taken as 100%, and changes were calculated with respect to this value. The reported data are the overall results of three different experiments. The error bar denotes the S.E. A probability level $P<0.05$ was taken to be statistically significant. Statistical evaluations were performed with Student's t-test.

3. Results

3.1. Immunohistochemical localization of presenilin-1 in the sciatic nerve and sensory axons

To investigate the morphological localization of PS-1 in the various tissue samples, both the N-terminal (AB1575)

and the C-terminal loop (AB5308) antibodies were used: they gave similar immunohistochemical staining. The immunoreactivity in the sciatic nerve was revealed in a discontinuous manner in the axons of the myelinated nerve fibres (Fig. 1A). Similar axonal staining was seen in the sensory axons (not documented) leaving the L5 and L6 dorsal root ganglia, and in a number of Schwann cells around the myelinated axons. No staining was present in the nerve samples from which the primary antibodies were omitted (Fig. 1B).

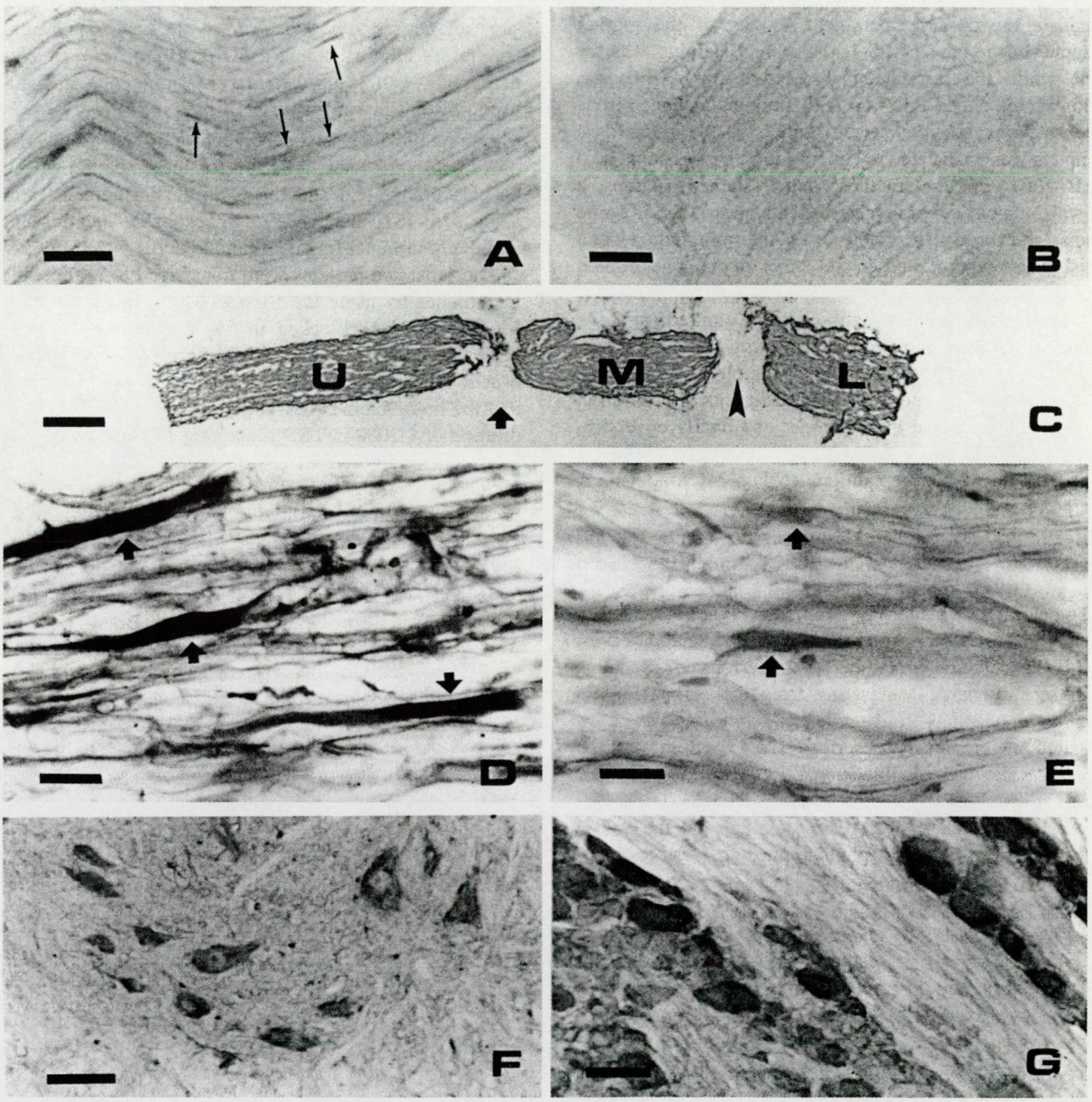

Fig. 1. Immunohistochemical demonstration of PS-1 in the various tissue samples, using AB1575 (A,C,E–G) and AB5308 (D) polyclonal antibodies. The two antibodies resulted in similar immunoreactivity. PS-1 staining appears in a discontinuous manner (arrows) in the axons of the control sciatic nerve bundle (A). No immunoreactivity was detected in the sciatic nerve samples without primary antibody (B). The arrangement of the double ligation on the sciatic nerve is demonstrated in C, where U indicates the segment above the proximal ligature (arrow), M the segment between the ligatures, and L the segment below the lower ligature (arrowhead). After 24 h of double ligation, a pronounced accumulation of PS-1 occurred above the proximal ligature (D, arrows). In the segment below the lower ligature, the staining for PS-1 was less expressed (E, arrows). PS-1 immunoreactivity occurred in the perikarya of the motoneurons (F) and the sensory nerve cell bodies of various sizes of the dorsal root ganglia (G). Scale bar=50 μm (A,B,F,G); 1.0 mm (C); 25 μm (D,E).

3.2. Immunohistochemical localization of presenilin-1 in the double-ligated sciatic nerve

To examine the bidirectional axonal transport of PS-1 or its fragments, a double-ligation technique was used (Fig. 1C). The sciatic nerve was ligated for 6, 12 or 24 h. The staining intensity was already increased after 6 h in the segments above the upper ligature and below the lower ligature. Between 6 and 24 h, however, the PS-1 staining gradually increased further only on the proximal side (Fig. 1D). After 6 h (Fig. 1E), the immunoreactivity did not increase further in the distal segment. Between the two ligatures, the immunostaining was observed only in the cytoplasm of the Schwann cells (not documented) after 24 h. When the N- or C-terminal fragment antibodies were used for the demonstration of PS-1, the motoric neurons in the ventral horn of the spinal cord (Fig. 1F) and the sensory ganglion cells (Fig. 1G) proved immunoreactive.

3.3. Immunohistochemical localization of presenilin-1 and histochemical demonstration of acetylcholinesterase in the double-ligated sciatic nerve

We next examined whether PS-1 is transported in the motoric, in the sensory or in both types of axons in the sciatic nerve. After 24 h, the double-ligated nerve was double-stained, first for AChE (brown colour) and then for PS-1 (bluish-black colour). In these samples, the two proteins appeared to be present in many axons, but separately within the same axon (Fig. 2A), both above and below the ligature. This staining pattern suggests that PS-1 and AChE are present in the motoric nerve. However, in other cases the brown (AChE) and the bluish-black (PS-1) staining reactions appeared in separate axons (Fig. 2B), suggesting that PS-1 may be present in the sensory axons too. In some other fibres the two colours appeared intermingled within the same axonal region. At higher magnification (Fig. 2C), the bluish-black end-product DAB–Ni appeared in dot-like structures within the region where the brownish DAB reaction product was present.

3.4. Immunohistochemical localization of amyloid precursor protein and histochemical demonstration of acetylcholinesterase in the double-ligated sciatic nerve

We have reported previously that AChE and APP are transported in the sciatic nerve of the rat [19,21,23]. It appeared necessary to answer the question of whether APP is conveyed similarly to PS-1 in the motoric and sensory axons, or whether they are transported in different axons. A double-staining technique revealed that, when the double-ligated sciatic nerve samples were incubated first for AChE activity, the brownish colour (due to the enzyme activity) appeared in some axons (Fig. 2D). When the same section was processed further to demonstrate the presence of APP (bluish-black colour), some of the axons proved to contain AChE only, some axons were double-labelled for AChE and APP, and in yet other axons only APP was present (Fig. 2E).

3.5. Immunohistochemical double-labelling for presenilin-1 and amyloid precursor protein in the double-ligated sciatic nerve

Since the PS-1 function is closely linked to γ-secretase activity for APP processing [8], we investigated the spatial relationships of these proteins in the sciatic nerve of the rat. The samples were incubated first for PS-1 and the reaction end-product was visualized with DAB. After photos of interesting areas had been taken, the sections were processed further for APP and the reaction end-product was intensified with Ni. This double-staining procedure revealed that those sites in the axons which reacted for PS-1 (Fig. 2F) were also positive for APP (Fig. 2G), suggesting that PS-1 and APP are either colocalized or there is an overlap of the staining for the two proteins.

3.6. Immunohistochemical demonstration of presenilin-1 and amyloid precursor protein in the presynaptic axon terminals at the neuromuscular junction

To demonstrate the sites of the destination of axonally transported fragments of PS-1, we compared the localization of PS-1 immunoreactivity with APP at the neuromuscular junction (NMJ) of the plantar muscle of the rat. In sections stained for APP, the axon varicosities appeared as discrete dots (Fig. 2H), but some immunoreactivity was diffuse. This latter staining could possibly be present in the postsynaptic membrane at the NMJ. When PS-1 was demonstrated in the muscle samples, similar well-discernible staining structures were revealed in the presynaptic axon terminals (Fig. 2I). To reveal the precise sites of these proteins, some of the sections were double-stained first for AChE (brown) and thereafter for PS-1 (bluish-black). In this case, the PS-1 reaction end-product was clearly visible within the NMJ, where the AChE histochemical staining was present (Fig. 2J,K).

3.7. Western blot detection of the accumulation of presenilin-1 in the double-ligated sciatic nerve

To validate the immunohistochemical results, the Western blot technique was used to detect the presence and the accumulation of the N- and C-terminal fragments and the full-length protein of PS-1 in a sciatic nerve which was double-ligated for 6, 12 or 24 h. The N-terminal of PS-1 was investigated with a polyclonal antibody (AB1575) directed against residues 14–33, while the C-terminal and the intact protein of PS-1 were demonstrated with an antibody (AB5308) directed against residues 275–367 of the PS-1 C-terminal loop region. The results of this technique accord well with the immunohistochemical

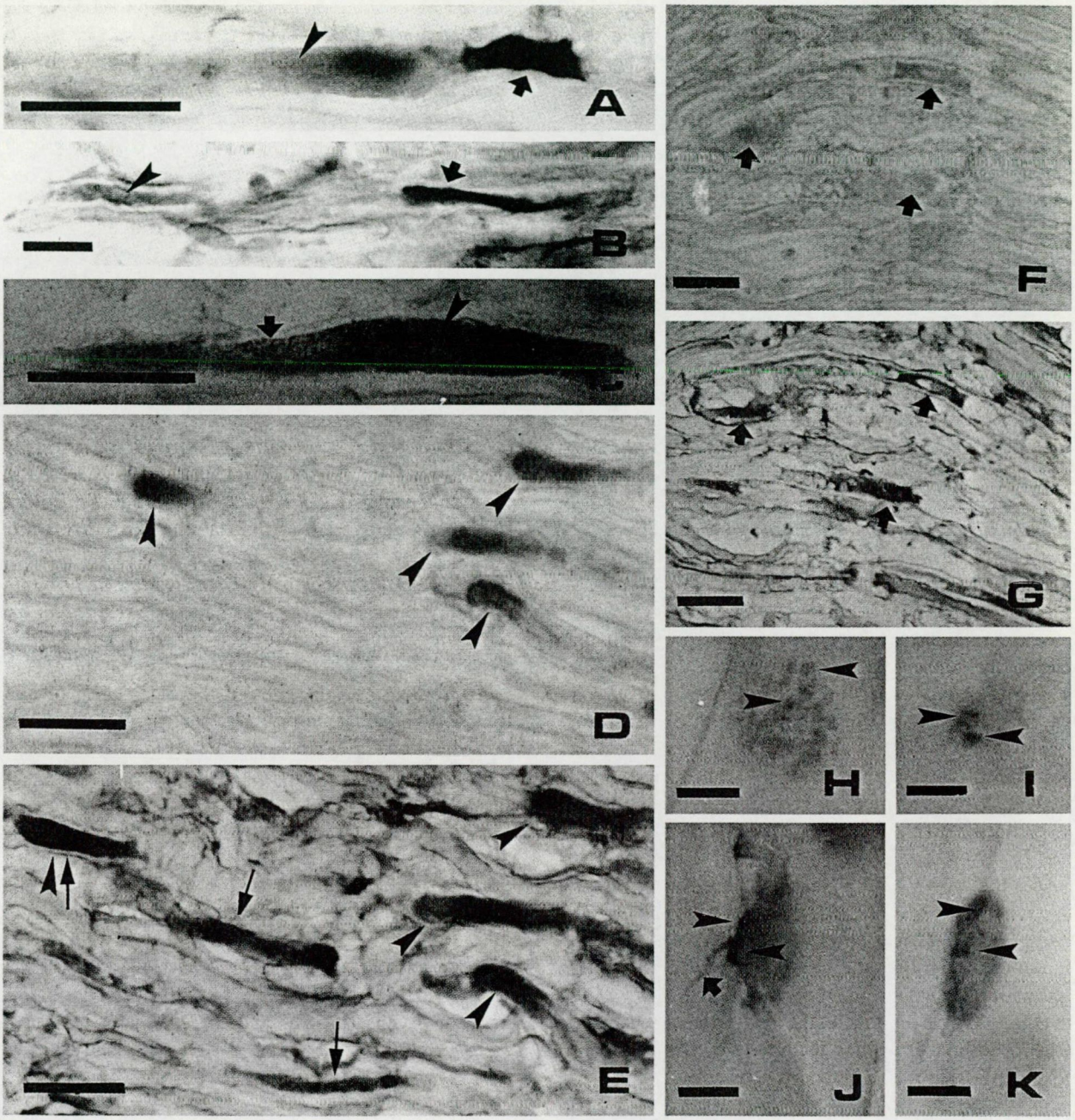

Fig. 2. Double-stained samples for AChE and PS-1 (A–C [AB1575], J–K [AB5308]), for AChE and APP (D,E) and for PS-1 and APP (G). In the sciatic nerve double-ligated for 24 h and double-stained first for AChE (brown, arrowhead) and thereafter for PS-1 (bluish-black, arrow), the two types of staining appeared either in distinct regions within the same axon (A) or in different axons (B) or in the same areas of the fibres (C) above the proximal ligature. In C, the PS-1 immunoreactivity is present in dot-like structures (arrow) in the region where the AChE (arrowhead) is present. In samples first stained for AChE (D, arrowheads) and thereafter for APP, either the two reaction end-products appeared in the same some axon (E, arrowhead plus arrow), or the AChE positivity (arrowheads) and the APP immunoreactivity (arrows) were present in separated fibres (E). The immunoreactivity for PS-1 (F, arrows) and for PS-1 and APP (G, arrows) could be revealed above the ligature in the same areas of the same axon in the double-ligated sciatic nerve for 24 h. In the muscle samples, the APP (H) and PS-1 (I) immunoreactivity appears as discrete dots (arrowheads). In double-stained muscle samples, the postsynaptic sites were delineated by the AChE histochemical reaction (J,K, brown) and the PS-1 immunoreactivity appeared in the motoric axon (J, arrow) and in the presynaptic axon terminals (J,K, arrowheads) at the NMJ. Scale bar=25 μm (A–G); 10 μm (H–K).

staining. It was shown that, besides large amounts of ~20-kDa C-terminal fragment and ~25-kDa N-terminal fragment, small amounts of the 45-kDa PS-1 holoprotein are present in the different segments both above the proximal ligature and below the distal ligature. After ligation, the C-terminal fragment (Fig. 3A,B), the N-terminal fragment (Fig. 3C,D) and intact PS-1 (Fig. 3E,F) accumulated in a time-dependent manner up to 24 h above

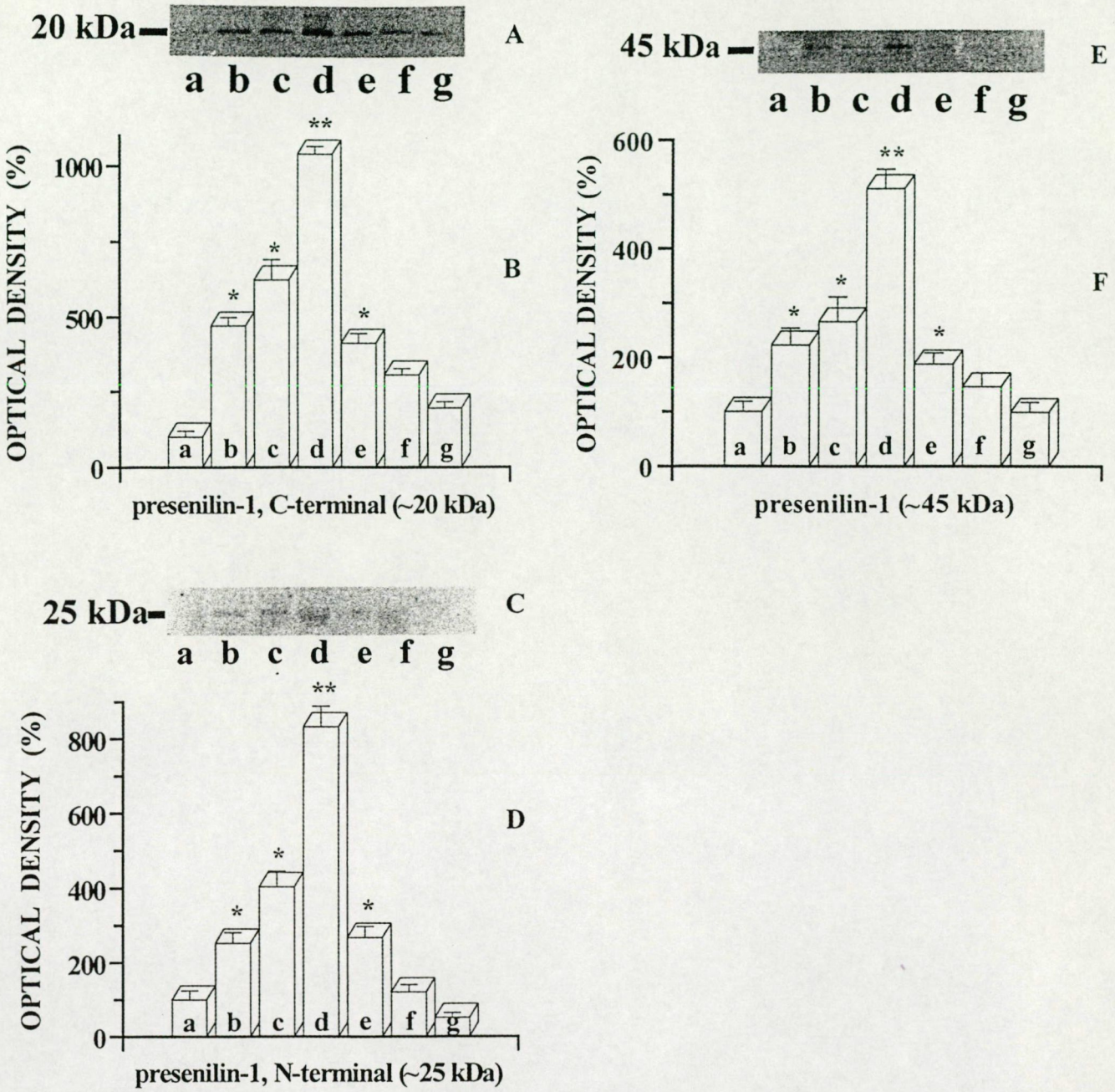

Fig. 3. Western blot of protein extracts from control samples (a) and from samples double-ligated for 6 h (b), 12 h (c) or 24 h (d) above the proximal ligature, or for 6 h (e), 12 h (f) or 24 h (g) below the distal ligature of the sciatic nerve. The polyclonal antibody AB5308 detected ~20-kDa (A) protein corresponding to the C-terminal and intact ~45-kDa (E), while antibody AB1575 detected ~25 kDa (C) protein corresponding to the N-terminal PS-1. The A, C and E immunoblot results were quantified and are demonstrated in histograms B, D and F, respectively. The optical density is expressed as a percentage of that for the control sample (100%). The reported data are the overall results of three different experiments. The error bar denotes the S.E. Statistical evaluations were performed with Student's *t*-test. Significant difference from the control sample: * $P<0.05$, ** $P<0.001$.

the proximal ligature, and up to 6 h below the distal ligature. No accumulation of these proteins could be revealed between the two ligatures (not documented). The accumulation of the C- and N-terminal fragments was more rapid than that of the full-length PS-1, suggesting a rapid endoproteolytic cleavage of PS-1 within the axons. After a 24-h ligation, the amount of the C-terminal fragment above the proximal ligature (Fig. 3B) was 10 times more than those found in the control, whereas the intact protein of PS-1 was increased by only five times (Fig. 3F) in the same segment as compared with the control sample of the sciatic nerve.

4. Discussion

This study has demonstrated three important points. First, N- and C-terminal PS-1 immunoreactivity is present in a large number of motoric and sensory axons of the sciatic nerve of rat. Second, the Western immunoblot technique revealed that not only the ~20-kDa C- and the ~25-kDa N-terminal fragments, but a small amount of the intact 45-kDa holoprotein of PS-1, is conveyed bidirectionally in the sciatic nerve. Third, the morphological appearance of the immunohistochemical staining of PS-1 in the presynaptic axon terminal is similar to that of APP.

4.1. Presence of presenilin-1 in the motoric and sensory axons

Some previous studies on the immunocytochemical localization of PS-1 suggested that it is restricted to the cell body and dendrites [6,29]. It was not found in significant amounts beyond the *cis*-Golgi compartments [2] (e.g. in the axons). Other studies have demonstrated the existence of PS-1 in the axons [10,27,34] and in the axoplasm [40]. The localization of PS-1 is similar to that of APP, which has been found in various axons [1,25,31,39,48] and axon terminals [5,17]. Our results support earlier data that both APP and PS-1 immunostaining may be present not only in the cell bodies and dendrites, but also in the axons of some neurons. PS-1 is suggested to have γ-secretase activity [8] and to cleave the transmembrane domain of APP, producing amyloid-beta (Aβ) peptide. In some immunohistochemical studies, no staining for PS-1 (γ-secretase activity) was demonstrated in the axons [2,6]. However, we were able to reveal Aβ staining in a number of axons and axon varicosities near and inside the senile plaques of the human hippocampus from AD individuals [49]. If this observation is correct, then Aβ would be produced in the axons having APP, but without PS-1. Such a result would indicate a spatial paradox for Aβ production. The present study therefore supports the earlier finding that PS-1 may be present in the axons [10,12,29,34]. The results presented here extend the earlier findings on the axonal localization of PS-1. Our double-labelling studies on PS-1 and AChE revealed that PS-1 staining is present not only in the AChE-positive motoric, but also in the AChE-negative sensory fibres [38]. In the AChE-positive motoric fibres, PS-1 was mostly localized in a segment where no AChE staining could be revealed. This result suggests that the two proteins may be localized in different axoplasmic structures or are transported at different axonal velocities. Our finding that PS-1 could be located in the different axons may have several explanations. First, we used a spinal cord and sciatic nerve model system, which may be different from the undifferentiated and transfected cell lines. Second, in this study both N- and C-terminal PS-1 antibodies were applied, with the same degree of success. Third, in none of the earlier experiments was a ligature introduced to facilitate the accumulation of PS-1 in a given segment of the nerve fibres. Our results therefore strengthen the findings that PS-1 may be present not only in the axons in some brain areas in rodents [10,29] and in the axon terminals of cortical and cerebellar neurons [37], but also in the axons and axon terminals of the motor neurons at the NMJ.

4.2. Anterograde and retrograde transport of presenilin-1 in the sciatic nerve of rat

By biochemical and light microscopic immunohistochemical means, PS-1 or its fragments has been demonstrated to be present at the cell surface [36], at the intercellular and synaptic contacts [13], in the synaptic plasma membranes [3], in the axon terminals [4] and in the axonal growth cones [3,4,12]. In accordance with these findings, PS-1 was detected ultrastructurally at the cell surface in transfected COS-7 cells [44], occasionally within presynaptic elements on typical synaptic vesicles of the monkey brain [29], and in the cerebellar cortex of the mouse and the rat [37]. All of these results support the suggestion that PS-1 may exit from the cell body and reach the cell surface plasma membrane or the synaptic regions in the neurons.

The results presented in this paper provide further experimental evidence and demonstrate that the N- and C-terminal fragments and intact PS-1 may be transported in the motoric and sensory axons. We used double ligatures that allow a more accurate assessment of bidirectional transport. Such an experimental set-up clearly indicates that the accumulation of PS-1 is due to bidirectional axonal movement, rather than accumulation at a site of axonal damage. The presence of 45-kDa holoprotein and fragments of PS-1 in the axons, and their accumulation in the segments above the proximal ligature and in the segments below the distal ligature, indicate that this protein may be cycling at all times in the sciatic nerve of the rat. Similarly to our finding of the bidirectional transport of PS-1, the fast anterograde [25,33,42] and retrograde [42] axonal movement of APP has already been demonstrated in the sensory nerves of the dorsal root ganglia of the rat [25,42]. However, the transport of APP and PS-1 is not restricted to the sensory nerves. Here, we have presented immunohistochemical evidence that the anterograde and retrograde movement of PS-1 may also occur in the motoric fibres of the sciatic nerve. The higher levels of the C- and N-terminal fragments and intact PS-1 adjacent to the proximal ligature as compared with the distal ligature may be due in part to the greater transport of PS-1 anterogradely. The mechanism of the transport of PS-1 holoprotein, the N-terminal and C-terminal fragments, and APP, however, may differ from that of AChE and choline acetyltransferase (ChAT), which are also present in the motoric axon. It has been shown that AChE [19,21] and ChAT [20,21] accumulate at different rates up to 24 h at the end proximal

to the ligature. The AChE activity rises not only in the proximal, but also in the distal segment up to 24 h, while the activity of ChAT does not change or slightly decreases distal to the ligature [21]. PS-1 and APP accumulate steadily up to 24 h above the upper ligature, while the highest accumulation of PS-1 in the segment distal to the ligature is observed up to 6 h after the lesion. Our data support the suggestion and provide further evidence that the various axoplasmic proteins may be conveyed inside the axon by various axonal structures [18], (e.g. AChE in axonal smooth surface endoplasmic tubules and vesicles [19], ChAT moves freely in the axoplasm [21], while PS-1 may be bound to coated transport vesicles [29], recycling endosomes [2] or small synaptic vesicles [3], and APP to clathrin-coated transport vesicles [32]. PS-1, PS-2 and APP KPI (751/770) immunostaining was recently demonstrated on the surface of the small synaptic vesicles in the presynaptic boutons and preterminal varicosities of the parallel fibres in the cerebellar cortex of the adult rat and mouse [37]. The question as to whether PS-1 and APP are transported in direct or indirect interactions remains to be answered.

4.3. Localization of presenilin-1 in relation to amyloid precursor protein in the presynaptic axon terminals at the neuromuscular junctions

There is an ongoing controversy as concerns the axonal localization of PS-1 in the central and peripheral nervous systems. In this study, we hoped not only to clarify the question of whether PS-1 can be found only in the axons, but also to reveal its presence in the axon terminals. The results of the immunostaining for PS-1 were compared with those for APP. Our findings clearly demonstrate that the localization of PS-1 is similar to that of APP in the axon terminals at the NMJ of the plantar muscle of the rat. APP has already been shown to be present in the axon terminals of the central nervous system [5,17]. The questions of whether PS-1 and APP are interconnected directly [45] or indirectly [24], and whether they are colocalized in the axon terminals at the NMJ or the immunostaining is merely overlapping, remain for further investigation.

4.4. The source of axonally transported presenilin-1

AD-associated PS-1 has previously been localized in various neuronal cell bodies [9–11,34] and in the muscle tissue [35]. Within the neuronal perikarya, it is present in the endoplasmic reticulum–Golgi intermediate compartment [2,7,26,29] and in the recycling endosomes [2,30]. Our observations indicate that there are at least three possible sources of PS-1 present in the axons of the sciatic nerve: (a) in the motoric axons, PS-1 may originate from the ventral horn neurons present in the grey matter of the spinal cord, while in the sensory fibres, PS-1 may be transported from the spinal ganglia, and (b) it may be taken up from the PS-1-positive Schwann cells surrounding the axons in the sciatic nerve, and (c) from the postsynaptic muscle tissues. Intensive PS-1 immunoreactivity has already been demonstrated in the large neurons of the grey matter of the spinal cord [10,15], and in the dorsal root ganglion cells of the mouse [15]. This and our own results lend strong support to our hypothesis that the motoneurons and the sensory ganglion cells are the primary sites of the source of PS-1 in the sensory and motoric axons in the sciatic nerve bundle. Furthermore, our results not only confirm the axonal localization of PS-1, but also extend the earlier findings demonstrating that PS-1 may be present in the motoric and sensory axons, where it is conveyed bidirectionally. The present immunohistochemical and Western blot study therefore argues against the suggestion that in general PS-1 can not be found beyond the endoplasmic reticulum and Golgi cisterna. Our results favour an axonal localization of PS-1 in the various neurons.

Acknowledgements

This work was supported by OTKA (T022683, T030339 and T032458) ETT (T-11/011/2000) and a Széchenyi Professorship to PK.

References

[1] S. Ahlgren, G.L. Li, Y. Olsson, Accumulation of beta-amyloid precursor protein and ubiquitin in axons after spinal cord trauma in humans: immunohistochemical observations on autopsy material, Acta Neuropathol. (Berl.) 92 (1996) 49–55.

[2] W.G. Annaert, L. Levesque, K. Craessaerts, I. Dierinck, G. Snellings, D. Westaway, P.S. George-Hyslop, B. Cordell, P. Fraser, B. De Strooper, Presenilin 1 controls γ-secretase processing of amyloid precursor protein in pre-Golgi compartments of hippocampal neurons, J. Cell Biol. 147 (1999) 277–294.

[3] D. Beher, C. Elle, J. Underwood, J.B. Davis, R. Ward, E. Karran, C.L. Masters, K. Beyreuther, G. Multhaup, Proteolytic fragments of Alzheimer's disease-associated presenilin 1 are present in synaptic organelles and growth cone membranes of rat brain, J. Neurochem. 72 (1999) 1564–1573.

[4] J. Busciglio, H. Hartmann, A. Lorenzo, C. Wong, K. Baumann, B. Sommer, M. Staufenbiel, B.A. Yankner, Neuronal localization of presenilin-1 and association with amyloid plaques and neurofibrillary tangles in Alzheimer,s disease, J. Neurosci. 17 (1997) 5101–5107.

[5] J.D. Buxbaum, G. Thinakaran, V. Koliatsos, J. O'Callahan, H.H. Slunt, D.L. Price, S.S. Sisoda, Alzheimer amyloid protein precursor in the rat hippocampus: Transport and processing through the perforant path, J. Neurosci. 18 (1998) 9629–9637.

[6] D.G. Cook, J.C. Sung, T.E. Golde, K.M. Felsenstein, B.S. Wojczyk, R.E. Tanzi, J.Q. Trojanowski, V.M.-Y. Lee, R.W. Doms, Expression and analysis of presenilin 1 in a human neuronal system: Localization in cell bodies and dendrites, Proc. Natl. Acad. Sci. USA 93 (1996) 9223–9228.

[7] J.G. Culvenor, F. Maher, G. Evin, F. Malchiodi-Albedi, R. Cappai, J.R. Underwood, J.B. Davis, E.H. Karran, G.W. Roberts, K. Beyreuther, C.L. Masters, Alzheimer's disease-associated presenilin

1 in neuronal cells: Evidence for localization to the endoplasmic reticulum–Golgi intermediate compartment, J. Neurosci. Res. 49 (1997) 719–731.

[8] B. De Strooper, P. Saftig, K. Craessaerts, H. Vanderstichele, G. Guhde, W. Annaert, K. Von Figura, F. Van Leuven, Deficiency of presenilin-1 inhibits the normal cleavage of amyloid precursor protein, Nature 391 (1998) 387–390.

[9] A. Diehlmann, N. Ida, S. Weggen, J. Grunberg, C. Haass, C.L. Masters, T.A. Bayer, K. Beyreuther, Analysis of presenilin 1 and presenilin 2 expression and processing by newly developed monoclonal antibodies, J. Neurosci. Res. 56 (1999) 405–419.

[10] G.A. Elder, N. Tezapsidis, J. Carter, J. Shioi, C. Bouras, H.-C. Li, J.M. Johnston, S. Efthimiopoulos, V.L. Friedrich Jr., N.K. Robakis, Identification and neuron specific expression of the S182/presenilin I protein in human and rodent brains, J. Neurosci. Res. 45 (1996) 308–320.

[11] I. Fakla, I. Kovacs, H. Yamaguchi, C. Geula, P. Kasa, Expressions of amyloid precursor protein, synaptophysin and presenilin-1 in the different areas of the developing cerebellum of rat, Neurochem. Int. 36 (2000) 143–151.

[12] P.E. Fraser, D.-S. Yang, G. Yu, L. Lévesque, M. Nishimura, S. Arawaka, L.C. Serpell, E. Rogaeva, P.S. George-Hyslop, Presenilin structure, function and role in Alzheimer disease, Biochim. Biophys. Acta 1502 (2000) 1–15.

[13] A. Georgakopoulos, P. Marambaud, S. Efthimiopoulos, J. Shioi, W. Cui, H.C. Li, M. Schutte, R. Gordon, G.R. Holstein, G. Martinelli, P. Mehta, V.L. Friedrich Jr., N.K. Robakis, Presenilin-1 forms complexes with the cadherin/catenin cell–cell adhesion system and is recruited to intercellular and synaptic contacts, Mol. Cell. 4 (1999) 893–902.

[14] H.H. Hess, M.B. Lees, J.E. Derr, A linear Lowry–Folin assay for both water-soluble and sodium dodecyl sulfate-solubilized proteins, Anal. Biochem. 85 (1978) 295–300.

[15] D.P. Huynh, V.V. Ho, S.-M. Pulst, Characterization and expression of presenilin 1 in mouse brain, NeuroReport 7 (1996) 2423–2428.

[16] D.P. Huynh, H.V. Vinters, D.H. Ho, V.V. Ho, S.-M. Pulst, Neuronal expression and intracellular localization of presenilins in normal and Alzheimer disease brains, J. Neuropathol. Exp. Neurol. 56 (1997) 1009–1017.

[17] A.F. Ikin, W.G. Annaert, K. Takei, P. De Camilli, R. Jahn, P. Greengard, J.D. Buxbaum, Alzheimer amyloid protein precursor is localized in nerve terminal preparations to Rab5-containing vesicular organelles distinct from those implicated in the synaptic vesicle pathway, J. Biol. Chem. 271 (1996) 31783–31786.

[18] C. Kaether, P. Skehel, C.G. Dotti, Axonal membrane proteins are transported in distinct carriers: A two-color video microscopy study in cultured hippocampal neurons, Mol. Biol. Cell. 11 (2000) 1213–1224.

[19] P. Kasa, Acetylcholinesterase transport in the central and peripheral nervous tissue: The role of tubules in the enzyme transport, Nature 218 (1968) 1265–1267.

[20] P. Kasa, S.P. Mann, C.O. Hebb, Localization of choline acetyltransferase. Ultrastructural localization in spinal neurones, Nature 226 (1970) 814–816.

[21] P. Kasa, S.P. Mann, S. Karcsu, L. Toth, S. Jordan, Transport of choline acetyltransferase and acetylcholinesterase in the rat sciatic nerve: A biochemical and electron histochemical study, J. Neurochem. 21 (1973) 431–436.

[22] P. Kasa, H. Papp, P. Kasa Jr., I. Torok, Donepezil dose-dependently inhibits acetylcholinesterase activity in various areas and the presynaptic cholinergic and the postsynaptic cholinoceptive enzyme-positive structures in the human and rat brain, Neuroscience 101 (2000) 89–100.

[23] P. Kasa, H. Papp, I. Kovacs, M. Forgon, B. Penke, H. Yamaguchi, Human amyloid-β1-42 applied in vivo inhibits the fast axonal transport of proteins in the sciatic nerve of rat, Neurosci. Lett. 278 (2000) 117–119.

[24] S.S. Kim, Y.M. Choi, Y.H. Suh, Lack of interactions between amyloid precursor protein and hydrophilic domains of presenilin 1 and 2 using the yeast two hybrid system, J. Mol. Neurosci. 9 (1997) 49–54.

[25] E.H. Koo, S.S. Sisodia, D.R. Archer, L.J. Martin, A. Weidemann, K. Beyreuther, P. Fischer, C.L. Masters, D.L. Price, Precursor of amyloid protein in Alzheimer disease undergoes fast anterograde axonal transport, Proc. Natl. Acad. Sci. USA 87 (1990) 1561–1565.

[26] D.M. Kovacs, H.J. Fausett, K.J. Page, T.W. Kim, R.D. Moir, D.E. Merriam, R.D. Hollister, O.G. Hallmark, R. Mancini, K.M. Felsenstein, B.T. Hyman, R.E. Tanzi, W. Wasco, Alzheimer-associated presenilins 1 and 2: neuronal expression in brain and localization to intracellular membranes in mammalian cells, Nature Med. 2 (1996) 224–229.

[27] I. Kovacs, I. Torok, J. Zombori, P. Kasa, Immunohistochemical localization of presenilin-1 in hippocampus and entorhinal cortex of human brain samples, Clin. Neurosci. 51 (1998) 56–57.

[28] U.K. Laemmli, Cleavage of structural proteins during the assembly of the head of bacteriophage T4, Nature 227 (1970) 680–685.

[29] J.J. Lah, C.J. Heilman, N.R. Nash, H.D. Rees, H. Yi, S.E. Counts, A.I. Levey, Light and electron microscopic localization of presenilin-1 in primate brain, J. Neurosci. 17 (1997) 1971–1980.

[30] J.J. Lah, A.I. Levey, Endogenous presenilin-1 targets to endocytic rather than biosynthetic compartments, Mol. Cell Neurosci. 16 (2000) 111–126.

[31] G.L. Li, M. Farooque, A. Holtz, Y. Olsson, Changes of beta-amyloid precursor protein after compression trauma to the spinal cord: An experimental study in the rat using immunohistochemistry, J. Neurotrauma 12 (1995) 269–277.

[32] N.R. Marquez-Sterling, A.C.Y. Lo, S.S. Sisodia, E.H. Koo, Trafficking of cell-surface β-amyloid precursor protein: Evidence that a sorting intermediate participates in synaptic vesicle recycling, J. Neurosci. 17 (1997) 140–151.

[33] P.J. Morin, C.R. Abraham, A. Amaratunga, R.J. Johnson, G. Huber, J.H. Sandell, R.E. Fine, Amyloid precursor protein is synthesized by retinal ganglion cells, rapidly transported to the optic nerve plasma membrane and nerve terminals, and metabolized, J. Neurochem. 61 (1993) 464–473.

[34] S. Moussaoui, C. Czech, L. Pradier, V. Blanchard, B. Bonici, M. Gohin, A. Imperato, F. Revah, Immunohistochemical analysis of presenilin-1 expression in the mouse brain, FEBS Lett. 383 (1996) 219–222.

[35] C. Nilsberth, J. Luthman, L. Lannfelt, M. Schultzberg, Expression of presenilin-1 mRNA in rat peripheral organs and brain, Histochem. J. 31 (1999) 515–523.

[36] W.J. Ray, M. Yao, J. Mumm, E.H. Schroerter, P. Saftig, M. Wolfe, D.J. Selkoe, R. Kopan, A.M. Goate, Cell surface presenilin-1 participates in the γ-secretase-like proteolysis of Notch, J. Biol. Chem. 274 (1999) 36801–36807.

[37] C. Ribaut-Barassin, S. Moussaoui, B. Brugg, A.M. Haeberle, G. Huber, A. Imperato, N. Delhaye-Bouchaud, J. Mariani, Y.J. Bailly, Hemisynaptic distribution patterns of presenilins and beta-APP isoforms in the rodent cerebellum and hippocampus, Synapse 35 (2000) 96–110.

[38] W.W. Schlaepfer, Acetylcholinesterase activity of motor and sensory nerve fibers in the spinal nerve roots of the rat, Z. Zellforsch. 88 (1968) 441–456.

[39] W. Schubert, R. Prior, A. Weidemann, H. Dircksen, G. Multhaup, C.L. Masters, K. Beyreuther, Localization of Alzheimer beta A4 amyloid precursor protein at central and peripheral synaptic sites, Brain Res. 563 (1991) 184–194.

[40] Y. Sekijima, F. Kametani, K. Tanaka, M. Okochi, M. Usami, H. Mori, T. Tokuda, S. Ikeda, Presenilin-1 exists in the axoplasm fraction in the brains of aged Down's syndrome subjects and non-demented individuals, Neurosci. Lett. 267 (1999) 121–124.

[41] R. Sherrington, E.I. Rogaev, Y. Liang, E.A. Rogaeva, G. Levesque, M. Ikeda, H. Chi, C. Lin, G. Li, K. Holman, T. Tsuda, L. Mar, J.-F.

Foncin, A.C. Bruni, M.P. Montesi, S. Sorbi, I. Rainero, L. Pinessi, L. Nee, I. Chumakov, D. Pollen, A. Brookes, P. Sanseau, R.J. Polinsky, W. Wasco, H.A.R. Da Silva, J.L. Haines, M.A. Pericak-Vance, R.E. Tanzi, A.D. Roses, P.E. Fraser, J.M. Rommens, P.H. George-Hyslop, Cloning of a gene bearing missense mutations in early-onset familial Alzheimer's disease, Nature 375 (1995) 754–760.

[42] S.S. Sisodia, E.H. Koo, P.N. Hoffman, G. Perry, D.L. Price, Identification and transport of full-length amyloid precursor proteins in rat peripheral nervous system, J. Neurosci. 13 (1993) 3136–3142.

[43] H. Tago, H. Kimura, T. Maeda, Visualization of detailed acetylcholinesterase fiber and neuron staining in rat brain by a sensitive histochemical procedure, J. Histochem. Cytochem. 34 (1986) 1431–1438.

[44] A. Takashima, M. Sato, M. Mercken, S. Tanaka, S. Kondo, T. Honda, K. Sato, M. Murayama, K. Noguchi, Y. Nakazato, H. Takahashi, Localization of Alzheimer-associated presenilin 1 in transfected COS-7 cells, Biochem. Biophys. Res. Commun. 227 (1996) 423–426.

[45] M. Waragai, I. Imafuku, S. Takeuchi, I. Kanazawa, F. Oyama, Y. Udagawa, M. Kawabata, H. Okazawa, Presenilin 1 binds to amyloid precursor protein directly, Biochem. Biophys. Res. Commun. 239 (1997) 480–482.

[46] L.L. Weber, M.A. Leissring, A.J. Yang, C.G. Glabe, D.H. Cribbs, F.M. LaFerla, Presenilin-1 immunoreactivity is localized intracellularly in Alzheimer's disease brain, but not detected in amyloid plaques, Exp. Neurol. 143 (1997) 37–44.

[47] S. Weggen S, A. Diehlmann, R. Buslei, K. Beyreuther, T.A. Bayer, Prominent expression of presenilin-1 in senile plaques and reactive astrocytes in Alzheimer's disease brain, NeuroReport 9 (1998) 3279–3283.

[48] T. Yamazaki, D.J. Selkoe, E.H. Koo, Trafficking of cell surface beta-amyloid precursor protein: retrograde and transcytotic transport in cultured neurons, J. Cell Biol. 129 (1995) 431–442.

[49] J. Zombori, H. Papp, P. Kasa, Intraaxonal and intraneuronal presence of amyloid-beta peptide in Alzheimer's disease brain samples, Clin. Neurosci. 53 (Suppl. 1) (2000) 25–26.

IV

ELSEVIER

Brain Research 796 (1998) 239–246

BRAIN RESEARCH

Research report

Vulnerability of small GABAergic neurons to human β-amyloid pentapeptide

Magdolna Pakaski [a,*], Zoltan Farkas [a], Peter Kasa Jr. [b], Monika Forgon [a], Henrietta Papp [a], Marta Zarandi [c], Botond Penke [c], Peter Kasa Sr. [a]

[a] *Alzheimer's Disease Research Centre, Albert Szent-Györgyi Medical University, 4 Somogyi st., H-6720 Szeged, Hungary*
[b] *Department of Pharmaceutical Technology, Albert Szent-Györgyi Medical University, H-6720 Szeged, Hungary*
[c] *Department of Medical Chemistry, Albert Szent-Györgyi Medical University, H-6720 Szeged, Hungary*

Accepted 31 March 1998

Abstract

β-Amyloid peptide (Aβ), the principal component of senile plaques in Alzheimer's disease, has been found to be neurotoxic. The role of Aβ in the deficits of the GABAergic system in patients with Alzheimer's disease is unclear. It has been suggested that the cytotoxic activity of Aβ is localized to amino acid residues 25–35 of this peptide, which contains a total of 42 amino acid residues. We now report that the short amyloid peptide fragments corresponding to amino acids 31–35 (Aβ31–35) and 34–39 (Aβ34–39) are also toxic in vitro to the small GABAergic neuron population of basal forebrain cultures. Morphological changes were accompanied by an increased number of varicosities localized on the processes of the GABA-immunoreactive neurons and by the appearance of round cells without processes. The neurodegeneration was confirmed by means of scanning electron microscopy. Quantification of the morphological findings by image analysis demonstrated a size-related dependence of the degeneration of GABAergic neurons. The results suggest that fragments of Aβ shorter than Aβ25–35 may exert cytotoxic action and demonstrate the toxicity of these Aβ fragments in decreasing the number of small GABAergic neurons.

Keywords: Amyloid; Alzheimer's disease; Neuronal culture; GABA immunocytochemistry; Scanning electron microscopy; Image analysis

1. Introduction

Previous studies have demonstrated deficits of different transmitter-containing neurons in patients with Alzheimer's disease (AD) [9,19,23,27,36,37]. It has also been shown that β-amyloid peptide (Aβ) plays a role in the neuronal degeneration of AD both in vivo [3,6,15,16,35,38] and in vitro [1,21,28,31]. Whether there is a relationship between Aβ toxicity and the GABAergic deficit is an important question because controversial data have been reported concerning changes in GABAergic neurons after Aβ treatment. Studies on the Aβ neurotoxicity of GABAergic cells have led to reports both of their resistance [30] and of their vulnerability [11,12].

Aβ contains 42–43 amino acid residues. It has been proposed that its biologically active domain is the discrete 11-amino acid internal sequence of amino acids 25–35 (Aβ25–35) [21,39]. The biological activities of shorter Aβ fragments have also been investigated [13,24,25,31,33]. The results indicate that the neurotoxic action of Aβ is linked to the state of aggregation of the peptide. Pike et al. [33] demonstrated the formation of stable aggregates and induction of the neurotoxicity of synthetic Aβ containing the hydrophobic residues 29–35, suggesting that this region is vital for amyloid deposition and bioactivity.

With regard to these previous data, one purpose of the present study was to reevaluate the toxicity of Aβ1–42 on GABAergic cells in embryonic rat basal forebrain cultures; a second goal was to compare the toxic effects of different short fragments of Aβ on this neuron population. The morphology of neuronal cultures was investigated by means of GABA immunocytochemistry. To confirm the reliability of the degeneration process visualized by GABA immunostaining, we additionally examined the morphological changes by using scanning electron microscopy. To quan-

* Corresponding author. Fax: +36-62-312-849; E-mail: pakaski@comser.szote-u.szeged.hu

0006-8993/98/$19.00
PII S0006-8993(98)00358-8

tify our results, the numbers and sizes of GABAergic neurons were measured with an image analyser. In view of the fact that previous data indicated that Aβ kills neurons by an apoptotic mechanism [7,17], a check was also made on the manner of neuronal death by staining the cells with the fluorescent chromatin dye Hoechst 33,258.

2. Materials and methods

2.1. Tissue cultures

Primary basal forebrain cultures were prepared from 16–17-day-old (E16–17) rat embryos. The collected tissue samples were incubated for 10 min in 0.25% trypsin (Gibco) at 37°C. The tissue was mechanically dissociated by trituration with a fire-polished Pasteur pipette. The resulting cell suspension was centrifuged for 10 min at $1000 \times g$. The pellet was resuspended in Dulbecco's Modified Eagle Medium (DMEM) (Gibco) containing 10% fetal bovine serum (FBS) (Gibco), 100 U/ml penicillin and 100 μg/ml streptomycin. Cells were plated onto poly-L-lysine (Sigma) coated coverslips ($3.5–4 \times 10^4$ cells/cm^2) and were plated in a humidified 37°C incubator in air containing 5% CO_2.

2.2. Treatment of neuronal cultures

Since untreated neurons were observed to retain their viability for at least 10 days in this culture system, 4 days in vitro (DIV 4) after plating the cultures were treated with 20 μM Aβ1–42, Aβ31–35, Aβ34–39 or Aβ33–35. Aβ1–42 and the various fragments were dissolved in 35% acetonitrile plus 0.1% trifluoroacetic acid (ACN/TFA) and were diluted 50 × in growth medium as described by Yankner et al. [39]. Control cultures were maintained in DMEM/10% FBS for 4 days, and then supplemented with ACN/TFA. Exposure to Aβ1–42 and its fragments was carried out in the incubator (37°C, 5% CO_2). Cultures were assessed on days 1 (DIV 4 + 1), 3 (DIV 4 + 3) and 5 (DIV 4 + 5) after treatment.

2.3. Peptide synthesis

Human Aβ was synthesized in the Chemical Department of our University by a solid-phase technique involving Boc chemistry [26]. Peptide chains were elongated on MBHA resin (0.6–0.8 mmol/g) and the syntheses were carried out manually. Couplings were performed with dicyclohexylcarbodiimide, with the exception of Asn, which was incorporated in HOBt-ester form. The Boc group was removed by treatment with 50% TFA in CH_2Cl_2. After completion of the synthesis, the peptide was cleaved from the resin with liquid HF. Free peptides were solubilized in 95% TFA, filtered and lyophilized. The crude peptides were purified by RP-HPLC on an Astec-300 5 C_4 column. The purity was checked by RP-HPLC on a W-Porex 5 C_4 column. Amino acid analysis demonstrated the expected amino acid composition, and electrospray mass spectrometry gave the expected molecular ion.

2.4. Immunocytochemistry

One to five days after Aβ treatment, the cultures were fixed in 1% glutaraldehyde for 20 min. The cells were then incubated by using 0.2% Triton X-100 and 5% normal bovine serum (NBS) in Tris-buffered saline (TBS) for 4 h. The monoclonal antibody against GABA (1:3000; Immunotech, France) was applied overnight at 37°C. This was followed by incubation in goat-anti-rabbit IgG (1:30, Jackson Immunores. Lab., USA) for 1 h, and then in rabbit peroxidase–antiperoxidase complex (1:200, Nordic Immun. Lab., Germany) for 1 h. The cultures were washed twice for 10 min between sera. All the washing steps and the dilution of the antisera were carried out with 0.1 M TBS (pH 7.4) containing 5% NBS. The peroxidase reaction was developed by using 3,3′-diaminobenzidine tetrahydrochloride and $NiCl_2$.

The specificity of the immunostaining was controlled by omitting the first or second antibody from the incubation procedure. No residual immunoreactivity was found.

Cells were examined on a Nikon Microphot FXA microscope equipped with Nomarsky optics (Japan).

2.5. Assessment of neuronal death

The cells of control and Aβ1–42-treated cultures were fixed for 30 min in 4% paraformaldehyde and then exposed to 2 μM Hoechst 33,258 (Sigma) for 30 min. Cultures were washed twice with phosphate-buffered saline and twice with water. Fluorescence was visualized by using a 40 × lens: the dye was excited at 365 nm, and the emission was filtered with a 400 nm barrier filter.

2.6. Scanning electron microscopy

The control and Aβ-treated cultures were prefixed in 1.0% glutaraldehyde and 2.0% formaldehyde for 4 h, postfixed in buffered 1% OsO_4 for 2 h, dehydrated in a graded series of ethanol, and placed in acetone. Following critical point drying with liquid CO_2, the cultures were sputtered with gold and examined on a Tesla BS-300 electron microscope.

2.7. Image analysis

A Leica Q500 MC colour image analyser (Germany) was employed to measure the numbers and sizes of the GABAergic cells in the control and Aβ-treated cultures. The image analyser was controlled by QWIN software. Since binary operators separately labelled profiles, including the fragmentations of GABA-positive cells, the binary editing operator was used for further manipulation of the images. In binary editing, the light pen was used by

drawing the GABA-immunoreactive cells manually. After this step, a measurement routine was run which computes the numbers and diameters of GABAergic cells. These results were stored in a data file that was further analysed by means of Microsoft Excel 5.0 software. GABA-immunoreactive cells were counted in 5 randomly selected fields (5×0.3 mm^2) per experiment in 3 separate experiments. All statistical evaluations involved Student's *t*-test analysis.

3. Results

3.1. Demonstration of toxicity of Aβ fragments by GABA immunocytochemistry

To determine the neuronal toxic effects of Aβ and its fragments, the control and Aβ-treated cultures were immunostained for GABA. The staining pattern of the control

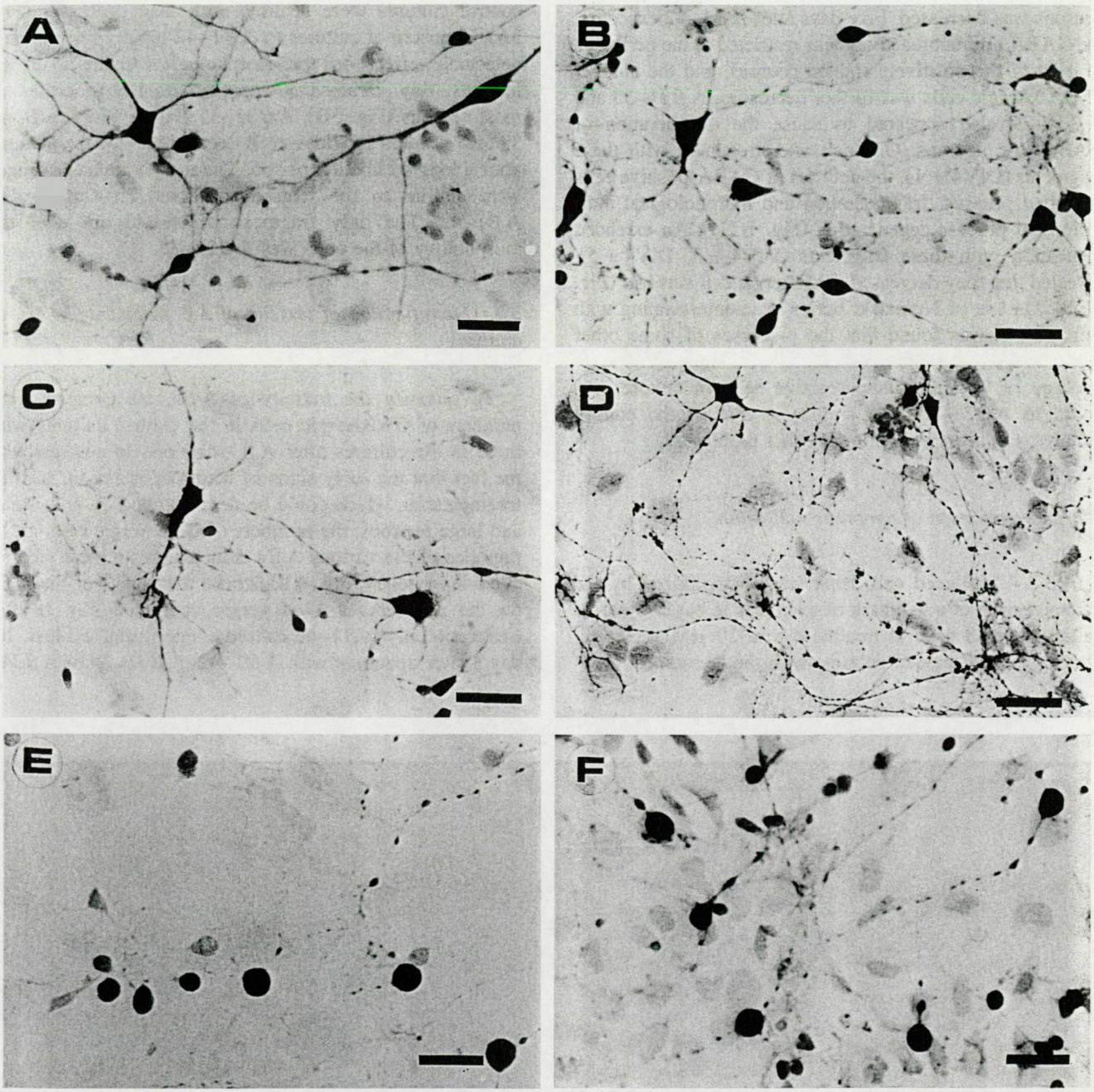

Fig. 1. Panels A–F present micrographs of basal forebrain cultures immunochemically stained with GABA antibody exposed for 1–3 days (DIV4 + 1, DID4 + 3) to the following treatments: A: solvent (control), (DIV4 + 1); B: 20 μM Aβ1–42 (DIV4 + 1); C: 20 μM Aβ31–35 (DIV4 + 1); D: 20 μM Aβ34–39 (DIV4 + 1); E: 20 μM Aβ31–35 (DIV4 + 5); F: 20 μM Aβ34–39 (DIV4 + 5). Essentially, all neurons appeared healthy in the control culture; in contrast, the vast majority of the neurons have degenerated after treatment (round perikaryons, fragmented neurites). Scale bar = 40 μm.

cultures demonstrated a diffuse intracellular distribution of GABA localized on the perikarya and long processes of the neurons (Fig. 1A). Neurons in the culture exposed to Aβ1–42 (20 μM) revealed characteristic morphological changes: 1 day after the Aβ1–42 treatment (DIV4 + 1) (Fig. 1B), varicosities could be detected on the processes of a large number of neurons. In the control cultures, only a few, spontaneous degenerated GABAergic neurons possessed fragmented neurites (Fig. 1A). By day 3 after Aβ1–42 incubation (DIV4 + 3), not only were varicosities visible, but the number of GABA-immunoreactive neurons was decreased. Five days after Aβ1–42 exposure, the GABA immunoreactivity was restricted to the perikarya in most of the positively stained neurons, and the number of GABAergic cells was further decreased. Aβ31–35 and Aβ34–39 also appeared to cause the degeneration of GABAergic neurons. One day after treatment with these fragments (DIV4 + 1), the neurites of GABA-positive cells exhibited pruning, fragmentation and morphological indications of process degeneration (Fig. 1C,D). An extended incubation with these fragments (DIV4 + 3, DIV4 + 5), revealed that they decreased GABAergic cell survival (Fig. 1E,F). On use of Nomarski optics or counterstaining with safranine, it was found that the processes of some other types (non-GABAergic) of neurons were intact. The morphology of GABA-immunoreactive cells in cultures exposed to Aβ33–35 was similar to that of the control cultures: the neurons had long, intact processes.

3.2. Demonstration of apoptotic cell death

Aβ1–42 induced cell death was characterized by the demonstration of a hallmark of apoptosis in basal forebrain cultures after 3 days of treatment with 20 μM Aβ1–42. Staining of Aβ-treated cultures with the fluorescent chromatin dye Hoechst 33,258 revealed numerous condensed nuclei (Fig. 2B); at the same time, this apoptotic feature was very scarce, although not absent, in control cultures (Fig. 2A).

3.3. Demonstration of toxicity of Aβ fragments by scanning electron microscopy

One to five days after incubation with the solvent (DIV4 + 1, DIV4 + 3 and DIV4 + 5), the neurons in the control cultures were healthy, with long processes (Fig. 3A). Exposure of cultures to Aβ1–42 rapidly resulted in a detectable effect on the morphological features of the neurons: tiny varicosities appeared on the processes of most neurons (Fig. 3B). Aβ31–35 (Fig. 3C) and Aβ34–39 also resulted in widespread degeneration of the neurons after a long incubation period. The morphological changes were similar to the features observed on exposure to Aβ1–42. The only fragment which did not alter the morphology of the cells was Aβ33–35.

3.4. Quantification of toxicity of Aβ fragments by image analysis

To quantify the toxicity of Aβs, we compared the numbers of GABAergic cells in the control cultures with those in the cultures after Aβ treatment. In contrast with the fact that the early signs of neurodegeneration, such as fragmentation which could be demonstrated on both small and large neurons, the numbers of GABAergic cells in the presence of the various Aβs demonstrated a clear size-related dependency. Fig. 4 illustrates the effects of the Aβs on the numbers of GABAergic cells. On day 1 after treatment, only Aβ1–42 caused a significant cell loss. By day 3 after treatment with Aβ1–42, Aβ31–35 or Aβ34–

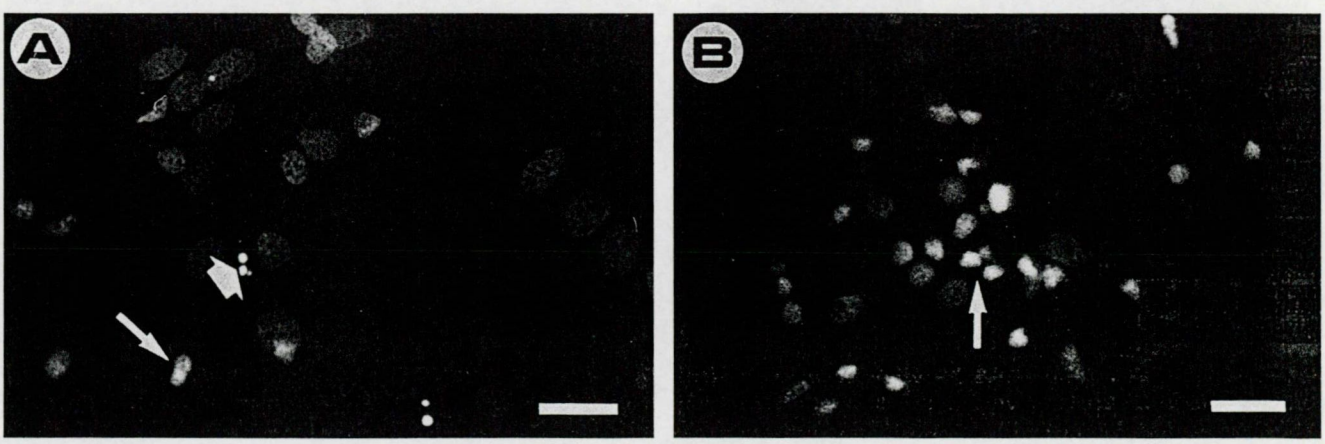

Fig. 2. Photomicrograph of basal forebrain cultures stained with the DNA dye Hoechst 33,258. A: control cultures exhibited nuclear staining typical of healthy cells; a few dying cells contained clumped DNA (arrow) and fragmented DNA (wide arrow); B: a 20 μM Aβ1–42-treated culture (DIV4 + 3) contained clumped DNA associated with a large number of apoptotic cells (arrow). Scale bar = 40 μm.

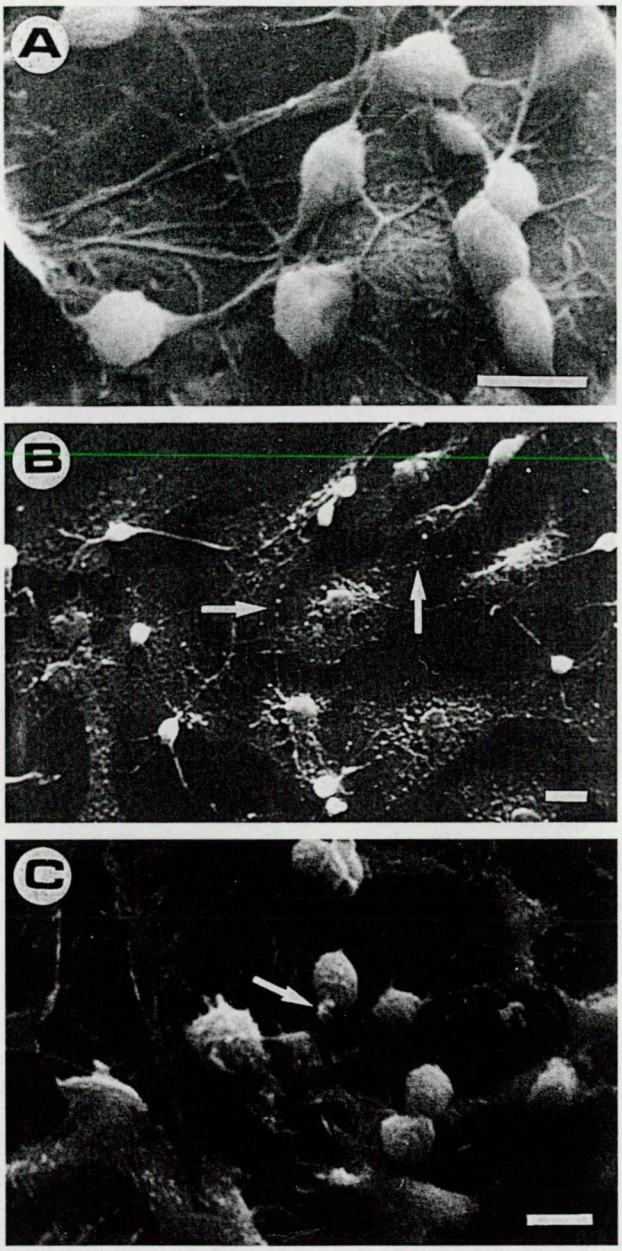

Fig. 3. Scanning electron microscopic images of basal forebrain cultures exposed for 3–5 days to the following treatments: A: solvent (control) (DIV4+3); B: 20 μM Aβ31–35 (DIV4+3) (a morphological sign of neuronal degeneration is visible, the arrow pointing to fragmented neurites); C: 20 μM Aβ31–35 (DIV4+5). Note the evidence of apoptosis of neurons: small protrusions on their soma. Scale bar = 20 μm.

39, the number of GABA-immunoreactive cells had decreased to 50–60% of that in the control culture. Following a 5-day exposure (Aβ1–42, Aβ31–35 or Aβ34–39), more serious damage to the GABAergic cells was observed. Treatment of cultures with Aβ33–35 did not induce a significant decrease in the number of GABA-positive cells.

Since morphological investigation of Aβ-treated cultures demonstrated that the small bipolar GABAergic cells are vulnerable after a shorter incubation period than for the large, multipolar ones, we analysed the effects of the Aβs on the cells of different sizes. Three types of neurons were distinguished by difference in somatic size: large neurons (longest diameter 15–20 μm), these being the least frequent cell type; medium-sized neuronal somata (diameter 10–15 μm); and small neurons (diameter 5–10 μm), these being the most frequent cell type in these neuronal cultures. Image analysis of the loss of these differently-sized neurons after Aβ treatment demonstrated that after exposure to Aβ1–42 for 1 day caused a selective loss of small GABAergic neurons (Fig. 5A), whereas the number of these small neurons remained unchanged following treatment with Aβ31–35, Aβ34–39 or Aβ33–35 (Fig. 5A). At this time, there was no significant decrease at all in the numbers of medium-sized or large neurons after exposure to the various Aβs.

On day 3 after treatment, not only Aβ1–42 but also Aβ31–35 and Aβ34–39 had induced the selective loss of small GABA-positive neurons (Fig. 5B). The numbers of medium-sized and large neurons were still not decreased significantly after any Aβ treatment relative to the controls (Fig. 5B).

On day 5 after exposure to the Aβs, the numbers of both small and medium-sized neurons were decreased significantly, but that of the large GABAergic neurons remained unchanged (Fig. 5C).

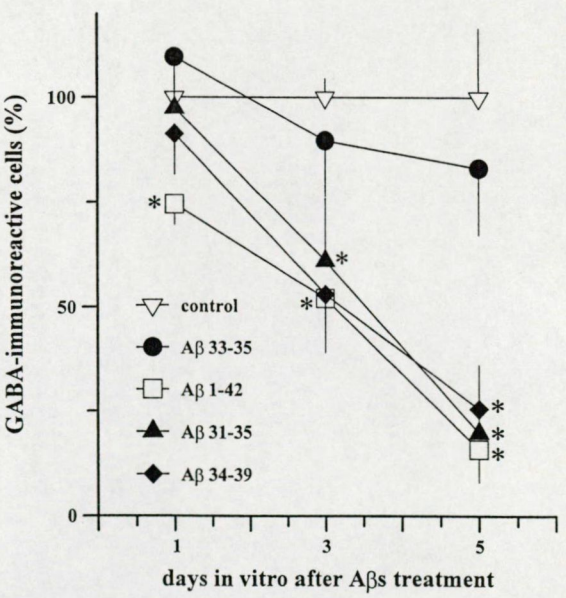

Fig. 4. Effects of different Aβs on numbers of GABAergic cells in embryonic rat basal forebrain cultures. The values for untreated cultures were taken as 100%. Data are means ± S.D. values from 5 randomly selected fields (5×0.3 mm^2) in each of 3 separate experiments. Significant toxicity is observed on day 1 after Aβ1–42 treatment, and on days 3 and 5 after Aβ1–42, Aβ31–35 and Aβ34–39 treatment (* $p < 0.001$, paired Student's t-test).

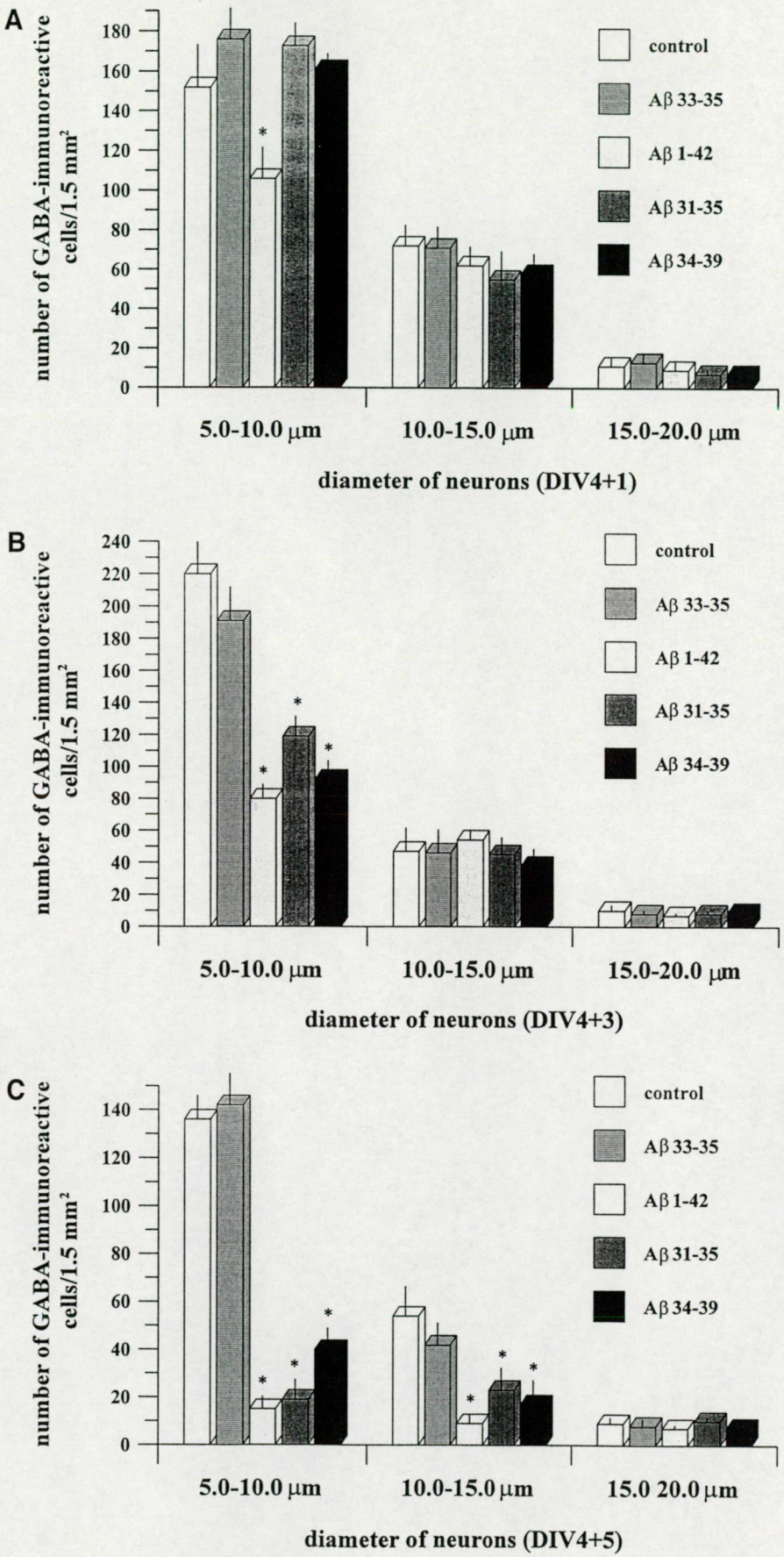
A
number of GABA-immunoreactive cells/1.5 mm²
control
Aβ 33-35
Aβ 1-42
Aβ 31-35
Aβ 34-39
5.0-10.0 μm
10.0-15.0 μm
15.0-20.0 μm
diameter of neurons (DIV4+1)
B
number of GABA-immunoreactive cells/1.5 mm²
control
Aβ 33-35
Aβ 1-42
Aβ 31-35
Aβ 34-39
5.0-10.0 μm
10.0-15.0 μm
15.0-20.0 μm
diameter of neurons (DIV4+3)
C
number of GABA-immunoreactive cells/1.5 mm²
control
Aβ 33-35
Aβ 1-42
Aβ 31-35
Aβ 34-39
5.0-10.0 μm
10.0-15.0 μm
15.0 20.0 μm
diameter of neurons (DIV4+5)

4. Discussion

Although post mortem AD brains have typically indicated severe reductions in the cholinergic marker choline acetyltransferase [5], an ever increasing number of data have been reported that point to damage to neurons containing other neurotransmitters. GABAergic cell injury in AD, for example, has been investigated extensively [9,19,23,37]. The present study revealed that not only Aβ1–42 itself, but also two of its fragments (Aβ31–35 and Aβ34–39) are toxic to the GABAergic neurons in rat basal forebrain cultures. The neurotoxic effects of Aβ1–42 and its fragment Aβ25–35 have been studied in considerable detail in both in vivo [3,6,15,16,35,38] and in vitro experiments [1,13,20,24,25,28,29,31], but information on shorter peptide fragments is almost completely lacking. A correlation has been demonstrated between Aβ aggregation and neurotoxicity [3,21,28,29,33]. Although we have not assessed their aggregation status, we suggest that Aβ31–35 and Aβ34–39 might aggregate at a slower rate than Aβ1–42, with the result that their toxic effects therefore would be more moderate during a given incubation period. The different effects of these fragments and Aβ33–35 may be due to their different aggregation states. We suggest that since Aβ33–35 cannot aggregate and so cannot be toxic, whereas Aβ31–35 and Aβ34–39 can presumably assemble and induce a neurotoxic effect.

Assessment of the mechanism of neuronal death proved that neurons in our experiments also died by apoptosis [7,17]. Although the apoptosis test and GABA immunocytochemistry were not performed on the same samples, it may be suggested that Aβ induces an apoptotic mechanism in the GABAergic neurons.

It is interesting to note that the Leu and Met at positions 34 and 35 of the amino acid sequence are common in Aβ31–35, Aβ33–35 and Aβ34–39. Our data suggest that Leu^{34} and Met^{35} may play a critical role in the biochemical mechanism of Aβ neurotoxicity. Since aggregation is important for toxicity, we concluded that a neurotoxic effect may be induced by Leu^{34} and Met^{35} in those fragments which contain more than three amino acids, which are long enough to be in a stable aggregation state. In agreement with the present data, the role of Met^{35} in Aβ toxicity has been indicated in earlier papers [10,18]. Manelli and Puttfarcken [18] found that the amino acid substitution Aβ1–42(Nle^{35}) decreased the toxicity towards rat hippocampal cells.

The image analysis data demonstrated the toxicity of Aβ1–42, Aβ31–35 and Aβ34–39 in decreasing the number of small GABAergic neurons. We do not know the reason for the prevailing loss of small GABAergic neurons. A subset of GABAergic neurons has been reported to express calcium-binding proteins [8,22,34]. There are suggestions that Aβ neurotoxicity involves an apoptotic cascade, driven in part by the destabilization of intracellular calcium [20,33]. Cells containing calcium-binding proteins are stated to reduce intracellular calcium levels more effectively than those that cannot bind calcium [4]. Although the sizes of neurons containing calcium-binding proteins have been investigated only in the striatum of rat [2] and human [14], both studies concluded that these neurons are medium to large in size. Based on the above data, we suggest that the small GABAergic neurons in our neuronal cultures may not contain any calcium-binding protein, and therefore the most vulnerable to Aβs. Pike and Cotman [32] investigated the vulnerability of calretinin-immunoreactive neurons. They reported that calretinin-positive neurons in hippocampal cultures are resistant to Aβ toxicity [32] and suggested that calretinin, with its enhanced calcium-buffering capacity, is responsible for the resistance of GABAergic cells. To prove or disprove our suggestion regarding the possibility of different contents of calcium-binding proteins in neurons of different sizes, further investigations are necessary, involving double immunocytochemical studies for different neurotransmitters colocalized with calcium-binding proteins (ongoing study).

In conclusion, the present study, aimed at obtaining a deeper insight into the cellular events leading to neuronal death, has provided morphological evidence that not only Aβ1–42 and its biologically active fragment Aβ25–35 are toxic to neuronal cells: Aβ31–35 and Aβ34–39 also induce neuronal degeneration in rat basal forebrain cultures. Our results lead us to conclude that Leu^{34} and Met^{35} may be responsible for the toxicity of amyloid peptides. It is presumed that the different sizes of neurons may be related to their different neurochemical phenotypes, which is one of the many factors influencing the neuronal vulnerability to amyloid toxicity. These observations suggest that the degeneration of small GABAergic neurons is an indicator of early pathological changes and of functionally and morphologically vulnerable sites.

Acknowledgements

The authors are indebted to V. Sz. Tóth and Mrs. I. Darányi for technical assistance. This study was supported by grants ETT: 584/1996, MKM: 36 and OTKA: T 022683.

Fig. 5. Effects of different Aβs on numbers of GABAergic cells of different sizes in embryonic rat basal forebrain cultures after different treatment periods. A: day 1 after treatment (DIV 4 + 1); B: day 3 after treatment; C: day 5 after treatment. Data are means ± S.D. values from 5 randomly selected fields (5 × 0.3 mm^2) in each of 3 separate experiments (* $p < 0.001$, paired Student's t-test).

References

[1] C. Behl, J.B. Davis, R. Lesley, D. Schubert, Hydrogen peroxide mediates amyloid β protein toxicity, Cell 77 (1994) 817–827.

[2] B.D. Bennett, J.P. Bolam, Characterization of calretinin-immunoreactive structures in the striatum of the rat, Brain Res. 609 (1993) 137–148.

[3] J. Busciglio, A. Lorenzo, B.A. Yankner, Methodological variables in the assessment of beta amyloid neurotoxicity, Neurobiol. Aging 13 (1992) 609–612.

[4] B. Cheng, M.P. Mattson, NGF and bFGF protect rat hippocampal and human cortical neurons against hypoglycemic damage by stabilizing calcium homeostasis, Neuron 7 (1991) 1031–1041.

[5] J.T. Coyle, D.L. Price, M.R. DeLong, Alzheimer's disease: a disorder of cortical cholinergic innervation, Science 219 (1983) 1184–1190.

[6] M. Emre, C. Geula, B.J. Ransil, M.-M. Mesulam, The acute neurotoxicity and effects upon cholinergic axons of intracerebrally injected β amyloid in the rat brain, Neurobiol. Aging 13 (1992) 553–560.

[7] G. Forloni, R. Chiesa, S. Smiroldo, L. Verga, M. Salmona, F. Tagliavini, N. Angeretti, Apoptosis mediated neurotoxicity induced by chronic application of beta amyloid fragment 25–35., Neuroreport 4 (1993) 523–526.

[8] T.F. Freund, GABAergic septohippocampal neurons contain parvalbumin, Brain Res. 478 (1989) 375–381.

[9] J. Hardy, R. Cowburn, A. Barton, G. Reynolds, P. Dodd, P. Wester, A.-M. O'Carrol, E. Lofdahl, B. Winblad, A disorder of cortical GABAergic innervation in Alzheimer's disease, Neurosci. Lett. 73 (1987) 192–196.

[10] K. Hensley, J.M. Carney, M.P. Mattson, M. Aksenova, M. Harris, J.F. Wu, R.A. Floyd, D.A. Butterfield, A model for β-amyloid aggregation and neurotoxicity based on free radical generation by the peptide: relevance to Alzheimer disease, Proc. Natl. Acad. Sci. U.S.A. 91 (1994) 3270–3274.

[11] P. Kasa, M. Pakaski, B. Penke, Synthetic human beta amyloid has selective vulnerable effects on different types of neurons and glial cells in in vitro cultures derived from embryonic rat brain cortex, Neurobiol. Aging 13 (1992) S104, Suppl. 1.

[12] P. Kasa, M. Pakaski, B. Penke, Synthetic human beta amyloid has selective vulnerable effects on different types of neurons, in: M. Nicolini, P.F. Zatta, B. Corain, (Eds.), Alzheimer's Disease and related disorders, Advances in the Biosciences, Vol. 12, Pergamon Press, Oxford, 1993, pp. 311–312.

[13] P. Kasa, Z. Farkas, M. Pakaski, K. Soós, B. Penke, Effects of β-amyloid peptides and their fragments on acetylcholine release in in vitro studies, Clin. Neurosci. 49 (1996) 48–49.

[14] H. Kita, T. Kosaka, C.V. Heizmann, Parvalbumin-immunoreactive neurons in the rat neostriatum: a light and electron microscopic study, Brain Res. 536 (1990) 1–15.

[15] N.W. Kowall, M.F. Beal, J. Busciglio, L.K. Duffy, B.A. Yankner, An in vivo model for neurodegenerative effects of β amyloid and protection by substance P, Proc. Natl. Acad. Sci. U.S.A. 88 (1991) 7247–7251.

[16] N.W. Kowall, A.C. McKee, B.A. Yankner, M.F. Beal, In vivo neurotoxicity of beta amyloid [β(1–40)] and the [β(25–35)] fragment, Neurobiol. Aging 13 (1992) 537–542.

[17] D.T. Loo, A. Copani, C.J. Pike, E.R. Whittemore, A.J. Walencewicz, C.W. Cotman, Apoptosis is induced by beta-amyloid in cultured central nervous system neurons, Proc. Natl. Acad. Sci. U.S.A. 90 (1993) 7951–7955.

[18] A.M. Manelli, P.S. Puttfarcken, β-Amyloid-induced toxicity in rat hippocampal cells: in vitro evidence for the involvement of free radicals, Brain Res. Bull. 38 (1995) 569–576.

[19] T.J. Marczynski, GABAergic deafferentation hypotheses of brain aging and Alzheimer's disease revisited, Brain Res. Bull. 45 (1998) 341–379.

[20] M.P. Mattson, B. Cheng, D. Davis, K. Bryant, I. Lieberburg, R.E. Rydel, β-amyloid peptides destabilize calcium homeostasis and render human cortical neurons vulnerable to excitotoxicity, J. Neurosci. 12 (1992) 376–389.

[21] M.P. Mattson, K.J. Tomaselli, R.E. Rydel, Calcium-destabilizing and neurodegenerative effects of aggregated β-amyloid peptide are attenuated by basic FGF, Brain Res. 621 (1993) 35–49.

[22] R. Miettinen, A.I. Gulyas, K.G. Baimbridge, D.M. Jacobowitz, T.F. Freund, Calretinin is present in non-pyramidal cells of rat hippocampus: II. Co-existence with other calcium binding proteins and GABA, Neuroscience 48 (1992) 29–43.

[23] P. Mohanakrishnan, A.H. Fowler, J.P. Vonsattel, M.M. Husain, P.R. Jolles, P. Liem, R.A. Komoroski, An in vitro ^{1}H nuclear magnetic resonance study of the temporoparietal cortex of Alzheimer brains, Exp. Brain Res. 102 (1995) 503–510.

[24] M. Pakaski, K. Soós, B. Penke, P. Kasa, Neurotoxic effects of beta-amyloid and different amyloid peptides on cholinergic, gabaergic and parvalbumin containing neurons, Clin. Neurosci. 49 (1996) 24.

[25] H. Papp, M. Pakaski, B. Penke, P. Kasa, Effects of β-amyloid and its fragments on cholinergic and cholinoceptive neurons in vitro, Clin. Neurosci. 49 (1996) 49–50.

[26] B. Penke, K. Soós, Z.E. Szabó, J. Márky-Zay, M. Pakaski, P. Kasa, Synthesis and investigation of the β-amyloid 1–42 polypeptide and its analogs, in: C.H. Schneider, A.N. Eberle, (Eds.), Peptides, Escom Science Publishers, 1992, pp. 792–793.

[27] E.K. Perry, J.A. Court, S. Lloyd, M. Johnson, M.H. Griffiths, D. Spurden, M.A. Piggott, J. Turner, R.H. Perry, Beta amyloidosis in normal aging and transmitter signalling in human temporal lobe, Ann. New York Acad. Sci. 777 (1996) 388–392.

[28] C.J. Pike, A.J. Walencewicz, C.G. Glabe, C.W. Cotman, In vitro aging of β-amyloid protein causes peptide aggregation and neurotoxicity, Brain Res. 563 (1991) 311–314.

[29] C.J. Pike, A.J. Walencewicz, C.G. Glabe, C.W. Cotman, Aggregation-related toxicity of synthetic β-amyloid protein in hippocampal cultures, Eur. J. Pharmacol. 207 (1991) 367–368.

[30] C.J. Pike, C.W. Cotman, Cultured GABA-immunoreactive neurons are resistant to toxicity induced by β-amyloid, Neuroscience 56 (1993) 269–274.

[31] C.J. Pike, D. Burdick, A.J. Walencewicz, C.G. Glabe, C.W. Cotman, Neurodegeneration induced by β-amyloid peptides in vitro: the role of peptide assembly state, J. Neurosci. 13 (1993) 1676–1687.

[32] C.J. Pike, C.W. Cotman, Calretinin-immunoreactive neurons are resistant to β-amyloid toxicity in vitro, Brain Res. 671 (1995) 293–298.

[33] C.J. Pike, A.J. Walencewicz, J. Kosmoski, D.H. Cribbs, C.G. Glabe, C.W. Cotman, Structure-activity analyses of β-amyloid peptides: contributions of the β25–35 region to aggregation and neurotoxicity, J. Neurochem. 64 (1995) 253–265.

[34] J.H. Rogers, Immunohistochemical markers in rat cortex: co-localization of calretinin and calbindin-D28k with neuropeptides and GABA, Brain Res. (1992) 147–157.

[35] D.K. Rush, S. Aschmies, M.C. Merriman, Intracerebral β-amyloid (25–35) produces tissue damage: is it neurotoxic?, Neurobiol. Aging 13 (1992) 591–594.

[36] D. Storga, K. Vrecko, J.G. Birkmayer, J.G. Reibnegger, Monoaminergic neurotransmitters, their precursors and metabolites in brains of Alzheimer patients, Neurosci. Lett. 203 (1996) 29–32.

[37] H. Tohgi, T. Abe, S. Takahashi, M. Kimura, A selective reduction of excitatory amino acids in cerebrospinal fluid of patients with Alzheimer type dementia compared with vascular dementia of the Binswanger type, Neurosci. Lett. 141 (1992) 5–8.

[38] J. Waite, G.M. Cole, S.A. Frautschy, D.J. Connor, L.J. Thal, Solvent effects on beta protein toxicity in vivo, Neurobiol. Aging 13 (1992) 595–599.

[39] B.A. Yankner, L.K. Duffy, D.A. Kirschner, Neurotrophic and neurotoxic effects of amyloid β protein: reversal by tachykinin neuropeptides, Science 250 (1990) 279–282.

V

Acta Biologica Hungarica 49 (1), pp. 43–54 (1998)

EFFECTS OF BETA-AMYLOID ON CHOLINERGIC, CHOLINOCEPTIVE AND GABAergic NEURONS*

Magdolna PÁKÁSKI[1], Henrietta PAPP[1], Mónika FORGON[1], P. KÁSA JR.[2] and B. PENKE[3]

[1]Alzheimer's Disease Research Centre, [2]Department of Pharmaceutical Technology, [3]Department of Medical Chemistry, Albert Szent-Györgyi Medical University, Szeged, Hungary

(Received: 1998-06-12; accepted: 1998-06-26)

Alzheimer's disease is primarily characterized by neurofibrillary tangles, senile plaques and a cholinergic hypofunction. In this study, the morphological signs of toxicity of amyloid β (Aβ) 1–42 and short amyloid peptide fragments corresponding to amino acids 31–35 and 34–39 were investigated on cholinergic, cholinoceptive and GABAergic neuronal populations of basal forebrain cultures.

The applied Aβ fragments were toxic to cholinergic, cholinoceptive and GABAergic neurons. In cholinergic and cholinoceptive neurons, the toxic effect caused a redistribution of the acetylcholinesterase within the cells; the characteristic morphological changes in the GABAergic neurons involved the fragmentation and disappearance of the processes.

These results suggest that the vulnerability of neurons to Aβ toxicity does not depend on their transmitter content, but the morphological manifestation of this vulnerability differs in the various neuronal populations. The results of experiments with short Aβ fragments led to the conclusion that Leu^{34} and Met^{35} may be responsible for the toxicity of amyloid peptides.

Keywords: Alzheimer's disease – amyloid – neuronal culture – GABA immunocytochemistry – acetylcholinesterase – vesicular acetylcholine transporter

INTRODUCTION

Alzheimer's disease (AD) is characterized by the extracellular deposition in the brain and its blood vessels of insoluble aggregates of the amyloid β (Aβ) peptide. AD can also be related to damage to the basal forebrain cholinergic system, and in particular the nucleus basalis of Meynert, which undergoes significant neuronal loss in AD [2, 4]. Although the GABAergic population is typically spared from severe neuronal loss in AD, the evidence does indicate the presence of neuritic abnormalities in these cells [25]. Previous studies have also demonstrated deficits of other neurotransmitters, including the GABA system, in patients with AD [15, 22].

*Dedicated to Professor Péter Kása on the occasion of the 25th anniversary of his appointment as Head of the Central Research Laboratory and the Alzheimer's Disease Research Centre.

Send offprint requests to: Dr. Magdolna Pákáski, Alzheimer's Disease Research Centre, Albert Szent-Györgyi Medical University, H-6723 Szeged, Somogyi u. 4, Hungary. E-mail: pakaski@comser.szote-u.szeged.hu.

0236-5383/98/$ 5.00

Aβ has been shown to be toxic to neurons *in vitro* [3, 18, 26] and to rats and aged primates *in vivo* [10, 11]. Although the relationship between Aβ toxicity and the cholinergic system was investigated *in vivo* [5, 6], we have little information about *in vitro* findings [17]. Another interesting question is how GABAergic neurons react to Aβ. Earlier investigations provided controversial results concerning the resistance [19] and vulnerability [7, 8] of GABAergic neurons in response to Aβ neurotoxicity.

The major protein component of the amyloid core of the senile plaques is the 40–42 amino acid residue Aβ. Earlier reports concluded that Aβ25–35 causes morphological indications of neuronal degeneration similar to those of the full-length Aβ1–42. It has been suggested that this 11-amino acid internal sequence of amino acids is the biologically active fragment and may be responsible for the toxic effect of Aβ1–42 [26]. Further analysis of a series of peptides derived from the proposed active fragment of Aβ revealed that Aβ29–35 is necessary for the neurotoxicity [20]. With regard to the cited data, the primary purpose of this study was to investigate the *in vitro* toxic effect of Aβ on cholinergic or cholinoceptive neurons in embryonic rat basal forebrain cultures; a second aim was to re-examine the morphological changes in the GABAergic neurons after Aβ treatment. Cholinergic or cholinoceptive neurons were identified by means of acetylcholinesterase (AChE) histochemistry and vesicular acetylcholine transporter (VAChT) immunohistochemistry. GABAergic neurons were demonstrated by GABA immunohistochemistry. These morphological methods were used to investigate the structural changes in the cholinergic, cholinoceptive and GABAergic neurons after Aβ1–42 treatment. After initial characterization of the activity of full-length Aβ1–42, the toxicities of shorter fragments, such as Aβ31–35, Aβ34–39 and Aβ33–35, were compared. To prove the neuronal damage by biochemical means, measurements were made on the mitochondrial dehydrogenase activity (MTT) reduction and lactate dehydrogenase (LDH) release into the medium.

MATERIALS AND METHODS

Tissue culture

Since the basal forebrain is a region typically affected in AD, primary basal forebrain cultures were utilized in our experiments. Basal forebrain tissue from embryonic rat pups on days 16 or 17 (E16–17) was dissected and then digested for 10 min in 0.25% trypsin (Gibco) at 37 °C. Following mechanical dissociation of the tissue, the suspension was settled for 10 min at 1000 × *g*. The cell pellet was resuspended in Dulbecco's Modified Eagle Medium (DMEM) (Gibco) containing 10% fetal bovine serum (FBS) (Gibco), 100 U/ml penicillin and 100 μg/ml streptomycin. Cells were plated onto coverslips coated with poly-L-lysine (Sigma) at a density of $3.5–4 \times 10^4$ cells/cm^2 and were grown in a humidified incubator at 37 °C in 5% CO_2.

Peptide solutions

Human Aβ was synthesized in the Chemical Department of our University by a solid-phase technique involving Boc chemistry, purified by HPLC, and subjected to electrospray mass spectral analysis [12]. Aβ1–42, Aβ31–35, Aβ34–39 or Aβ33–35 was solubilized in 35% acetonitrile plus 0.1% trifluoroacetic acid (ACN/TFA). Peptide solutions were diluted into the growth medium immediately after solubilization to yield a final concentration of 20 μM for Aβs as described by Yankner et al. [26]. Peptides were added to cultures on 4 day *in vitro* (DIV 4) after plating. Control cultures were maintained in DMEM/10% FBS for 4 days, and then supplemented with vehicle alone. Morphological changes in the cells were monitored on days 1 (DIV 4+1), 3 (DIV 4+3) and 5 (DIV 4+5) after treatment.

AChE histochemistry

To visualize the signs of Aβ toxicity on cholinergic and cholinoceptive neurons, the cultures were fixed in 4% paraformaldehyde for 20 min and then stained for AChE by the technique of Tago et al. [23]. Ethopropazine (10^{-4} M) was always used as non-specific cholinesterase inhibitor. After incubation with a reaction mixture containing acetylthiocholine iodide (1 mg/ml) as substrate, the reaction product was detected with 3,3'-diaminobenzidine tetrahydrochloride and $NiCl_2$. During the microscopic examination, 300 AChE-positive neurons were counted both in the control and in the Aβ1–42-treated cultures and they were classified according to their size and the staining pattern.

VAChT immunohistochemistry

For a more exact identification of cholinergic neurons, the cultures were immunostained for VAChT. The cells were fixed in 4% paraformaldehyde for 20 min and were incubated with 0.1% Triton X-100 and 5% normal rabbit serum (NGS) in Tris-buffered saline (TBS) for 2 h. The polyclonal antibody against VAChT (1:32 000, Chemicon, USA) was applied for 48 h. This was followed by incubation in rabbit-anti-goat IgG-biotin (1:200, Jackson Immunores. Lab., USA) for 1 h, and then in streptavidin-horseradish peroxidase (1:500, Zymed, USA) for 1 h. The cultures were washed twice with 0.1 M TBS (pH 7.4) for 10 min between sera. The peroxidase reaction was developed by using 3,3'-diaminobenzidine tetrahydrochloride and $NiCl_2$.

GABA immunohistochemistry

To assess the neuronal damage caused to the GABAergic neurons by the Aβs, the cultures were immunostained for GABA by the peroxidase-antiperoxidase method. After fixation in 1% glutaraldehyde for 20 min, the cells were permeabilized and the non-specific staining was blocked by incubation with 0.2% Triton X-100 and 5% normal bovine serum

(NBS) in TBS for 4 h. The monoclonal antibody against GABA (1:3000; Immunotech, France) was applied overnight at 37 °C. Goat-anti-rabbit secondary antibody (1:30, Jackson Immunores. Lab., USA) and rabbit peroxidase-antiperoxidase complex (1:200, Nordic Immun. Lab., Germany) were applied consecutively for 1 h at room temperature. Staining was revealed with a solution containing 3,3'-diaminobenzidine tetrahydrochloride, $NiCl_2$ and H_2O_2 in Tris-HCl. In immunocytochemical control experiments, immunostaining was blocked by deletion of the GABA antibody. The results of morphological observations were quantified by image analysis. A Leica Q500 MC colour image analyser (Germany) was employed to measure the numbers of GABAergic cells in the control and Aβ-treated cultures after different time intervals.

Biochemical investigations

As one of the early indicators of toxicity of Aβs [23], the MTT reduction was measured 2 and 6 h after Aβ treatment. 200 µl/culture of 5 mg/ml MTT (3-[4,5-dimethylthiazol-2-yl]-2,5-diphenyltetrazolium bromide) stock was added and, after a 4 h incubation, 300 µl of reaction solution containing 50% dimethylformamide and 20% SDS was added to solubilize the insoluble formazan precipitates produced by MTT reduction. The next day, the absorbance of the purple dye was read at 570 nm.

After a longer incubation with Aβs (DIV4+3; DIV4+4 and DIV 4+5), the LDH activity in the culture medium was evaluated by measuring the rate of disappearance of NADH (after addition of pyruvate and NADH), monitored spectrophotometrically at 340 nm by the method of Wróblewski and LaDue [25].

RESULTS

Demonstration of toxicity of Aβs on cholinergic and cholinoceptive neurons

In the control cultures, two types of neurons could be distinguished on the basis of their morphological features after AChE histochemistry. The majority of the AChE-positive neurons (66%–76%) were small and bipolar, but this basal forebrain culture contained a relatively large number of multipolar neurons with extensively arborized processes (24%–34%). The specific staining for AChE was localized on the perikarya and processes of neurons (Fig. 1A). After Aβ1–42 treatment, the localization of the staining pattern was changed. It did not fill the whole perikarya and could be observed near the plasma membrane or sometimes near the somatodendritic region (Fig. 1B). Similarly, treatment of the cultures with shorter peptides (Aβ31–35 or Aβ34–39) also caused alterations in the enzyme localization within the cholinoceptive and cholinergic neurons (Fig. 1C). Aβ33–35 had no effect at all. Figure 2 demonstrates the quantitative distribution of the healthy and damaged AChE-positive neurons of different sizes in the control and Aβ1–42-treated cultures. The numbers of both large, multipolar and small, bipolar neurons displaying diffuse

perikaryonal staining (healthy cells) were decreased after Aβ1–42 treatment. At the same time, the number of neurons with a staining pattern localized near the plasma membrane (damaged cells) was increased. The increase in the number of damaged cells was not essentially different in the small, bipolar (3-fold) and large, multipolar (4-fold) neurons.

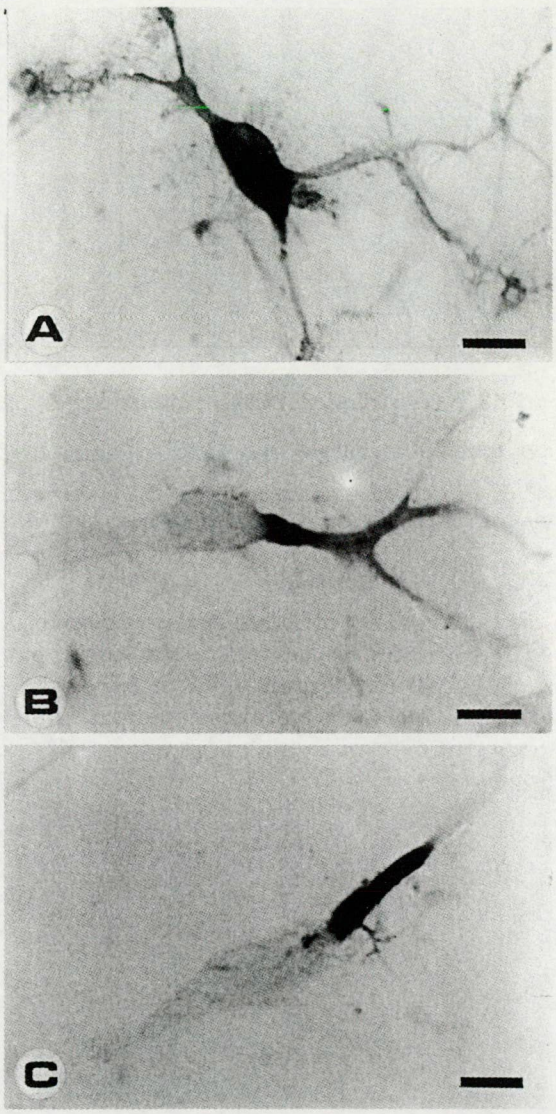

Fig. 1. Panels A–C: micrographs of basal forebrain cultures histochemically stained for AChE exposed for 1 day (DIV4+1) to the following treatments: A: solvent (control); B: 20 μM Aβ1–42; and C: 20 μM Aβ31–35. The neurons appear intact in the control culture; in contrast, the neurons are damaged after treatment (the specific staining is localized around the membrane). Scale bar = 10 μm

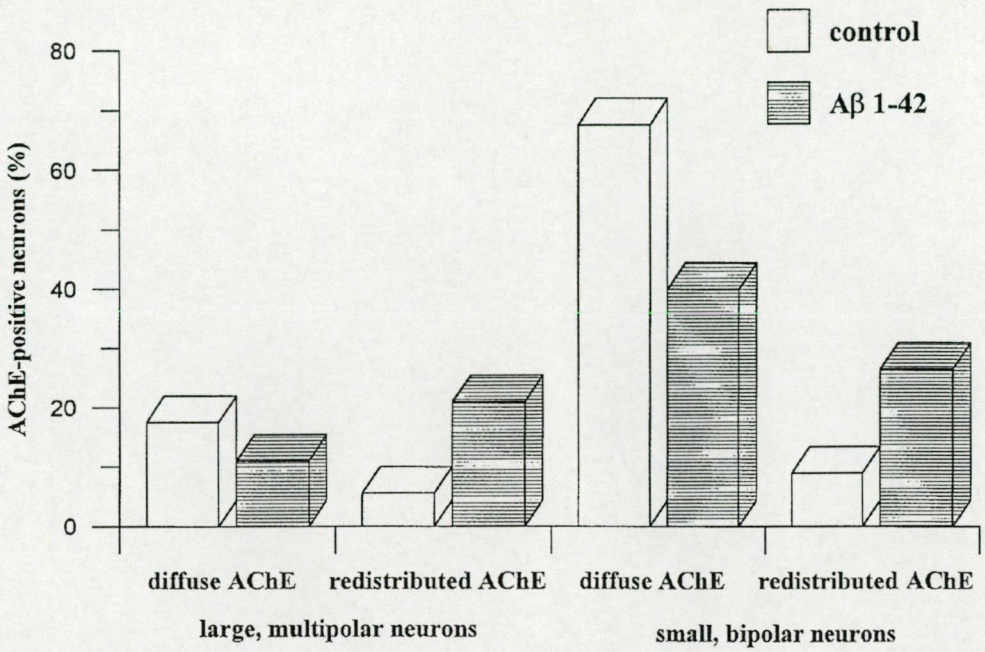

Fig. 2. Effect of Aβ1–2 on the localization of the AChE staining in the large, multipolar and small, bipolar AChE-positive neurons. The counted 300 cells of the cultures were taken as 100%

To confirm that the cultures really contained cholinergic neurons, the cells were immunostained for VAChT. Figure 3 illustrates the specific staining of cholinergic neurons. The immunostaining of VAChT was localized to the perikarya, where it appeared as vesicular distribution, and sometimes to the processes of neurons.

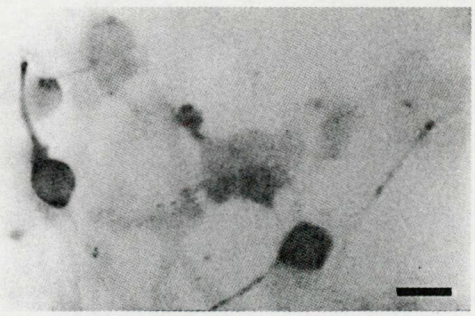

Fig. 3. Photomicrograph of basal forebrain cultures immunostained with VAChT antibody. Scale bar = 10 μm

Demonstration of toxicity of Aβs on GABAergic neurons

When the control and Aβ-treated cultures were immunostained for GABA, there were again morphological differences between them. In the untreated cultures, the GABA-immunoreactive neurons were healthy and their long processes were intact (Fig. 4A). Initially (DIV4+1), tiny varicosities appeared on the processes of the GABA-positive neurons in the Aβ1–42 treated cultures (Fig. 4B). On longer incubation (DIV4+3), more fragmented neurites could be observed. By day 5 after Aβ1–42 treatment, the signs of degeneration had become more serious: the majority of the GABAergic cells had lost their processes and the number of this type of neurons had decreased. Aβ31–35 (Fig. 4C) and Aβ34–39 (Fig. 4D) had similar toxic effects on the GABAergic basal forebrain neurons. There were no changes in the morphology of GABA-immunoreactive neurons after Aβ33–35 treatment. Table 1 illustrates the effects of the Aβs on the numbers of GABAergic cells counted by image analysis. On day 1 after treatment, only Aβ1–42 caused a significant cell loss. By day 3 after treatment with Aβ1–42, Aβ31–35 or Aβ34–39, the number of GABA-immunoreactive cells had decreased to 50-60% of that in the

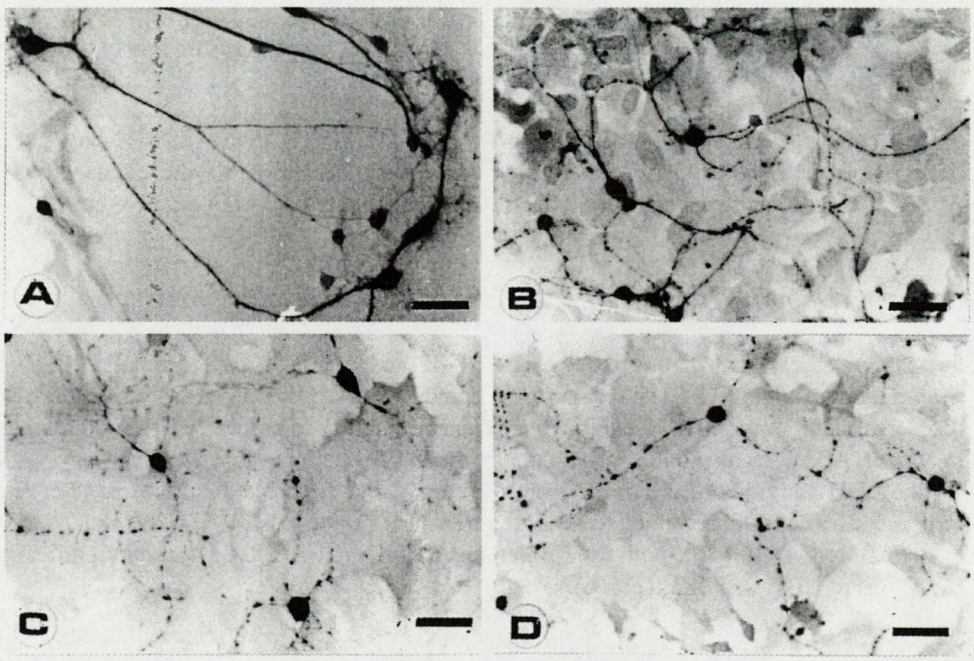

Fig. 4. Photomicrograph of basal forebrain cultures immunostained with GABA antibody exposed for 1 or 3 days (DIV4+1, DID4+3) to the following treatments: A: solvent (control) (DIV4+1); B: 20 μM Aβ1–42 (DIV4+1); C: 20 mM Aβ31–35 (DIV4+3) and D: 20 mM Aβ34–39 (DIV4+3); neurons have long, intact processes in the control culture; in contrast, the vast majority of the neurons are degenerated after treatment (fragmented neurites). Scale bar = 30 μm

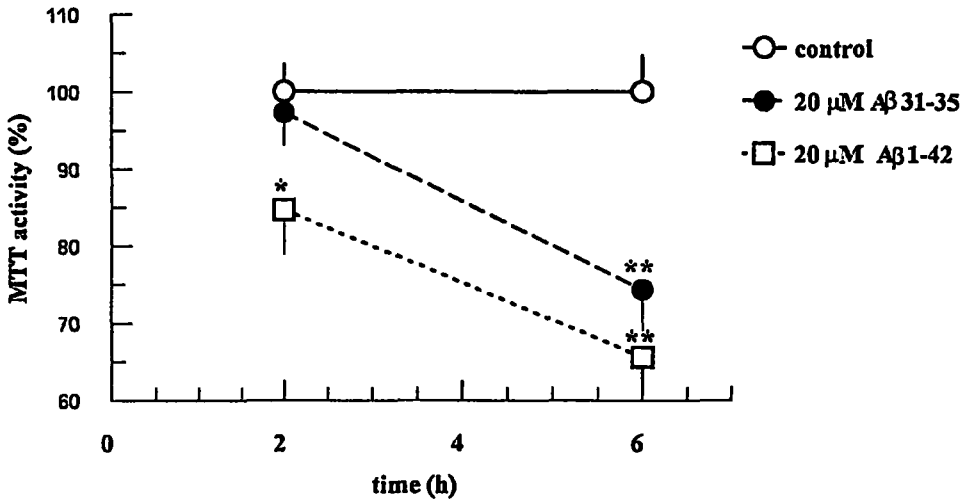

Fig. 5. Inhibition of MTT reduction caused by Aβ1–42 and Aβ31–35 in embryonic rat basal forebrain cultures. The values for untreated cultures (vehicle alone) were taken as 100%. Results on treated cultures are expressed as percentages of the control absorbance. Data are means ± SD values of results on 5 separate sample. Significant toxicity is observed at 2 h after Aβ1–42 treatment, and at 6 h after Aβ1–42 or Aβ31–35 treatment (*$p < 0.001$, **$p < 0.002$, paired Student's *t*-test)

control culture. Following a 5-day exposure to Aβ1–42, Aβ31–35 or Aβ34–39, more serious damage to the GABAergic cells was observed. Treatment of the cultures with Aβ33–35 did not induce a significant decrease in the number of GABA-positive cells.

Demonstration of toxicity of Aβs by biochemical means

For further assessment of the toxicity of Aβ1–42 and Aβ31–35 on the basal forebrain neuronal culture, the MTT test was performed and LDH activity was measured. After a 2-h Aβ treatment, only Aβ1–42 exhibited a diminished ability to reduce MTT. By 6 h after treatment, Aβ31–35 also potentially inhibited the MTT reduction (Fig. 5).

The LDH activities of the media from the control and Aβ-treated cultures did not reveal any significant difference after a 3-day treatment period (DIV4+3). One and 2 days later (DIV4+4, DIV 4+5), both the full-length Aβ1–42 and Aβ31–35 caused significant elevations of LDH activities (Fig. 6).

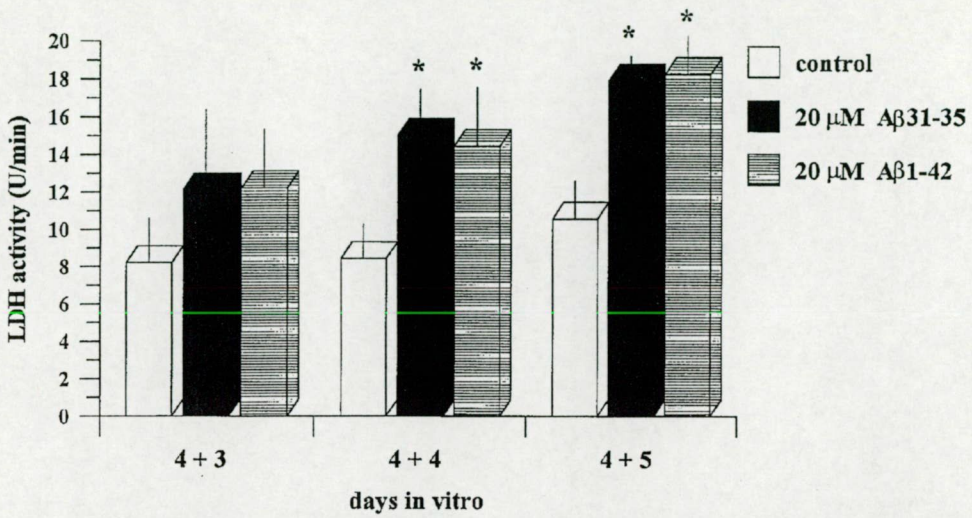

Fig. 6. Effects of Aβ1–42 and Aβ31–35 on LDH release from embryonic rat basal forebrain cultures. Data are means ± SD values of results on 5 separate samples. Significant toxicity is observed on days 4 and 5 after Aβ1–42, Aβ31–35 and Aβ34–39 treatment (*$p < 0.001$, paired Student's *t*-test)

DISCUSSION

The earliest data emphasized the relatively selective vulnerability of the cholinergic system of the basal forebrain in AD [2, 4]. A few years later, increasing evidence indicated damage to other transmitter systems, including the GABAergic neurons [15, 22, 25].

There were no *in vitro* or *in vivo* data relating to comparisons of the vulnerability of cholinergic and GABAergic neurons to Aβ toxicity. The present study revealed that Aβs are toxic to cholinergic, cholinoceptive and GABAergic neurons in rat basal forebrain cultures.

Table 1
Effects of different Aβs on numbers of GABAergic cells in embryonic rat basal forebrain cultures

	Aβ1–42	Aβ31–35	Aβ34–39	Aβ34–35
DIV4+1	74.5 ± 4.8*	97.4 ± 5.7	91.3 ± 9.7	109.7 ± 7.5
DIV4+3	52.0 ± 6.2*	61.0 ± 15*	53.0 ± 14*	89.7 ± 13.2
DIV4+5	15.9 ± 7.8*	19.9 ± 6.2*	25.6 ± 4.2*	83.1 ± 15.9

The values are expressed as % of control cultures. Data are means ± SD values from 5 randomly selected fields (5×0.3 mm^2) in each of 3 separate experiments. Significant toxicity is observed on day 1 after Aβ1–42 treatment, and on days 3 and 5 after Aβ1–42, Aβ31–35 and Aβ34–39 treatment (*$p < 0.001$, paired Student's *t*-test).

The histochemical results on the human cerebral cortex [14] indicate that the AChE-positive neurons that may be considered cholinergic exhibit extensive dendritic arborizations and the reaction of the secreted enzyme is also positive around the perikarya. Since our basal forebrain cultures contained a relatively large number of this latter type of AChE-positive neurons, the morphological changes in the cholinoceptive and the cholinergic neurons in consequences of Aβ toxicity had already been demonstrated [9]. This is the first *in vitro* study which provides information about the quantification of the signs of toxicity in cholinergic and cholinoceptive neurons after treatment with full-length Aβ. The change in localization of AChE within the cell can be regarded as an early sign of neurotoxicity [9], when the synthesis of the enzyme has almost totally stopped and it is translocated around the membrane.

The morphological signs of the toxic effects of Aβ1–42, Aβ31–35 and Aβ34–39 could also be detected on the GABAergic neurons, but they differed from those on the cholinergic and cholinoceptive neurons. Our results disprove the data of Pike and Cotman [19], who found the GABAergic neurons to be resistant. We hypothesize that the controversial data may arise from differences in the solvent and in the concentrations of the peptides applied in the different experiments. Another difference lies in the age and origin of the cultures used by ourselves and by Pike and Cotman. Our previous results [15] demonstrated that the vulnerability of GABAergic neurons depends on their sizes: the most vulnerable GABA-immunoreactive neurons were the small ones (diameter 5–10 μm), since only the number of these was decreased on 1 day after Aβ1–42 treatment. Monitoring the numbers of three different sizes of GABAergic neurons for 5 days after treatment revealed the relative resistance of the large cells to Aβ treatment. We postulated that the differences in vulnerability within the GABAergic neurons may depend on other neurochemical differences. Since the GABAergic neurons are nearly always colocalized with one of several different calcium-binding proteins, our suggestion relates to the finding of Pike and Cotman [21], who reported the resistance of calretinin-immunoreactive neurons to Aβ toxicity. On the basis of the results mentioned above, we proposed that the small GABAergic neurons do not contain one of the calcium-binding proteins, and they may therefore be vulnerable to Aβ.

On the basis of the toxicity of both Aβ31–35 and Aβ34–39, we suggested that the amino acids Leu^{34} and Met^{35} may play a role in the neurodegenerative effect of βAP. This suggestion seems to confirm earlier results [11]. Manelli and Puttfarcken found that the amino acid substitution Aβ1–42(Nle^{35}) decreased the toxicity towards rat hippocampal cells.

Abe and Kimura [1] demonstrated that Aβ toxicity consists of two phases, which are distinguished on the basis of differences in duration and in Ca^{2+} dependence. The early phase could be detected by the MTT assay, and the late phase by the LDH release assay. Our study, with these methods confirmed these findings. We found that the two phases of toxicity caused by Aβ31–35 can also be proved by these cytotoxic assays.

In summary, we have identified and characterized the morphological changes induced by Aβ in cholinergic, cholinoceptive and GABAergic neurons. The signs of toxicity display characteristic features for the given neuronal population. The results of experiments with short Aβ fragments lead us to conclude that Leu^{34} and Met^{35} may also be important for the toxicity of amyloid peptides.

ACKNOWLEDGEMENT

This work was supported by grants of OTKA T022683 and ETT 584/1996.

REFERENCES

1. Abe, K., Kimura, H. (1996) Amyloid β toxicity of a Ca^{2+}-independent early phase and a Ca^{2+}-dependent late phase. *J. Neurochem. 67,* 2074–2078.
2. Bartus, R. T., Dean, R. L. III, Beer, B., Lippa, S. (1982) The cholinergic hypothesis of geriatric memory dysfunction. *Science 217,* 408–414.
3. Busciglio, J., Lorenzo, A., Yankner, B. A. (1992) Methodological variables in the assesssment of beta amyloid neurotoxicity. *Neurobiol. Aging. 13,* 609–612.
4. Coyle, J. T., Price, D. L., DeLong, M. R. (1983) Alzheimer's disease: a disorder of cortical cholinergic innervation. *Science 219,* 1184–1190.
5. Emre, M., Geula, C., Ransil, B. J., Mesulam, M.-M. (1992) The acute neurotoxicity and effects upon cholinergic axons of intracerebrally injected β-amyloid in the rat brain. *Neurobiol. Aging 13,* 553–559.
6. Harkány, T., Lengyel, Zs., Soós, K., Penke, B., Luiten, P. G. M., Gulya, K. (1995) Cholinotoxic effects of β-amyloid$_{(1-42)}$ peptide on cortical projections of the rat nucleus basalis magnocellularis. *Brain Res. 695,* 71–75.
7. Kása, P., Pákáski, M., Penke, B. (1992) Synthetic human beta amyloid has selective vulnerable effects on different types of neurons and glial cells in *in vitro* cultures derived from embryonic rat brain cortex. *Neurobiol. Aging 13, Suppl. 1,* S104.
8. Kása, P., Pákáski, M., Penke, B. (1993) Synthetic human beta amyloid has selective vulnerable effects on different types of neurons. In: Nicolini, M., Zatta, P. F., Corain, B. (eds) *Alzheimer's Disease and Related Disorders. Advances in the Biosciences 12,* Pergamon Press, Oxford, pp. 311–312.
9. Kása, P., Pákáski, M., Zarándi, M., Forgon, M., Papp, H., Rakonczay, Z. (1998) Alterations in the distribution of acetylcholinesterase within the cholinergic and cholinoceptive neurons in *in vitro* tissue cultures in response to human amyloid β peptide and some of its fragments. *Neurobiol. Aging 19,* 549.
10. Kowall, N. W., Beal, M. F., Busciglio, J., Duffy, L. K., Yankner B. A. (1991) An *in vivo* model for neurodegenerative effects of β amyloid and protection by substance P. *Proc. Natl. Acad. Sci. USA 88,* 7247–7251.
11. Kowall, N. W., McKee, A. C., Yankner, B. A., Beal, M. F. (1992) In vivo neurotoxicity of beta amyloid [β(1-40)] and the [β(25-35)] fragment. *Neurobiol. Aging 13,* 537–542.
12. Laskay, G., Zarándi M., Varga, J., Jost, K., Fónagy, A. Torday, C., Latzkovits, L., Penke, B. (1997) A putative tetrapeptide antagonist prevents β-amyloid-induced long-term elevation of $[Ca^{2+}]_i$ in rat astrocytes. *Biochem. Biophys. Res. Commun. 235,* 479–481.
13. Manelli, A. M., Puttfarcken, P. S. (1995) β-Amyloid-induced toxicity in rat hippocampal cells: in vitro evidence for the involvement of free radicals. *Brain Res. Bull. 38,* 569–576.
14. Mesulam, M. M., Geula, C. (1992) Overlap between acetyl-cholinesterase-rich and choline acetyltransferase-positive (cholinergic) axons in human cerebral cortex. *Brain Res. 577,* 112–120.
15. Mountjoy, C. Q., Rossor, M. N., Iversen, L. L, Roth, M. (1984) Correlation of cortical cholinergic and GABA deficits with quantitative neuropathological findings in senile dementia. *Brain 107,* 507–518.
16. Pákáski, M., Farkas, Z., Kása, P. Jr., Forgon, M., Papp, H., Zarándi, M., Penke, B., Kása, P. (1998) Vulnerability of small GABAergic neurons to human β-amyloid pentapeptide. *Brain Res. 796,* 239–246.
17. Papp, H., Pákáski, M., Penke, B, Kása, P. (1996) Effects of β-amyloid and its fragments on cholinergic and cholinoceptive neurons in vitro. *Clin. Neurosci. 49,* 49–50.
18. Pike, C. J., Walencewicz, A. J., Glabe, C. G, Cotman, C. W. (1991) In vitro aging of β-amyloid protein causes peptide aggregation and neurotoxicity. *Brain Res. 563,* 311–314.

19. Pike, C. J., Cotman, C. W. (1993) Cultured GABA-immunoreactive neurons are resistant to toxicity induced by β-amyloid. *Neuroscience 56,* 269–274.
20. Pike, C. J., Burdick, D., Walencewicz, A. J., Glabe, C. G, Cotman, C. W. (1993) Neurodegeneration induced by β-amyloid peptides in vitro: the role of peptide assembly state. *J. Neurosci. 13,* 1676–1687.
21. Pike, C. J., Cotman, C. W. (1995) Calretinin-immunoreactive neurons are resistant to β-amyloid toxicity in vitro. *Brain Res. 671,* 293–298.
22. Rossor, M. N., Garret, N. J., Johnson, A. L., Mountjoy, C. Q., Roth, M., Iversen, L. L. (1982) A post-mortem study of the cholinergic and GABA systems in senile dementia. *Brain 105,* 313–330.
22. Shearman, M. S., Ragan, C. I., Iversen, L. L. (1994) Inhibition of PC12 cell redox activity is a specific, early indicator of the mechanism of β-amyloid-mediated cell death. *Proc. Natl. Acad. Sci. USA 91,* 1470–1474.
23. Tago, H., Kimura, H., Maeda, T. (1986) Visualization of detailed acetylcholinesterase fiber and neuron staining in rat brain by a sensitive histochemical procedure. *J. Histochem. Cytochem. 34,* 1431–1438.
24. Walker, L. C., Kitt, C. A., Struble, R. G., Schmechel, D. E., Oertel, W. H., Cork, L. C., Price, D. L. (1985) Glutamic acid decarboxylase-like immunoreactive neurites in senile plaques. *Neurosci. Lett. 59,* 165–169.
25. Wróblewski, F., LaDue, J. S. (1955) Lactic dehydrogenase activity in blood. *Proc. Soc. Exp. Biol. Med. 90,* 210–213.
26. Yankner, B. A., Duffy, L. K., Kirschner, D. A. (1990) Neurotrophic and neurotoxic effects of amyloid β protein: reversal by tachykinin neuropeptides. *Science 250,* 279–282.

VI

AMYLOID-β1-42 TREATMENT DOES NOT HAVE A SPECIFIC EFFECT ON CHOLINERGIC NEURONS IN *IN VITRO* BASAL FOREBRAIN NEURONAL CULTURES OF RAT

HENRIETTA PAPP[1*], P. KASA, Jr.,[2] MAGDOLNA PAKASKI[1],

L. BALASPIRI[3] and P. KASA, Sr.[1]

[1]Alzheimer's Disease Research Centre, Department of Psychiatry,

[2]Department of Pharmaceutical Technology and

[3]Department of Chemistry, University of Szeged,

H-6720 Szeged, Hungary

Corresponding author: H. Papp

Alzheimer's Disease Research Centre

Department of Psychiatry

University of Szeged

H-6720 Szeged, Hungary

E-mail: papph@comser.szote.u-szeged.hu

Running title: Aβ1-42 does not specifically affect cholinergic neurons

The neurotoxic effect of amyloid-beta peptide(1-42) was investigated in cultures of neuronal tissue derived from the basal forebrain of embryonic rat. The axonal varicosities of the cholinergic cells were revealed by vesicular acetylcholine transporter staining, and the axonal varicosities in general by synaptophysin immunohistochemistry. The results demonstrate that the treatment of *in vitro* neuronal cultures with 20 μM amyloid-beta peptide (1-42) for 2 days on day 5, 12 or 15 exerted a neurotoxic effect on both the cholinergic and the non-cholinergic neurons. In the same cultures, the absolute number of synaptophysin-positive axon varicosities was reduced to greater extent (control: 203±37/field *vs* treated: 101±16/field) than the number of vesicular acetylcholine transporter-immunoreactive (control: 48±4/field *vs* treated: 0/field) structures. It is concluded that amyloid-beta peptide (1-42) does not have a specific effect only on the cholinergic neurons, but affects non-cholinergic neurons as well.

Key words: amyloid-beta peptide – neurotoxicity - neuronal cultures - vesicular acetylcholine transporter - synaptophysin

INTRODUCTION

A cholinergic deficit is one of the major features of Alzheimer's disease (AD), where the hypofunction may be caused by amyloid-beta peptide (Aβ). Such a neurotoxic effect of Aβ has been demonstrated both in *in vivo* experiments [10] and *in vitro,* using neuronal cultures [11, 13, 15, 20].

The nervous system functions are dependent on the proper working of the synaptic apparatus. Diverse synaptic proteins such as synaptophysin (SYN) and the vesicular acetylcholine transporter (VAChT) that are distributed in various subcellular compartments in the axons and axon terminals may regulate the neurotransmission at the synaptic sites. In AD, the cholinergic deficit is well documented. It may be due to presynaptic alterations in the synthesis (choline acetyltransferase, ChAT) and the reduced release of acetylcholine (ACh), the decreased presence of receptors for ACh and the relative increased activity of acetylcholinesterase (AChE). VAChT is unique for the cholinergic neurons [2, 7]. It mediates the accumulation of ACh in the synaptic vesicles [3], which is largely built up from SYN. Reduced levels of these proteins may effectively influence the appropriate functioning of the synapse.

The cholinergic neurotransmission in the brain depends not only on the activities of ChAT and AChE, but also on the adequacy of the VAChT function and on the intactness of the synaptic vesicles, from which most of the ACh can be released. It remains to be elucidated how these proteins are damaged by the neurotoxic Aβ1-42 in the various transmitter-containing neurons. Through the use of [^{3}H]vesamicol quantitative autoradiography, the reduction of VAChT has been demonstrated in Aβ-infused rats [8]. Our present aim therefore was to shed more light on the *in vitro* effects of Aβ1-42 on the VAChT and SYN-immunoreactive structures present in the axon varicosities and axon terminals in cultures of neuronal tissue derived from embryonic rat basal forebrain.

MATERIALS AND METHODS

Materials

The substances used in this study were trypsin, Dulbecco's modified Eagle's medium (DMEM) and foetal bovine serum (FBS) from Gibco; poly-L-lysine, normal sheep serum, normal rabbit serum and 3,3'-diaminobenzidine.4HCl tetrahydrochloride from Sigma-Aldrich (St Louis, MO, USA); polyclonal anti-synaptophysin (902314) from Boehringer (Mannheim, Germany); polyclonal anti-VAChT antibody (AB1578) from Chemicon International Inc. (Temecula, CA, USA); sheep-anti-mouse IgG-biotin and rabbit-anti-goat IgG-biotin from Jackson Immunores. Lab. (West Grove, PA, USA); and streptavidin-horseradish peroxidase

from Zymed Laboratories Inc. (South San Francisco, CA, USA). All other reagents were of either laboratory or analytical grade from various suppliers.

Tissue cultures

Primary rat embryonic basal forebrain cultures were established via the protocol previously described [12]. In brief: the basal forebrain was dissected from the brains of embryonic rat pups on day 18 (E18), incubated in 0.25% trypsin for 10 min and dissociated by gentle trituration, and the suspension was settled for 10 min at 1000 x g. After resuspension, the cells were seeded at a density of $3.5\text{-}4x10^{-4}$ cells/cm^2 on poly-L-lysine-coated glass coverslips in DMEM supplemented with 10% (vol/vol) FBS, streptomycin (100 μg/ml) and penicillin (100 U/ml). The neuronal cultures were grown in a humidified incubator at 37 °C in 5% CO_2.

Treatment of tissue cultures

Human Aβ1-42 (synthesized in the Department of Chemistry at our University) was dissolved, and the cultures were treated after dilution in DMEM. The Aβ1-42 (20 μM Aβ1-42) was added to cultures on DIV5, DIV12 or DIV15 and the treated samples were cultivated for a further 2 days in a serum-free condition. Control cultures were maintained under similar conditions, but supplemented with the vehicle alone. The numbers of stained varicosities and/or axon terminals were monitored on DIV7, DIV14 or DIV17.

Synaptophysin immunohistochemistry

For identification of axonal varicosities and axonal terminals, the tissue cultures were immunostained for SYN. After fixation, the control and Aβ1-42-treated samples were incubated with 2.5% Triton X-100, and then with 5% normal sheep serum in phosphate buffer. The polyclonal antibody against SYN (1:1000) was applied for 48 h. This was followed by incubation in sheep-anti-mouse IgG-biotin (1:1000) for 1.5 h, and then in streptavidin-horseradish peroxidase (1:1000) for 1.5 h. The peroxidase reaction was developed by using 3,3'-diaminobenzidine tetrahydrochloride and $NiCl_2$.

Vesicular acetylcholine transporter immunohistochemistry

The cholinergic neurons and their axonic varicosities and axon terminals in the cultures were evaluated by immunohistochemistry for VAChT. After fixation, the control and the Aβ-treated neuronal cultures were incubated with 2.5% Triton X-100, and then with 5% normal rabbit serum in phosphate buffer. The polyclonal antibody against VAChT (1:32000) was applied for 48 h. This was followed by incubation in rabbit-anti-goat IgG-biotin (1:1000) for 1.5 h, and then in streptavidin-horseradish peroxidase (1:1000) for 1.5 h. The peroxidase reaction was developed by using 3,3'-diaminobenzidine tetrahydrochloride and $NiCl_2$.

Image analysis

The cholinergic neurons and the numbers of VAChT and SYN-immunoreactive axon varicosities and/or axon terminals in the cultures were evaluated by image analysis. The number of immunoreactive axonal varicosities was determined with a Quantimet 500MC Image Analysis System (Leica Cambridge) linked to a JVC-Color camera mounted on a Leica Laborlux "S" Leitz microscope.

The immunohistochemical reactions in the axonal varicosities were visualized and the digitized image (256 grey levels) was displayed on a colour monitor with 1024x768 pixel resolution. The neurotoxic effect of Aβ1-42 on the immunohistochemical staining was evaluated. Randomly selected areas of the control and treated cell cultures on coverslips were taken from 5 fields per cover slip. The numbers of immunoreactive axon varicosities in the control and the Aβ1-42-

treated samples were counted. All measurements were made under the same optical light conditions.

RESULTS

Effects of amyloid-beta peptide on the number of synaptophysin-positive axon terminals

In control tissue cultures, the SYN-positive immunoreactive axon varicosities and the axon terminals could be revealed diffusely distributed among neurons of various sizes. They were present on the soma of the neurons and closely related to some dendrites. The SYN-immunopositive structures differed considerably in size. The number of axonal varicosities increased as the duration of cultivation progressed (Fig. 1A-C). After 20 μM Aβ1-42 treatment of the basal forebrain tissue cultures for 2 days, the numbers of SYN-positive structures were diminished on DIV7, DIV14 and DIV17 (Fig. 1D-F).

For quantitative determination, the numbers of SYN-positive axon varicosities in the control and the Aβ-treated samples of the cultures were investigated by means of image analysis at various times (DIV7, DIV14 and DIV17). The results of the analyses of the control and Aβ-treated samples are summarized in Fig. 2.

Effects of amyloid-beta peptide on the number of vesicular acetylcholine transporter-positive axon terminals

In the control tissue cultures, besides the various types of cholinergic neurons (bipolar and multipolar), the VAChT-immunoreactive axon varicosities and axon terminals were distributed similarly to the SYN (Fig. 3A-C), but their number was much lower, as revealed by qualitative analysis of the stained samples. The immunopositive axon varicosities were among the VAChT-negative cell bodies and near the positively stained neuronal perikarya. VAChT immunoreactivity could also be revealed mainly as puncta and to a lesser extent as diffuse staining in neurons of different sizes.

Two days after 20 μM Aβ1-42 treatment, the VAChT immunoreactivity in the axon varicosities in the DIV7, DIV14 and DIV17 samples was dramatically reduced or even eliminated (Fig. 3D-F). Evaluation of the VAChT-positive axon varicosities and axon terminals in the control and Aβ1-42-treated samples by means of image analysis is illustrated in Fig. 4.

DISCUSSION

The results presented here support earlier findings that VAChT immunohistochemistry is a unique and useful means for the demonstration of cholinergic neurons, their axon varicosities and axon terminals both in the adult central and peripheral nervous systems [2, 18] and during development in tissue cultures [14].

Our immunohistochemical study resulted in three principal findings. First, various types of cholinergic neurons (small bipolar and larger multipolar) can be revealed in the primary neuronal cell culture. Second, the VAChT-positive axon varicosities are more sensitive than the SYN immunoreactive neuronal structures to this Aβ treatment. Third, the use of embryonic basal forebrain neuronal tissue cultures and their treatment with the neurotoxic Aβ provides a good *in vitro* cellular model with which to investigate the effects of various chemical agents on the cholinergic neurons and also to study the pathomechanism related to AD.

One of the primary features of AD is a cholinergic deficit, which may be caused by the neurotoxic Aβ. A reduction in the cholinergic terminal integrity has been demonstrated through use of a vesamicol analogue [^{125}I]MIBT [5], which is known to block the uptake of ACh into the cholinergic synaptic vesicles [1]. It has been suggested that the demonstration of VAChT can be a useful marker for assessment of the loss of cholinergic structures in AD. Indeed, the VAChT immunoreactivity in the axon varicosities furnishes a good possibility to detect

pathophysiological alterations in the cholinergic neurons. Such alterations, as demonstrated here, can be induced not only under *in vivo* circumstances, but *in vitro* as well.

The toxic effect of Aβ has already been demonstrated at micromolar concentrations in several tissue models [see refs. 6, 16, 19]. More recently, however, Blusztajn and Berse [4] reported that synthetic Aβ at submicromolar concentrations does not cause cytotoxicity, but rather reduces the expression of cholinergic markers in neuronal cells. This is supported by an earlier experiment in which we observed that Aβ affects the cholinergic neurons within 2 h in primary neuronal cultures [15]. At present, however, we are unable to decide whether the neurotoxic effect or the reduced expression of the cholinergic marker proteins was revealed in our experiments. The neurotoxic effect has been revealed in an *in vivo* experiment, demonstrating that Aβ1-42 inhibits the fast axonal transport of various types of proteins (including VAChT) in the sciatic nerve of rat [9].

A reduced level of presynaptic vesicle protein SYN occurs in the hippocampus of individuals with AD [17]. In our tissue culture model, a reduction in the SYN-immunoreactive structures was similarly observed after Aβ1-42 treatment. However, the decrease in the SYN staining is probably due not only to a reduction in the cholinergic axonal varicosities, but rather to the neurotoxic effect of Aβ on other neurotransmitter-containing neurons too. This is supported by experimental evidence. Pakaski et al. [12] demonstrated that Aβ1-42 *in vitro* not only affects the AChE-positive neurons, but also a neurodegenerative effect on GABAergic neurons. Further studies are required to clarify whether the reduction in the SYN-positive axon varicosities is due to the degeneration of cholinergic and GABAergic neurons or the degeneration of other transmitter containing neurons. Such investigations are currently in progress in our laboratory.

ACKNOWLEDGEMENT

This work was supported by OTKA (T022683, T030339 and T032458) ETT (T-11/011/2000) and a Széchenyi Professorship to P.K.

REFERENCES

1. Adam-Vizi, V., Deri, Z., Vizi, E. S., Sershen, H., Lajtha, A. (1991) Ca2-o-independent veratridine-evoked acetylcholine release from striatal slices is not inhibited by vesamicol (AH5183): mobilization of distinct transmitter pools. *J. Neurochem. 56,* 52-58.
2. Arvidsson, U., Riedl, M., Elde, R., Meister, B. (1997) Vesicular acetylcholine transporter (VAChT) protein: A novel and unique marker for cholinergic neurons in the central and peripheral nervous systems. *J. Comp. Neurol. 378,* 454-467.
3. Barbosa, J. Jr., Massensini, A. R., Santos, M. S., Meireles, S. I., Gomez, R. S., Gomez, M. V., Romano-Silva, M. A., Prado, V. F., Prado, M. A. M. (1999) Expression of the vesicular acetylcholine transporter, proteins involved in exocytosis, and functional calcium signaling in varicosities and soma of a murine septal cell line. *J. Neurochem. 73,* 1881-1893.
4. Blusztajn, J. K., Berse, B. (2000) The cholinergic neuronal phenotype in Alzheimer's disease. *Metab. Brain Dis. 15,* 45-64.
5. Efange, S. M., Garland, E. M., Staley, J. K., Khare, A, B., Mash, D. C. (1997) Vesicular acetylcholine transporter density and Alzheimer's disease. *Neurobiol. Aging 18,* 407-413.
6. Forloni, G. (1993) β-amyloid neurotoxicity. *Funct. Neurol. 8,* 211-225.
7. Gilmor, M. L., Nash, N. R., Roghani, A., Edwards, R. H., Yi, H., Hersch, S. M., Levey, A. I. (1996) Expression of the putative vesicular acetylcholine transporter in rat brain and localization in cholinergic synaptic vesicles. *J. Neurosci. 16,* 2179-2190.

8. Ikeda, E., Shiba, K., Mori, H., Ichikawa, A., Sumiya, H., Kuji, I., Tonami, N. (2000) Reduction of vesicular acetylcholine transporter in β-amyloid protein-infused rats with memory impairment. *Nucl. Med. Commun. 21,* 933-937.
9. Kasa, P., Papp, H., Kovacs, I., Forgon, M., Penke, B., Yamaguchi, H. (2000) Human amyloid-β1-42 applied in vivo inhibits the fast axonal transport of proteins in the sciatic nerve of rat. *Neurosci. Lett. 278,* 117-119.
10. Kowall, N. W., McKee, A. C., Yankner, B. A., Beal, M. F. (1992) In vivo neurotoxicity of β-amyloid [β(1-40)] and the β(25-35) fragment. *Neurobiol. Aging 13,* 537-542.
11. Ma, W., Zheng, W. H., Belanger, S., Kar, S., Quirion, R. (2001) Effects of amyloid peptides on cell viability and expression of neuropeptides in cultured rat dorsal root ganglion neurons: a role for free radicals and protein kinase C. *Eur. J. Neurosci. 13,* 1125-1135.
12. Pakaski, M., Papp, H., Forgon, M., Kasa, P. Jr., Penke, B. (1998) Effects of β-amyloid on cholinergic, cholinoceptive and GABAergic neurons. *Acta Biol. Hung. 49,* 43-54.
13. Papp, H., Pakaski, M., Penke, B., Kasa, P. (1996) Effects of β-amyloid and its fragments on cholinergic and cholinoceptive neurons in vitro. *Clin. Neurosci. 49,* 49-50.
14. Papp, H., Pakaski, M., Kovacs, I., Kasa, P. (1998) Characterization of the developmental expression of the vesicular acetylcholine transporter and acetylcholinesterase in cultured neurons. *Clin. Neurosci. 51,* 57.
15. Papp, H., Pakaski, M., Kasa, P. (1999) Identification of cholinergic neurons and their synaptic connections in rat embryonic neuronal culture and effects of human β-amyloid-42 on the cholinergic neurons. *Neurobiology 7,* 368-369.
16. Papp, H., Pakaski, M., Balaspiri, L., Kasa, P. (2000) In vitro effects of human amyloid-β peptide (Aβ1-42) and its fragments on the vesicular acetylcholine transporter and synaptophysin immunoreactive axon terminals. *Neurobiology 8,* 379-380.
17. Sze, C. I., Troncoso, J. C., Kawas, C., Mouton, P., Price, D. L., Martin, L. J. (1997) Loss of the presynaptic vesicle protein synaptophysin in hippocampus correlates with cognitive decline in Alzheimer disease. *J. Neuropathol. Exp. Neurol. 56,* 933-944.
18. Weihe, E., Tao-Cheng, J.-H., Schäfer, M. K.-H., Erickson, J. D., Eiden, L. (1996) Visualization of the vesicular acetylcholine transporter in cholinergic nerve terminals and its targeting to a specific population of small synaptic vesicles. *Proc. Natl. Acad. Sci. USA 93,* 3547-3552.
19. Yankner, B. A., Dawes, L. R., Fisher, S., Villa-Komaroff, L., Oster-Granite, M. L., Neve, R. L. (1989) Neurotoxicity of a fragment of the amyloid precursor associated with Alzheimer's disease. *Science 245,* 417-420.
20. Yankner, B. A., Duffy, L. K., Kirschner, D. A. (1990) Neurotrophic and neurotoxic effects of amyloid β protein: reversal by tachykinin neuropeptides. *Science 250,* 279-282.

Legends to Figures

Fig. 1. Light microscopic localization of synaptophysin immunoreactivity in the axon varicosities and in the axon terminals during development in the control basal forebrain neuronal cultures. Note the increased density of staining after the various time intervals. A: DIV7, B: DIV14 and C: DIV17. The synaptophysin-immunoreactive axon varicosities are reduced in the cultures after treatment with 20 μM Aβ1-42 for 2 days (E: DIV7, F: DIV14 and G: DIV17). Bar = 20 um.

Fig. 2. Evaluation of synaptophysin-positive axon varicosities and/or axon terminals by image analysis in control and Aβ1-42-treated basal forebrain tissue cultures. The control samples

were treated with the vehicle, and the other *in vitro* cultures with 20 μM Aβ1-42 for 2 days on days 5, 12 or 15.

Fig. 3. Light microscopic localization of vesicular acetylcholine transporter immunoreactivity in the cholinergic axon varicosities and in the axon terminals. Note that the number of small and large labelled puncta increase during the *in vitro* development of cholinergic neurons (A: DIV7; B: DIV14 and C: DIV17). After treatment with 20 μM Aβ1-42 for 2 days, the vesicular acetylcholine transporter immunoreactivity disappears in the basal forebrain tissue culture (E: DIV7; F: DIV14 and D: DIV17). Bar = 20 um.

Fig. 4. Evaluation of vesicular acetylcholine transporter-positive axon varicosities and/or axon terminals by image analysis in control and Aβ1-42-treated basal forebrain tissue cultures. The control samples were treated with the vehicle, and the other *in vitro* cultures with 20 μM Aβ1-42 for 2 days on days 5, 12 or 15.

Copy

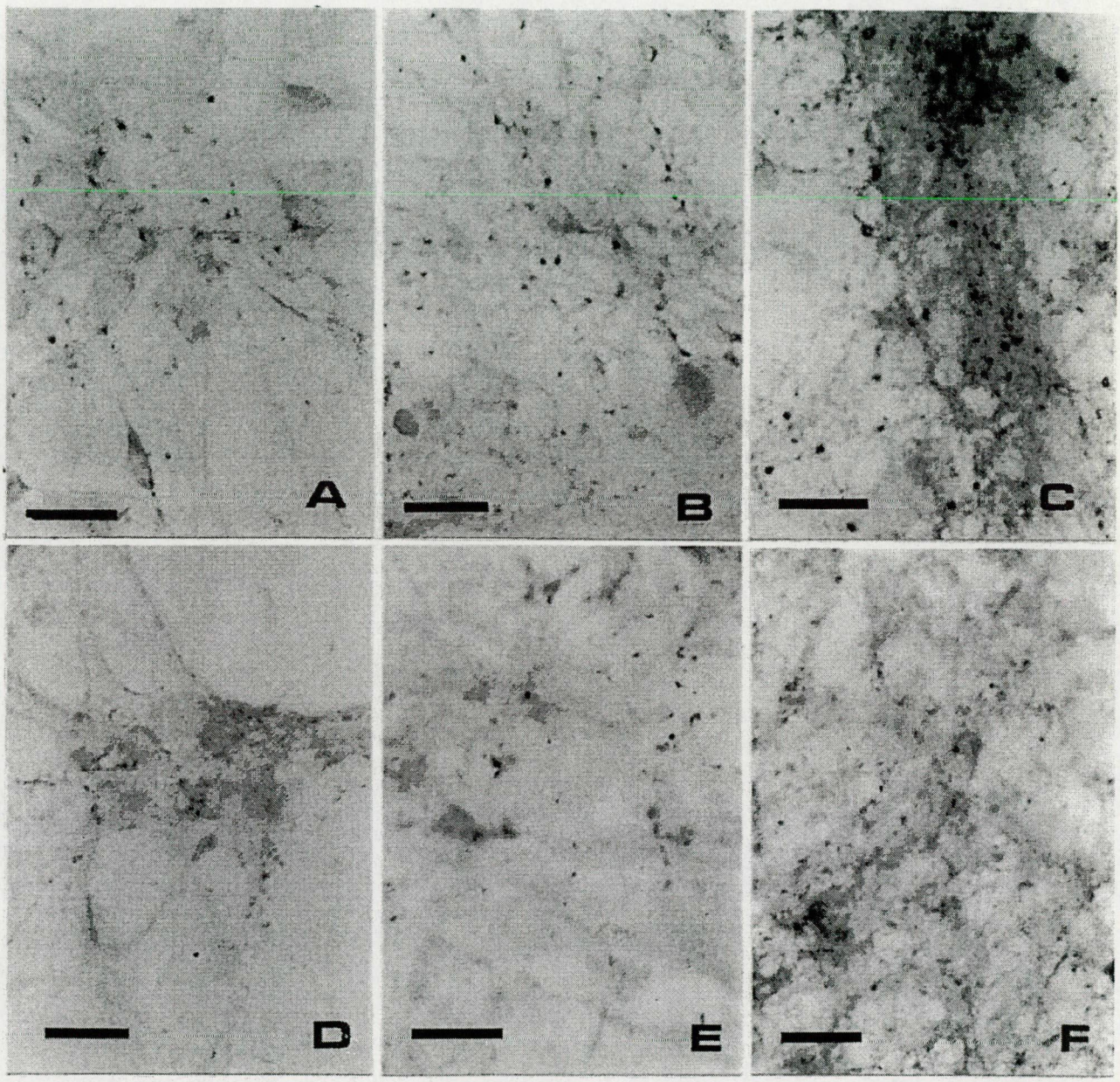

Fig. 1.

Evaluation of synaptophysin-positive axon varicosities and/or axon terminals by image analysis in control and Aß1-42-treated basal forebrain tissue cultures

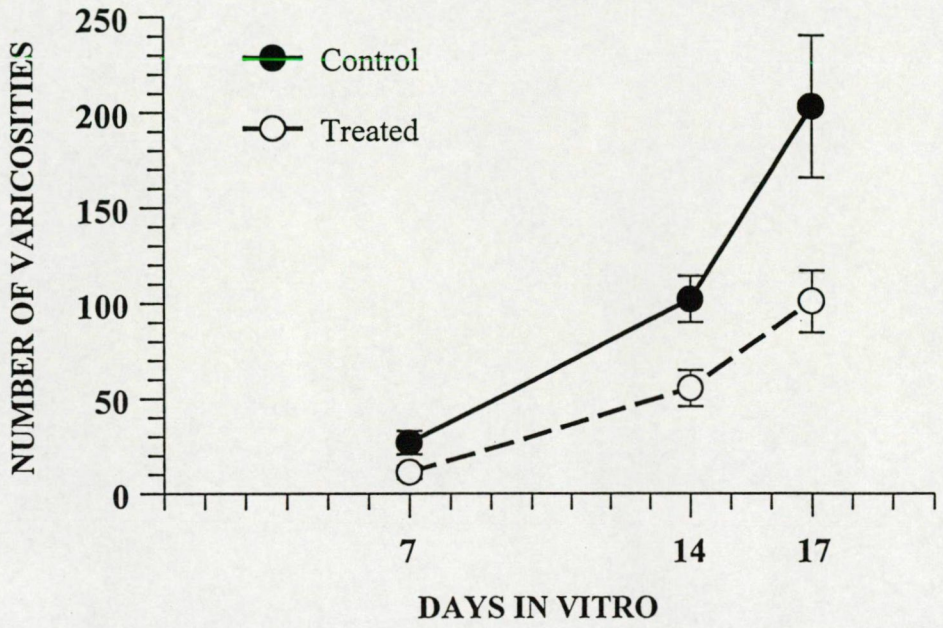

The control samples were treated with the vehicle, and the other in vitro cultures with 20 μM Aß1-42 for 2 days on days 5, 12 or 15.

Fig. 2.

Copy

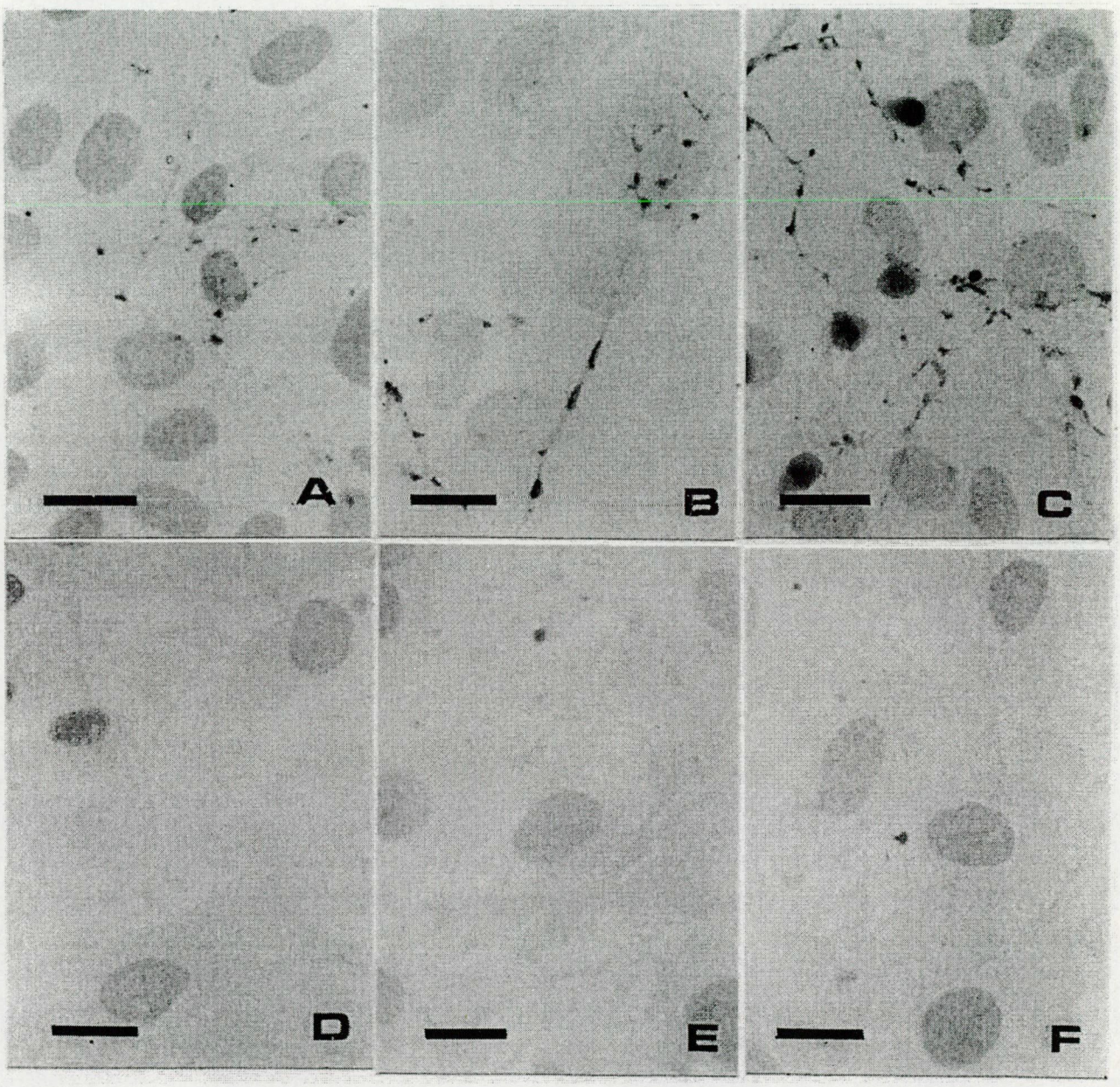

Fig. 3.

Evaluation of vesicular acetylcholine transporter-positive axon varicosities and/or axon terminals by image analysis in control and Aß1-42-treated basal forebrain tissue cultures

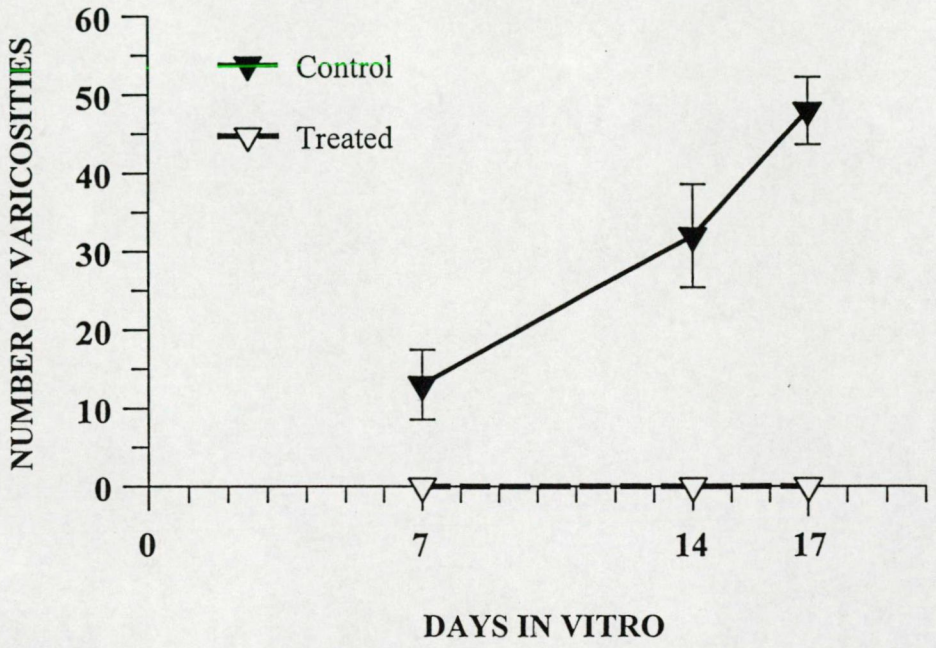

The control samples were treated with the vehicle, and the other in vitro cultures with 20 μM Aß1-42 for 2 days on days 5, 12 or 15.

Fig. 4.